



Systematics of *Pseudotothyris* (Loricariidae: Hypoptopomatinae)

FERNANDA O. MARTINS^{1*}, HERALDO A. BRITSKI² and FRANCISCO LANGEANI¹

¹UNESP – Universidade Estadual Paulista Instituto de Biociências, Letras e Ciências Exatas, Laboratório de Ictiologia, Rua Cristóvão Colombo, 2265, 15054-000, São José do Rio Preto, SP, Brazil

²MZUSP – Museu de Zoologia da Universidade de São Paulo, Avenida Nazaré, 481, Caixa Postal 7172, 01051-000, São Paulo, SP, Brazil

Received 17 April 2013; revised 17 October 2013; accepted for publication 21 October 2013

Pseudotothyris Britski & Garavello, 1984 is a genus of small catfishes distributed only in coastal basins in southern and south-eastern Brazil, between Rio de Janeiro and Santa Catarina states. Schaefer (1991), in a phylogenetic analysis of the Hypoptopomatinae, did not find any uniquely derived character to diagnose *Pseudotothyris*, and thus questioned its taxonomic validity, suggesting that a more detailed comparative analysis would be necessary to find exclusive diagnostic characters of the genus. Based on this, the present study aimed to perform a phylogenetic analysis and taxonomic revision of the genus, evaluating its specific composition, its monophyly, and its phylogenetic relationships. For this, we performed a phylogenetic analysis with 92 characters observed across 57 terminal taxa, including members of the Delturinae, Loricariinae, Hypostominae, Neoplecostominae, and all valid genera of Hypoptopomatinae. Our results corroborate the monophyly of the genus, which is supported by a uniquely derived synapomorphy: anterior snout odontodes well developed only on dorsal region. As expected and already suggested by other authors, *Pseudotothyris* is recovered as the sister group of *Otothyris*, another genus that occurs in coastal drainages. Additionally, as a result of the taxonomic revision, we present a redescription of the genus and of the two valid species, and the description of a new species.

© 2014 The Linnean Society of London, *Zoological Journal of the Linnean Society*, 2014, 170, 822–874.
doi: 10.1111/zoj.12107

ADDITIONAL KEYWORDS: cascudinhos – catfish – coastal rivers – freshwater – Neotropical region – phylogeny – Siluriformes – taxonomy.

INTRODUCTION

Pseudotothyris Britski & Garavello, 1984, includes two species, *Pseudotothyris obtusa* (Miranda-Ribeiro, 1911) and *Pseudotothyris janeirensis* Britski & Garavello, 1984, which are distributed in coastal drainages of southern and south-eastern Brazil, from Rio de Janeiro to Santa Catarina state. Originally, the genus was characterized by having the tip of the snout formed by small plates bearing poorly

developed odontodes, compound pterotic with large fenestrae, pectoral girdle usually entirely exposed, and abdomen naked or partially covered with small and scattered plates.

Schaefer (1991, 1998) included *Pseudotothyris* within the *Otothyris* and recovered it as the sister to *Otothyris* Myers, 1927, and this clade as sister to *Schizolecis* Britski & Garavello, 1984, two genera also from coastal drainages. Although the author had suggested the absence of subocular plate as a synapomorphy for the genus, he emphasized that uniquely derived characters to diagnose the genus were still lacking.

*Corresponding author. E-mail: fernanda_martins2@hotmail.com

Some years later, Gauger & Buckup (2005) also recovered these three genera as a monophyletic group. However, contrary to Schaefer (1991, 1998), Gauger & Buckup (2005) suggested the absence of the spinelet as a synapomorphy for *Pseudotothyris*, and did not recover the Otothyriini as monophyletic. At the same time, Ribeiro, Carvalho & Melo (2005) described *Otothyropsis* from the upper rio Paraná system, suggesting a close relationship of this new genus and the clade *Pseudotothyris* + *Otothyris*. More recently, Calegari, Lehmann & Reis (2011) described a new species of *Otothyropsis*, but did not recover the genus as closely related to the clade *Pseudotothyris* + *Otothyris*.

Recent molecular phylogenetic analyses are discordant to morphological ones in the position of *Pseudotothyris*. According to Cramer *et al.* (2007) and Cramer, Bonatto & Reis (2011), *Pseudotothyris* is closely related to *Hisonotus francirochai* (Ihering, 1928), whereas *Otothyris* and *Schizolecis* form a monophyletic group. In another hypothesis, Chiachio, Oliveira & Montoya-Burgos (2008) found *Pseudotothyris* as sister to a larger clade that includes species of *Epactionotus* Reis & Schaefer, 1998, *Eurycheilichthys* Reis & Schaefer, 1992, *Hisonotus* Eigenmann & Eigenmann, 1889, *Microlepidogaster* Eigenmann & Eigenmann, 1889, *Otothyris*, *Otothyropsis*, and *Parotocinclus* Eigenmann & Eigenmann, 1889.

Based on this, we present herein the taxonomic review to *Pseudotothyris*, including the redescription of the genus and species, the description of a new species, and a phylogenetic analysis including all species of *Pseudotothyris* and *Otothyris*.

MATERIAL AND METHODS

TAXONOMIC REVIEW

Measurements were performed with digital callipers, point-to-point, on the left side of the specimens and to the nearest 0.1 mm, following Boeseman (1968) with the modifications of Armbruster & Page (1996), Schaefer & Provenzano (1993), Ribeiro *et al.* (2005), and Martins & Langeani (2011a). Morphometric data were expressed as per cent of standard length (SL), except subunits of the head, which were expressed as per cent of head length (HL). Plate counts and nomenclature followed Schaefer (1997), except for 'parietosupraoccipital' instead of 'supraoccipital' (Arratia & Gayet, 1995). Additional counts included: teeth on ceratobranchial 5 and on the upper pharyngeal toothplate. Plates, procurrent rays, vertebrae and teeth on ceratobranchial 5 and on upper pharyngeal toothplate were counted on cleared and stained (c&s) specimens, prepared according to Taylor & Van Dyke (1985). Vertebrae counts included five from the

Weberian apparatus, and the compound caudal centrum was counted as a single element. Dorsal-fin rays include the spinelet as the first unbranched ray. The mode of each count is given in parentheses after the respective count (sometimes the values were bimodal). Sex determination was made based on the presence of dimorphic secondary sexual characters in males, such as the dorsal skin flap on the pelvic-fin spine and the conspicuous papilla after the genital pore.

PHYLOGENETIC ANALYSIS

Sixty-one characters were based on the literature, following Schaefer (1987, 1991, 1998, 2003b), Armbruster (2004), Gauger & Buckup (2005), Lehmann (2006), and Calegari (2010). Thirty-one new characters are proposed here.

We examined 57 terminal taxa representing five Loricariidae subfamilies: Delturinae, Loricariinae, Hypostominae, Neoplecostominae, and Hypoptopomatinae. *Isbrueckeirichthys*, *Kronichthys*, *Pareiorhaphis*, *Pareiorhina*, and *Neoplecostomus* were considered as Neoplecostominae, as suggested by Gosline (1947) and modified by Armbruster (1998, 2004), Montoya-Burgos *et al.* (1998), Armbruster *et al.* (2000), and Reis, Pereira & Armbruster (2006).

The ingroup was composed of the three *Pseudotothyris* species and members of all 19 other valid hypoptopomatine genera in order to test the monophyly and the phylogenetic relationships of the genus amongst the other Hypoptopomatinae. We also included *Nannoplecostomus*, to date a genus of uncertain position within the Loricariidae. As outgroups we included representatives of all Neoplecostominae genera, *Hypostomus careopinnatus* Martins *et al.*, 2012, representing the Hypostominae, *Harttia kronei* Miranda-Ribeiro, 1908, representing the Loricariinae, and *Delturus carinotus* (La Monte, 1933), representing the Delturinae, which was used as the root to the tree.

Missing data were assigned in the matrix by '?' if the character was considered undetermined, and '-' if the character was considered inapplicable.

Phylogenetic analysis was performed using TNT v. 1.1 (Goloboff, Farris & Nixon, 2008). All characters were considered non-additive and received equal weights. To find the most parsimonious tree, we performed a heuristic search using new technology: ratched (with 200 iterations) and drift (with 50 iterations), with random addition sequences, 1000 replicates and maximum retention of 10 000 trees. From the equally parsimonious trees we constructed a strict consensus tree. Bremer support was performed in TNT v. 1.1, using suboptimal trees with up to 20 steps more than the fundamental trees.

INSTITUTIONAL ABBREVIATIONS

All from Brazil except for AMNH and MHNG. AMNH, American Museum of Natural History, New York, NY, USA. DZSJRP, Coleção de Peixes do Departamento de Zoologia e Botânica do Instituto de Biociências, Letras e Ciências Exatas, Universidade Estadual Paulista, São José do Rio Preto, São Paulo; LBP, Laboratório de Biologia de Peixes, Instituto de Biociências, Universidade Estadual Paulista, Botucatu, São Paulo; LIRP, Laboratório de Ictiologia da Universidade de São Paulo, Ribeirão Preto, São Paulo; MCN, Fundação Zoobotânica do Rio Grande do Sul; MCP, Museu de Ciências e Tecnologia da Pontifícia Universidade Católica do Rio Grande do Sul, Porto Alegre; MHNCI, Museu de História Natural Capão da Imbuia, Curitiba, Paraná; MHNG, Muséum d'histoire naturelle, Genève, Switzerland; MNRJ, Museu Nacional do Rio de Janeiro, Rio de Janeiro, Rio de Janeiro; MZUEL, Museu de Zoologia da Universidade Estadual de Londrina, Londrina, Paraná; MZUSP, Museu de Zoologia da Universidade de São Paulo, São Paulo, São Paulo; UFRGS, Departamento de Zoologia da Universidade Federal do Rio Grande do Sul, Porto Alegre, Rio Grande do Sul.

RESULTS

TAXONOMIC REVIEW

PSEUDOTOOTHYRIS BRITSKI & GARAVELLO, 1984

Pseudotothyris Britski & Garavello, 1984: 232 (*Otocinclus obtusus* Miranda-Ribeiro, 1911, type species by original designation) (distribution: coastal rivers of south-eastern Brazil, from Rio de Janeiro to Santa Catarina state); Schaefer, 1997: 41 (identification key); Eschmeyer, 1998: 2099 (catalogue); Schaefer, 2003a: 327 (catalogue); Ferraris, 2007: 290 (catalogue).

Diagnosis: *Pseudotothyris* differs from all other Hypoptopomatinae by having odontodes on anterior region of snout unequal in size, those on dorsal surface well developed, longer and wider than the other on ventral portion, which are more similar to the odontodes on the rest of the head (Fig. 1B) (vs. either small or well-developed odontodes on both surfaces of the snout or well-developed odontodes restricted to ventral portion). Additionally, *Pseudotothyris* can be diagnosed from all hypoptopomatines except *Otothyris* by having the compound pterotic with an elongate posterior extension, easily distinguished from the main body of the bone, its distal portion surpassing the rib of the sixth vertebra [vs. posterior extension absent, or if present never surpassing the rib of the sixth vertebra (Fig. 2)]. *Pseudotothyris* is readily distinguished from *Otothyris* by having 14 branched rays on the caudal fin (vs. 12); abdominal plates, when present, numerous and small (vs. abdomen plates

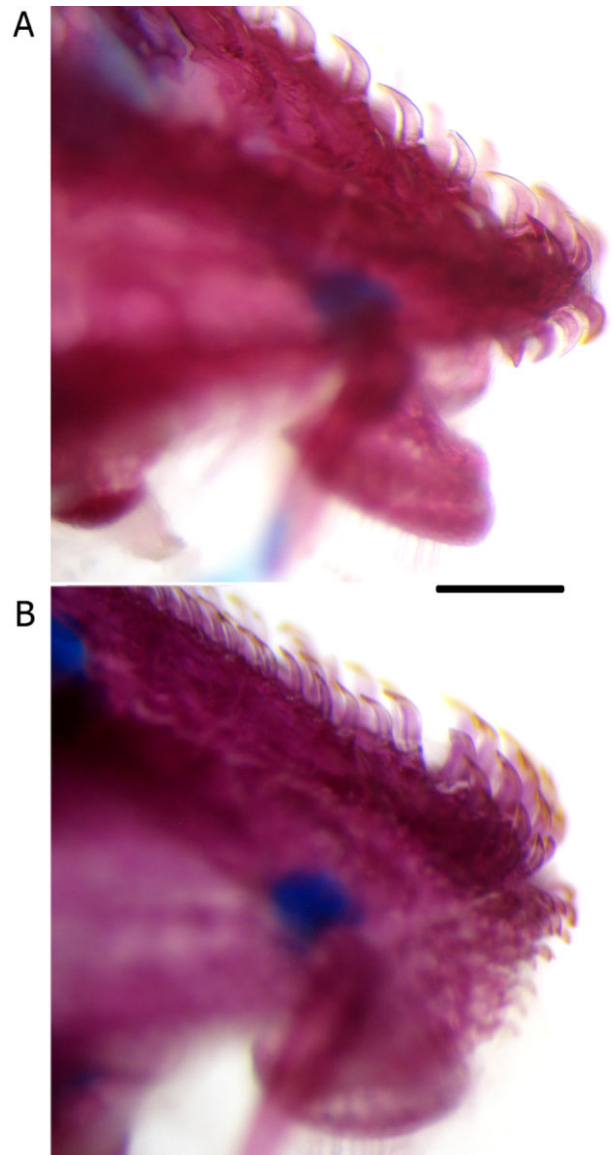


Figure 1. Odontodes at anterior margin of snout. A, *Otothyris lophophanes*, MNRJ 22985, 20.0 mm standard length (SL), female. B, *Pseudotothyris obtusa*, MCP 31726, 24.2 mm SL, female. Scale bar = 0.5 mm.

always present, few and large); anterior portion of snout with four elongate plates (Fig. 3C) [vs. two quadrangular plates (Fig. 3B)]; canal of the second infraorbital present (Fig. 4B) [vs. absent in most specimens (Fig. 4C)]; and mesethmoid extending beyond the condyle, with the anterior portion rounded and narrow (Fig. 5B) [vs. mesethmoid never extending beyond the condyle, the anterior portion truncated and laterally expanded (Fig. 5A)].

Additionally, *Pseudotothyris* can be easily distinguished from *Schizolecis* by having the arrector fossae entirely closed and pectoral girdle often totally

exposed, sometimes with a small median area without odontodes, covered only by skin (vs. arrector fossae partially open and pectoral girdle exposed only laterally); a raised tuft of well-developed odontodes on the parietosupraoccipital in adults (vs. absent); and first pelvic-fin ray with a dorsal fleshy flap in males (vs. absent). Finally, *Pseudotothyris* differs from *Otothyropsis* by having the anterior portion of snout with four elongate plates (vs. a single plate); iris operculum absent (vs. present); and upper pharyngeal toothplate small and rounded, its length less than 50% of the length of ceratobranchial 5 (vs. upper pharyngeal toothplate relatively large and wedge-shaped, its length more than 50% of the length of ceratobranchial 5).

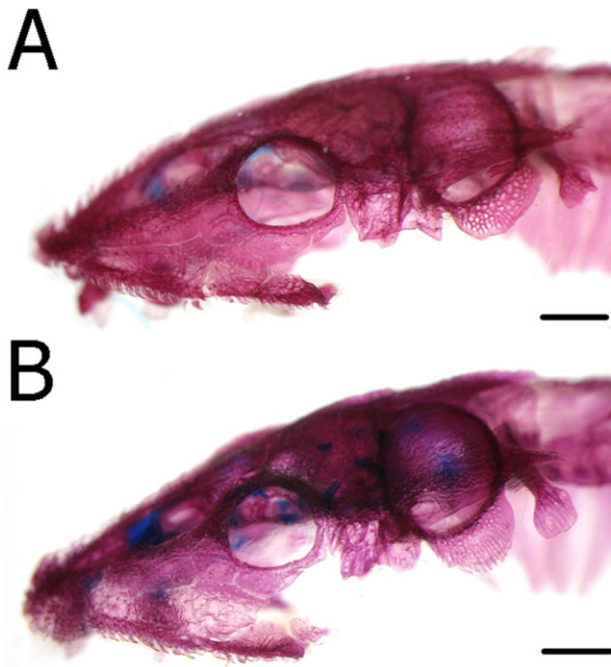


Figure 2. Skull in lateral view (left side, dissected). A, *Otothyris lophophanes*, MNRJ 22985, 20.0 mm standard length (SL), female. B, *Pseudotothyris obtusa*, MCP 31726, 24.2 mm SL, female. Scale bars = 1 mm.

Distribution: *Pseudotothyris* occurs in southern and south-eastern Brazilian coastal drainages, from Rio de Janeiro to Santa Catarina state (Fig. 6). The region includes three subareas as defined by Abell *et al.* (2008): Fluminense (from Rio de Janeiro mountain region, near Macaé, to Santos); Ribeira de Iguape (from Santos to São Paulo and Paraná state limits), and Sudeste Mata Atlântica (from São Paulo and Paraná states' division to Florianópolis). In the transition between Fluminense and Ribeira de Iguape subareas there is a gap in the genus distribution. This region is known to have low richness (Sabino & Castro, 1990; Esteves & Lobón-Cerviá, 2001; Ribeiro *et al.*, 2006), not having many species that are common in neighbouring areas. This is probably related to the geographical formation of the area, which is characterized by a reduced coastal plain, with numerous waterfalls and drainage area reduced, which could decrease the habitat for many species of fishes, including *Pseudotothyris* species.

***PSEUDOTOTHYRIS* *IGNOTA* SP. NOV.**

(FIG. 8; TABLES 1, 2)

Pseudotothyris obtusa non Miranda-Ribeiro, 1911; Britski & Garavello, 1984: 232 (*partim*, material from Paraná and Santa Catarina states); Schaefer, 1991: 8 (fig. 2c, compound pterotic), 39 (examined material to phylogenetic analysis); Schaefer, 1998: 400 (examined material to phylogenetic analysis, *partim*, material from Santa Catarina state).

Material examined

Holotype: Brazil: Santa Catarina: UFRGS 16404 (32.7 mm SL), stream tributary to lago Acaraí, São Francisco do Sul (26°17'33"S, 48°35'21"W), 26.i.2007, L. R. Malabarba, R. Quevedo, V. Bertaco.

Paratypes: Brazil: São Paulo: MZUSP 71836 (3, 28.7–31.8 mm SL), Itapitanga-Ariri road, Cananéia (25°00'36"S, 47°55'12"W), 28.ii.1991, W. Wosiacki col.

KEY TO *PSEUDOTOTHYRIS* SPECIES

- 1A. Dorsal-fin spinelet present; transverse dark saddles on the dorsum absent; subocular cheek plate absent.....
.....*Pseudotothyris janeirensis*
- 1B. Dorsal-fin spinelet absent; three transverse dark saddles on the dorsum; subocular cheek plate generally present.
.....2
- 2A. Anterior margin of snout with an odontode-free band (Fig. 7C); first anal-fin pterygiophore contacting the 12th vertebra; ceratobranchial 5 with 12–15 teeth; upper pharyngeal toothplate with 20–30 teeth.....
.....*Pseudotothyris obtusa*
- 2B. Anterior margin of snout completely covered in odontodes (Fig. 7A); first anal-fin pterygiophore contacting the 13th vertebra; ceratobranchial 5 with 15–31 teeth; upper pharyngeal toothplate with 32–47 teeth.....
.....***Pseudotothyris ignota* sp. nov.**

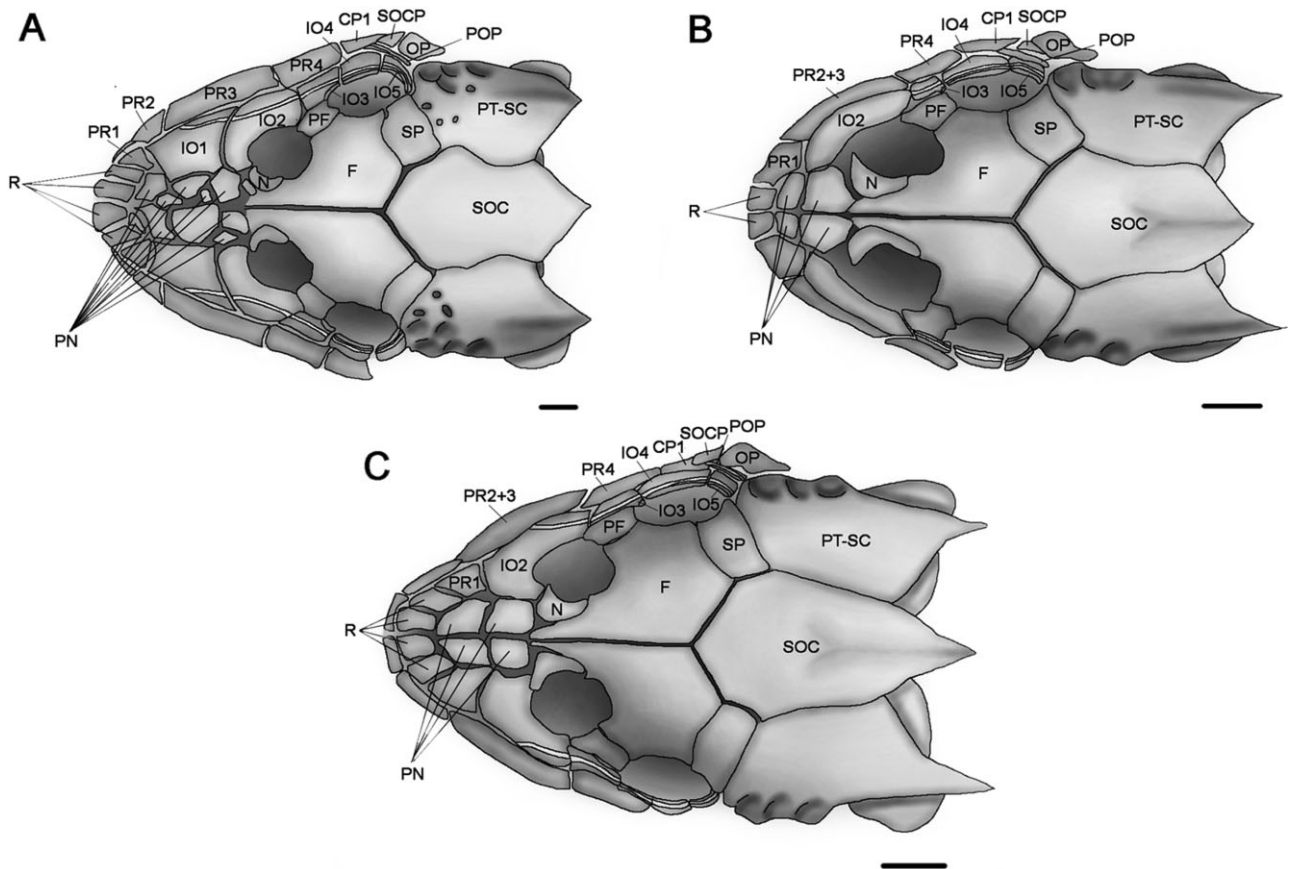


Figure 3. Skull in dorsal view (specimens dissected on the left). A, *Schizolecis guntheri*, DZSJRP 6525, 32.9 mm standard length (SL), male. B, *Otothyris lophophanes*, MNRJ 22958, 20.0 mm SL, sex undetermined. C, *Pseudotothyris obtusa*, MCP 31726, 24.2 mm SL, female. Abbreviations: CP1, canal-bearing plate 1; F, frontal; IO1–6, infraorbitals 1–6; N, nasal; OP, opercle; PF, prefrontal plate; PN, prenasal plates; POP, preopercle; PR1–4, postrostral plate 1–4; PT-SC, compound pterotic; R, rostral plate(s); SOC, parietosupraoccipital; SOCP, subocular cheek plate; SP, sphenotic. Scale bars = 1 mm.

UFRGS 10336 (42 + 2 c&s, 18.6–32.7 mm SL), stream at Km 63 by SP-222 road, Iguape (24°43'48"S, 47°35'55"W), V. Bertaco, F. Carvalho, F. Jerop, A. J. Thomaz. UFRGS 10339 (2, 28.2–29.7 mm SL), stream by the road between Iguape and Icapara (24°39'41"S, 47°25'35"W), V. Bertaco, F. Carvalho, F. Jerop, A. J. Thomaz. Paraná: MCP 18262 (3, 15.6–31.9 mm SL), rio Dois de Fevereiro, Antonina, 14.iii.1995, A. Côrtes, F. Popazoglo, L. F. Duboc. MCP 20030 (5 + 1 c&s, 24.4–30.1 mm SL), artificial canal in Guaraguaçu, Paranaguá, Km 7 by PR-407 road (25°38'S, 48°35'W), 7.ix.1988, P. A. Buckup, E. H. Pereira, P. Azevedo. MCP 27425 (1, 29.6 mm SL), rio Dois de Fevereiro, Paranaguá drainage, Antonina (25°26'S, 48°43'W), 15.xi.2000, F. Popazoglo. MCP 30710 (1, 24.7 mm SL), tributary to rio Nhundiaquara by PR-411 road, Morretes (25°25'20"S, 48°52'29"W), 23.ix.2002, L. R. Malabarba, V. A. Bertaco, M. A. Azevedo. MCP 31731 (1, 21.5 mm SL), tributary to rio Xaxim by PR-340 road, Antonina (25°22'26"S, 48°46'42"W), 23.ix.2002,

L. R. Malabarba, V. A. Bertaco, M. A. Azevedo. MZUSP 24773 (4, 18.6–29.7 mm SL), 5 km from Morretes (25°28'S, 48°48'59"W), 03.xii.1975, P. S. Santos-Filho. MZUSP 42411 (12 + 1 c&s, 20.4–28.2 mm SL), rio Veríssimo, Morro Inglês district, near Paranaguá-Curitiba road, Paranaguá (25°31'S, 48°32'W), 13.ii.1989, A. A. Andreatta, C. Oliveira. Santa Catarina: AMNH 260737 (5, 25.1–31.9 mm SL); DZSJRP 15882 (9 + 1 c&s, 14.3–32.0 mm SL); UFRGS, 9057 (55, 16.2–33.0 mm SL), collected with holotype. DZSJRP 15881 (1 c&s, 28.1 mm SL); MCP 37651 (12, 20.6–31.6 mm SL), tributary to rio Palha, 3 km from SC-406 road, in São João do Rio Vermelho (27°28'59"S, 48°26'14"W), 28.ii.2005, A. Bertaco. MCP 10706 (2, 26.1–26.8 mm SL), rio Canela, Joinville, 24.iv.1985, G. Sato. MCP 31727 (13, 24.9–32.6 mm SL), tributary to rio Miranda at Ilha de São Francisco do Sul, road to Laranjeiras, canal do Linguado (26°19'36"S, 48°39'04"W), 19.ix.2002, L. R. Malabarba, V. A. Bertaco, M. A. Azevedo. MCP 31729

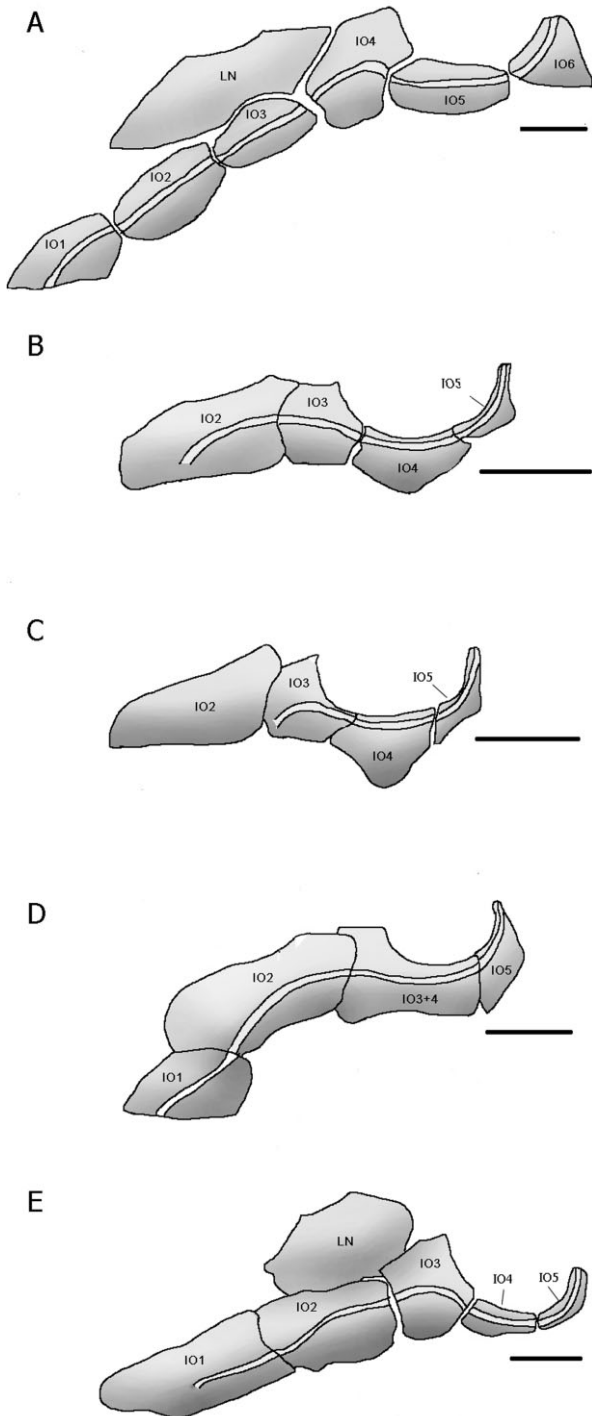


Figure 4. Infraorbital series, lateral view (left side). A, *Isbrueckerichthys duseni*, DZSJRP 13670, 48.3 mm standard length (SL), sex undetermined. B, *Pseudotothyris obtusa*, MCP 31726, 24.2 mm SL, female. C, *Otothyris lophophanes*, MNRJ 22985, 20.0 mm SL, female. D, *Microlepidogaster* sp. nov., MZUSP 95291, 38.1 mm SL, female. E, *Gymnotocinclus anosteos*, UFRGS 11296, 43.7 mm SL, male. Abbreviations: IO1–6, infraorbitals 1–6; LN, lateronasal plate. Scale bars = 1 mm.

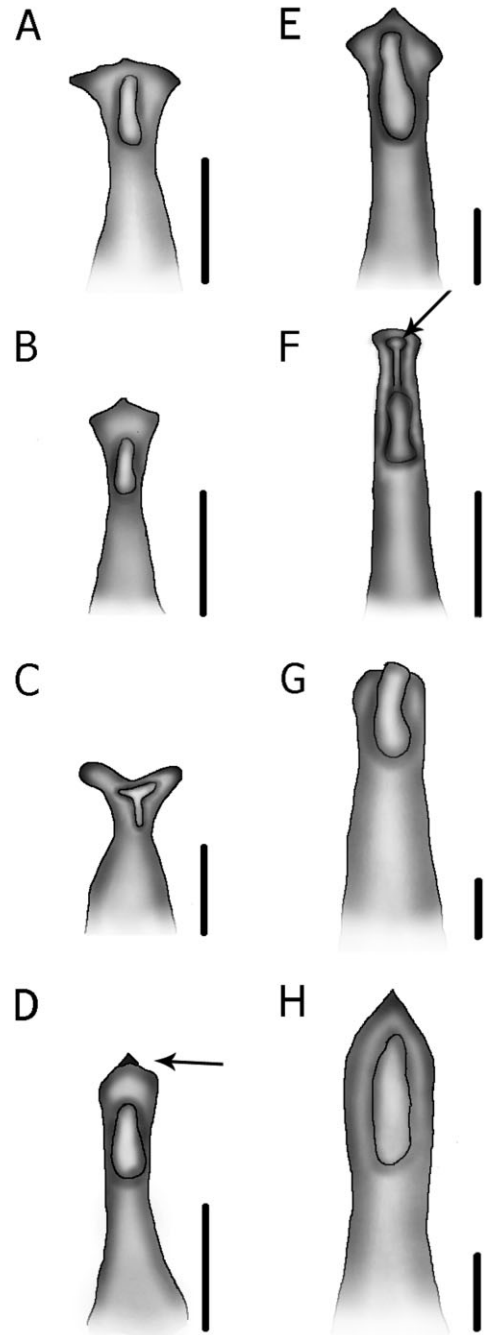


Figure 5. Mesethmoid in ventral view. A, *Otothyris rostrata*, MCN 18943, 23.6 mm standard length (SL), male. B, *Pseudotothyris obtusa*, MCP 31726, 24.2 mm SL, female. C, *Otocinclus affinis*, DZSJRP 7610, 31.5 mm SL. D, *Rhinolekos britskii*, DZSJRP 6983, 36.0 mm SL, female. E, *Pareiorhina rudolphi*, DZSJRP 13713, unmeasured, sex undetermined. F, *Hisonotus notatus*, DZSJRP 13852, 31.5 mm SL, female. G, *Neoplecostomus microps*, DZSJRP 2768, unmeasured, sex undetermined. H, *Isbrueckerichthys duseni*, DZSJRP 13670, 48.3 mm SL, sex undetermined. Arrows showing the cartilaginous process (D), and process anterior to the condyle (F). Scale bars = 1 mm.

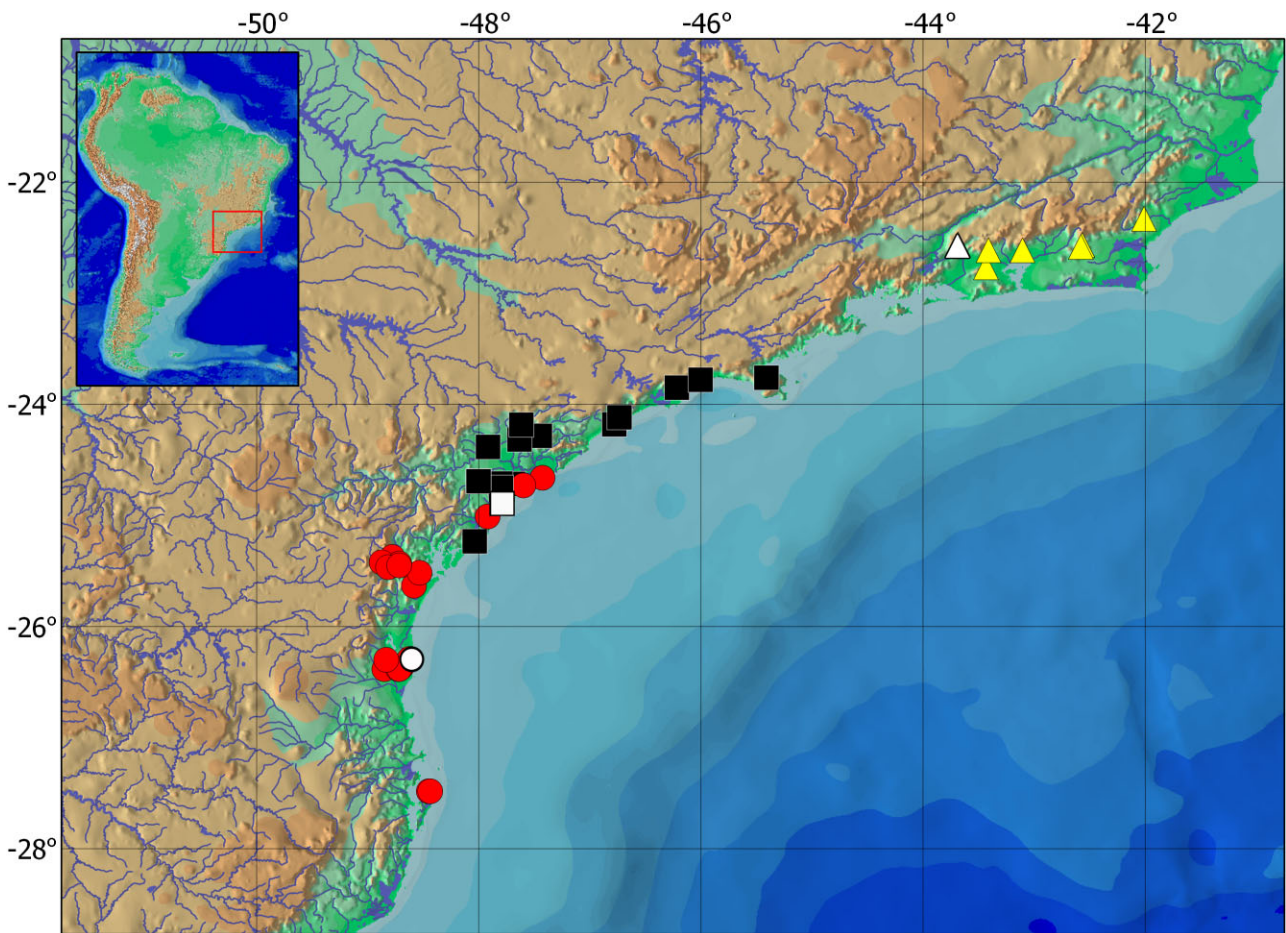


Figure 6. Geographical distribution of *Pseudotothyris* species in southern and south-eastern Brazilian coastal drainages: *Pseudotothyris ignota* sp. nov. (dots), *Pseudotothyris obtusa* (squares), and *Pseudotothyris janeirensis* (triangles). The symbols can represent more than one sampling locality. Open symbols represent type localities.

(17, 22.6–30.8 mm SL), tributary to rio Parati, 1 km from Araquari by BR-280 road (26°22'58"S, 48°43'33"W), 19.ix.2002, L. R. Malabarba, V. A. Bertaco, M. A. Azevedo. MCP 31730 (4, 25.5–29.6 mm SL), tributary to canal do Linguado at Ilha de São Francisco do Sul, Araquari (26°22'8"S, 48°42'4"W), 20.ix.2002, L. R. Malabarba, R. Quevedo, V. A. Bertaco. MCP 37647 (3, 18.5–27.2 mm SL), tributary to rio Palha, 3 km from SC-406 road, in São João do Rio Vermelho, Florianópolis (27°28'59"S, 48°26'14"W), 10.ii.2005, V. A. Bertaco. MZUSP 28997 (11 + 1 c&s, 25.7–29.9 mm SL), rio Zoada tributary to rio Pirai, Joinville (26°22'59"S, 48°50'59"W), 10.i.1985, G. Sato. MZUSP 51010 (6, 22.9–23.4 mm SL), Rio Vermelho, Barra do Sul, Araquari, 23.ix.1977. UFRGS, 9058 (2, 30.0–30.4 mm SL, stream by the road, São Francisco do Sul (26°16'32"S, 48°36'33"W), L. R. Malabarba, R. Quevedo, V. A. Bertaco. UFRGS, 9059 (9, 23.0–29.8 mm SL), rio Ribeiro in

Tapera district, Tapera (48°35'19"S, 26°17'12"W), L. R. Malabarba, R. Quevedo, V. A. Bertaco.

Diagnosis: *Pseudotothyris ignota* differs from all congeners by having the anterior margin of snout with an odontode-free band, (Fig. 7A, D) [vs. the anterior margin of snout completely covered by odontodes (Fig. 7B, C, E, F)]. Additionally, *Pseudotothyris ignota* can be distinguished from *Pseudotothyris obtusa* by having the upper pharyngeal toothplate bearing 32–47 teeth (Fig. 9A) [vs. 20–30 (Fig. 9B, C)]; ceratobranchial 5 bearing 15–31 teeth (Fig. 9A) [vs. 12–15 (Fig. 9B, C)]; first anal-fin pterygiophore contacting the 13th vertebra (vs. 12th); and metapterygoid-hyomandibula suture complete, the bones contacting each other dorsally to the suture (Fig. 10F) [vs. metapterygoid-hyomandibula suture reduced, the bones not contacting each other dorsally to the suture (Fig. 10E)]. Finally, *Pseudotothyris*

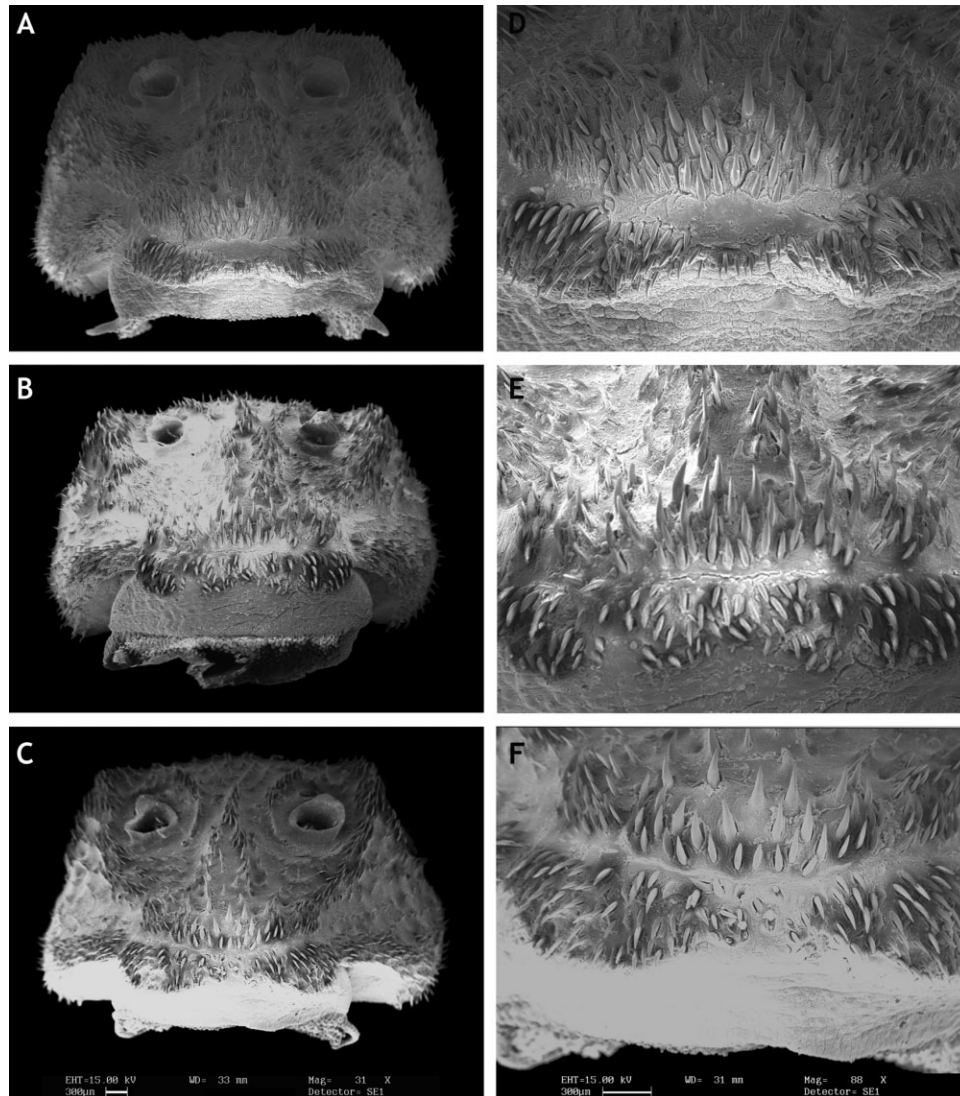


Figure 7. Scanning electron micrographs of snout of *Pseudotothyris ignota* sp. nov., UFRGS 9057, 30.4 mm standard length (SL), female (A, D); *Pseudotothyris janeirensis*, MNRJ 17701, 25.5 mm SL, female (B, E); and *Pseudotothyris obtusa*, MZUSP 53682, 28.3 mm SL, female (C, F).

ignota differs from *Pseudotothyris janeirensis* by having three transverse dark saddles on the dorsum (vs. transverse dark saddles on dorsum absent); spinelet absent [vs. present (Fig. 11A)]; subocular cheek plate generally present [vs. always absent (Fig. 12B)]; and odontodes on lateral plates randomly distributed (vs. odontodes aligned in well-defined series).

Description: Morphometric and meristic data in Tables 1 and 2. Dorsal body profile convex from tip of snout to dorsal-fin origin; descending posteriorly at dorsal-fin base; almost straight from end of dorsal-fin base to caudal-fin origin. Ventral body profile almost straight; ascending at pelvic-fin base; straight to caudal-fin origin. Greatest body depth at

parietosupraoccipital tip. Greatest body width at pectoral girdle, gradually tapering towards snout and caudal fin. Caudal peduncle almost ellipsoid in transverse section. Head deep; compound pterotic and parietosupraoccipital with longitudinal crests; tuft of well-developed odontodes at parietosupraoccipital tip. Anterior margin of snout almost rounded in dorsal view; tip of snout with four elongate plates, their length greater than their width; well-developed odontodes restricted to dorsal portion of snout; other odontodes equal in size and randomly distributed on remainder of head and body, not forming conspicuous rows. Poorly developed keels in median and midventral plate series. Eye small, dorsolaterally placed, not visible in ventral view. Iris operculum



Figure 8. *Pseudotothyris ignota* sp. nov., UFRGS 16404, holotype, 32.7 mm standard length, female, Brazil, Santa Catarina state, São Francisco do Sul municipality, stream to lago Acaraí.

Table 1. Morphometric data for *Pseudotothyris ignota* sp. nov.; holotype (H) and 94 paratypes; range includes holotype

Character	H	Minimum	Maximum	Mean	SD
Standard length (mm)	32.7	18.5	33.0	27.3	–
Per cent of standard length					
Predorsal length	45.7	44.6	50.3	47.3	1.3
Preanal length	61.2	59.1	65.5	62.2	1.4
Prepectoral length	25.0	23.7	29.4	26.3	1.1
Prepelvic length	41.3	38.7	46.6	42.3	1.4
Postanal length	33.7	29.9	36.5	33.4	1.4
Thoracic length	19.3	17.0	21.9	19.3	1.1
Abdominal length	22.0	17.9	23.2	20.3	1.0
Caudal–peduncle depth	9.0	7.9	10.7	9.3	0.6
Head length	37.6	36.0	41.5	38.7	1.2
Cleithral width	25.5	24.5	29.2	26.6	0.9
Base of dorsal fin length	14.2	11.4	14.6	13.0	0.7
Dorsal-fin unbranched ray length	24.0	19.4	25.7	23.2	1.4
Pectoral-fin unbranched ray length	27.5	24.7	31.4	27.6	1.5
Pelvic-fin unbranched ray length	15.8	13.7	20.4	17.1	1.4
Dorsal to anal fin length	24.6	19.8	27.1	23.9	1.1
Snout–opercle length	24.7	22.9	28.9	25.5	1.0
Body depth	19.0	15.2	21.6	19.1	1.5
Per cent of head length					
Head width	66.1	59.8	69.3	64.4	2.0
Head depth	53.7	45.9	56.6	51.2	2.4
Snout length	42.8	40.5	46.4	43.1	1.1
Orbital diameter	15.2	12.4	18.0	15.1	1.0
Interorbital length	37.9	34.0	41.3	38.3	1.5
Maxillary barbel length	3.8	3.1	8.7	5.9	1.3
Prenasal length	28.5	24.0	32.5	27.9	1.6
Internasal length	13.7	8.7	14.1	11.0	1.2
Nasal chamber width	7.7	7.6	13.7	10.5	1.6
Females	–	7.6	10.7	9.3	0.8
Males	–	10.9	13.7	12.2	0.7
Nasal chamber length	13.7	11.1	19.4	14.7	2.1
Suborbital depth	23.0	17.1	25.5	21.6	1.7

SD, standard deviation.

absent. Elongate posterior extension on compound pterotic, forming dorsal part of broad swimbladder opening; large irregular fenestrae on posteroventral margin; infraorbital canal entering infraorbital series via compound pterotic or sphenotic. Parietosupra-occipital forming part of dorsal wall of swimbladder capsule.

Body entirely covered by dermal plates, except on ventral part of head and region overlying opening of swimbladder capsule. Abdomen partially naked, small plates randomly distributed; occasionally totally naked except for lateral abdominal and preanal plates; rarely totally covered by plates; four to six lateral abdominal plates; one to two preanal plates.

Lips oval, papillose; lower lip larger than upper, never reaching pectoral girdle; papillae gradually small to lip edge. Maxillary barbel reduced, free

from oral disk. Teeth slender and bifid; median cusp larger and rounded, lateral smaller and pointed. Premaxillary teeth 14–30 (20). Dentary teeth 9–26 (17). Premaxillary and dentary accessory teeth (according to description in Reis & Schaefer, 1992) present only in juveniles.

Dorsal fin, ii,6–7 (7); originating approximately at vertical through end of pelvic-fin base; tip of adpressed rays reaching or surpassing vertical line passing end of anal-fin base; spinelet absent. Anterior portion of compound supraneural first dorsal-fin proximal radial contacting neural spine of seventh vertebra. Pectoral fin i,5–6 (6); originating immediately behind opercular opening; tip of adpressed rays surpassing vertical through end of pelvic-fin base; well-developed odontodes on unbranched ray, gradually enlarged toward tip. Cleithrum and coracoid totally exposed,

Table 2. Frequency distribution of meristic data for *Pseudotothyris ignota* sp. nov.; holotype and 94 paratypes. Plate (counted on both sides whenever possible), procurrent ray, and vertebrae counts were carried out only for cleared and stained specimens. Holotype values are marked with an asterisk

Character	Frequency distribution	Range	Mode
Dorsal plates	21(1), 23(6), 24(2), 25(2), 26(1)	21–26	23
Mid-dorsal plates	16(5), 17(4), 18(3)	16–18	16
Median plates	21(2), 22(1), 23(3), 24(4)*, 25(2)	21–25	24
Anterior field plates	4(2), 5(7), 6(3)	4–6	5
Gap field plates	1(2), 2(2), 3(2), 4(2), 5(2), 6(2)	1–6	–
Posterior field plates	12(1), 13(2), 14(2), 15(3), 16(3), 17(1)	12–17	15/16
Nonperforated plates at caudal-peduncle end	2(3), 3(6), 4(2), 5(1)	2–5	3
Midventral plates	15(1), 16(5), 17(4), 18(1)	15–18	16
Ventral plates	18(2), 19(3), 20(4), 21(3)	18–21	20
Lateral abdominal plates	4(4), 5(2), 6(4)	4–6	4/6
Premaxillary teeth	14(1), 15(5), 16(4), 17(2), 18(14), 19(9), 20(24), 21(19), 22(18), 23(23), 24(22), 25(12)*, 26(9), 27(7), 28(1), 29(2), 30(1)	14–30	20
Dentary teeth	9(1), 13(3), 14(4), 15(7), 16(12), 17(32), 18(23), 19(21), 20(24), 21(27), 22(13)*, 23(5), 24(2), 25(4), 26(1)	9–26	17
Upper pharyngeal plate teeth	32(1), 35(2), 38(2), 39(1), 40(1), 41(1), 46(1), 47(1)	32–47	35/38
Ceratobranchial 5 teeth	15(1), 18(2), 19(1), 21(1), 23(2), 25(1), 28(1), 31(1)	15–31	18/23
Dorsal-fin branched rays	6(1), 7(94)*	6–7	7
Pectoral-fin branched rays	5(2), 6(93)*	5–6	6
Pelvic-fin unbranched rays	5(95)*	–	5
Anal-fin unbranched rays	5(95)*	–	5
Caudal-fin unbranched rays	13(6), 14(88)*, 15(1)	13–15	14
Dorsal procurrent rays	5(4), 6(2)	5–6	5
Ventral procurrent rays	3(1), 4(2), 5(2), 6(1)	3–6	4/5
Vertebrae	28(3), 29(2)	28–29	28

sometimes a small median area without odontodes, covered only by skin. Arrector fossae partially enclosed by ventral lamina of coracoids in juveniles, opening restricted to a small area near midline; completely closed in adults. Pectoral axillary slit present in juveniles and adults, about 3–4.5 times the orbital diameter, at an angle of 45° with body axis. Pelvic fin i,5; unbranched ray shorter than branched ones. Anal fin i,5; first proximal radial contacting haemal spine of 13th vertebra. Caudal fin i,13–15 (14),i; concave, lobes equal in size; 5–6 (5) dorsal and 3–6 (4/5) ventral procurrent rays. Adipose fin and azygous plates absent. Median lateral plate series 21–25 (24), usually complete from compound pterotic to caudal-fin base; sometimes truncated, ending anteriorly to caudal-fin origin, one to two plates of dorsal and ventral series contacting each other on midline of body; some specimens with single median plate after this truncation. Vertebrae 28–29 (28).

Coloration in alcohol: Ground colour of dorsal surface brown with three dark saddles connecting to a dark longitudinal stripe on lateral body; first bar near end of dorsal-fin base, incomplete at dorsal midline;

second at vertical through end of anal-fin base; third preceding dorsal procurrent rays. Mid-dorsal portion of head to parietosupraoccipital tip dark brown; a clear area between anterior margin of snout to nasal chamber edge. Ventral surface and lateroventral portion of body and head yellowish coloured.

Dorsal-, anal-, pectoral-, and pelvic-fin membranes hyaline. Dorsal- and anal-fin rays with dark bands, sometimes entirely dark; base of rays unpigmented, forming a clear area at dorsal-fin base. Pectoral- and pelvic-fin unbranched rays entirely dark; some specimens with dark bands. Anal-fin base with an anterolateral dark spot. Caudal fin densely pigmented, except for its tip and a circular unpigmented area on each lobe. Procurrent rays region yellowish coloured, sometimes extending to lateral portion of caudal peduncle.

Sexual dimorphism: Males with conspicuous urogenital papilla immediately posterior to anus; expanded flap of skin on dorsal surface of the first pelvic-fin ray; tip of adpressed pelvic fin generally reaching anal-fin origin; nasal chamber wider than in females (10.9–13.7% HL in males; 7.6–10.7% HL in females).

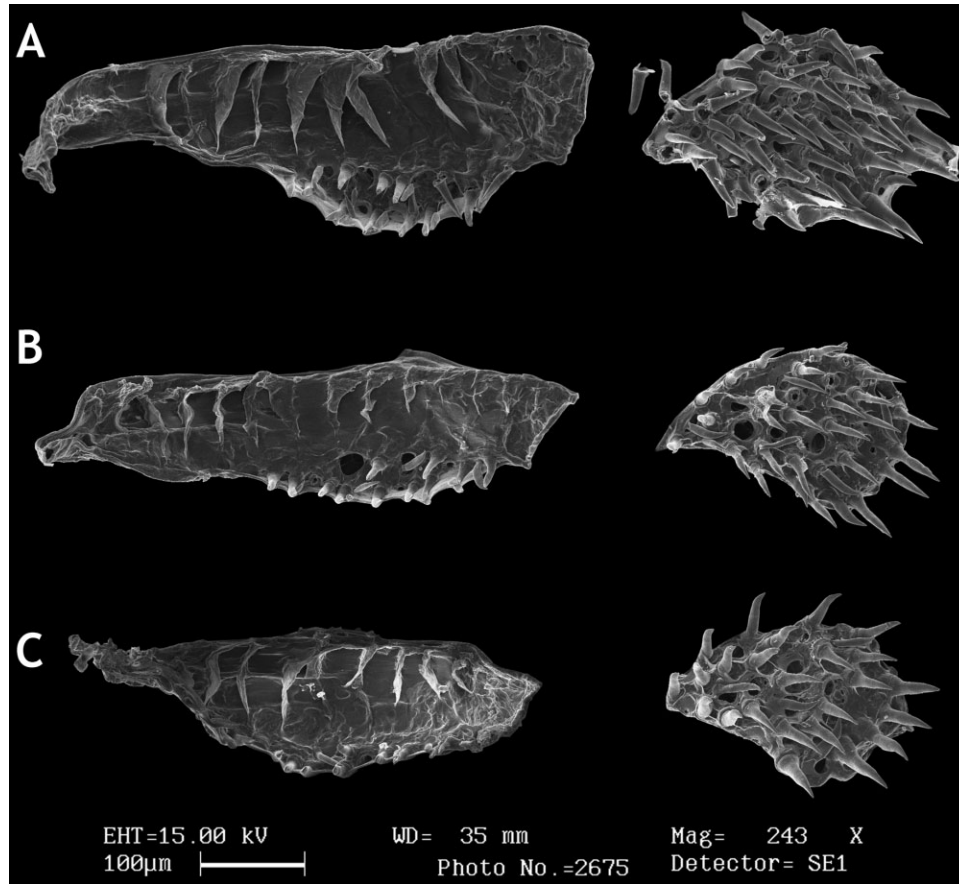


Figure 9. Scanning electron micrographs of ceratobranchial 5 and upper pharyngeal toothplate. A, *Pseudotothyris ignota* sp. nov., MCP 20030, 24.9 mm standard length (SL), female. B, *Pseudotothyris janeirensis*, MZUSP 80211, 24.9 mm SL, female. C, *Pseudotothyris obtusa*, MZUSP 101333, 24.0 mm SL, male.

Distribution: Coastal drainages from Iguape in São Paulo state to São João do Rio Vermelho in Santa Catarina state (Fig. 6). *Pseudotothyris ignota* sp. nov. and *Pseudotothyris obtusa* are sympatric in small coastal drainages in Iguape, Cananéia, and Ilha Comprida, which are adjacent to Ribeira de Iguape basin. This sympatry can be related to changes in sea level, as suggested by Weitzman, Menezes & Weitzman (1988), which recently allowed the dispersion of the two species to this intermediate area after the speciation process. Furthermore, the occurrence of *Pseudotothyris ignota* sp. nov. in coastal drainages and in Florianópolis and São Francisco islands may be associated with a recent separation between these islands and the continent (Milne, Long & Bassett, 2005).

Etymology: The specific epithet is from the Latin *ignotus* meaning unknown or ignored because this species has been identified as *Pseudotothyris obtusa* since the description of the older species in 1911.

PSEUDOTOTHYRIS JANEIRENSIS
BRITSKI & GARAVELLO, 1984
(FIGS 13, 14; TABLES 3, 4)

Pseudotothyris janeirensis Britski & Garavello, 1984: 234, 235, figs 9, 10 (photographs) [original description; type locality: Rio dos Macacos, Represa (açude) Engenho da Serra, [Engenheiro] Paulo de Frontin, Rio de Janeiro]; Eschmeyer, 1998: 800 (catalogue); Schaefer, 2003a: 327 (catalogue); Reis & Carvalho, 2007: 87 (catalogue); Ferraris, 2007: 290 (catalogue).

Material examined

All from Brazil: Rio de Janeiro state: holotype. MNRJ 10278 (33.9 mm SL), rio dos Macacos, Represa Engenho da Serra, Engenheiro Paulo de Frontin, H. Valle, 29.vi.1946. Paratypes. MNRJ 4707 (19 of 114 + 1 c&s, 16.7–33.6 mm SL); MNRJ 10283 (1, 28.3 mm SL); MNRJ 10280 (1, 30.3 mm SL); MNRJ 10289 (1, 32.3 mm SL); MNRJ 10286 (1, 29.9 mm SL); MNRJ 10293 (1, 32.2 mm SL), same data for

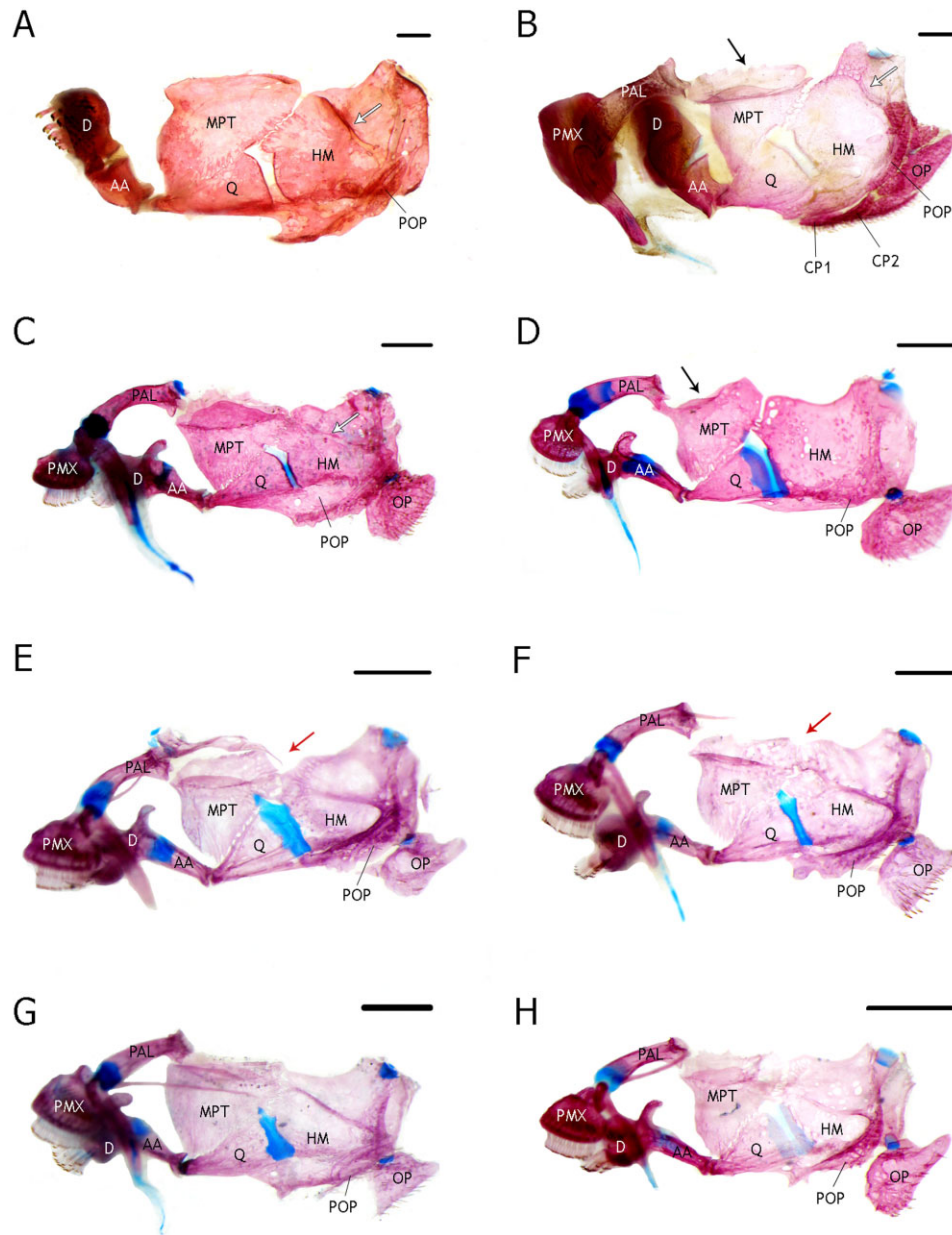


Figure 10. Suspensorium, lateral view (left side). A, *Neoplecostomus microps*, DZSJRP 2768, unmeasured, sex undetermined. B, *Isbrueckerichthys duseni*, DZSJRP 13670, 48.3 mm standard length (SL), sex undetermined. C, *Rhinolekos schaeferi*, DZSJRP 12192, 36.5 mm SL, sex undetermined. D, *Otocinclus affinis*, DZSJRP 7610, 31.5 mm SL, sex undetermined. E, *Pseudotothyris obtusa*, MCP 31726, 24.2 mm SL, female. F, *Pseudotothyris ignota* sp. nov., UFRGS 9057, 32.0 mm SL, female. G, *Schizolecis guntheri*, DZSJRP 6525, 32.9 mm SL, male. H, *Otothyris travassosi*, MNRJ 22947, 22.3 mm SL, female. Arrows show the metapterygoid channel and levator arcus palatine crest (A, B, C, D), and metapterygoid–hyomandibula suture (E, F). Abbreviations: AA, compound anguloarticular; CP1, 2, canal-bearing plate 1, 2; D, dentary; HM, hyomandibula; MPT, metapterygoid; OP, opercle; PAL, palatine; PMX, premaxilla; POP, preopercle; Q, quadrate. Scale bars = 1 mm.

holotype. MNRJ 5925 (1, 28.1 mm SL), rio da Taquara, Caxias, A. Passarelli-Filho. MNRJ 10066 (1, 23.8 mm SL), Tinguá. Nontypes. Additional material: Brazil: Rio de Janeiro: DZSJRP 12512 (2, 22.2–28.6 mm SP), rio Guandú drainage,

Engenheiro Paulo de Frontin-Paracambi (22°34'10"S, 43°41'24"W), 22.v.2010. DZSJRP 12518 (5 + 1 c&s, 22.0–33.0 mm SL), stream by road near the city, rio Guandú drainage, Engenheiro Paulo de Frontin (22°33'41"S, 43°41'8"W), 22.v.2010. DZSJRP 13846

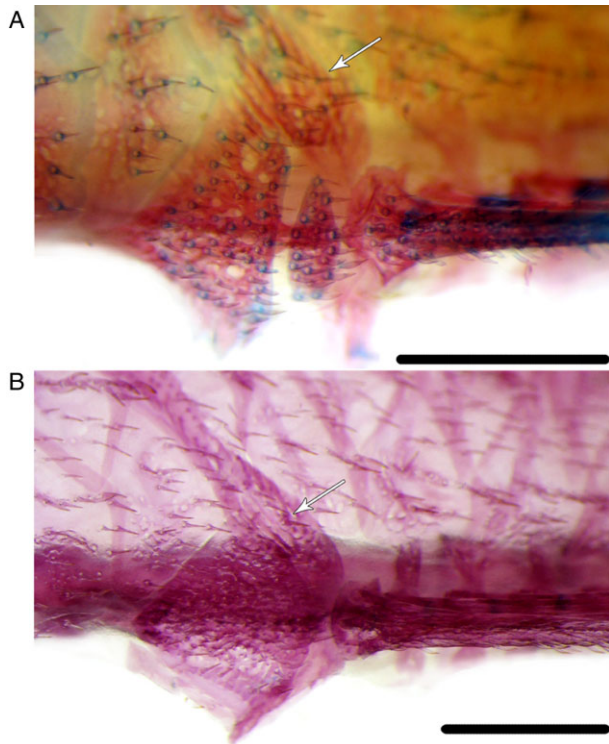


Figure 11. Dorsal-fin insertion in dorsal view. A, *Pseudotothyris janeirensis*, DZSJRP 12518, 23.1 mm standard length (SL), female. B, *Pseudotothyris obtusa*, MCP 31726, 24.2 mm SL, female. Arrows show the transverse process of first dorsal-fin pterygiophore exposed and bearing odontodes. Scale bars = 1 mm.

(3, 13.0–31.0 mm SL), tributary to rio São João, in Gaviões district, Silva Jardim (22°34'59"S, 42°34'44"W), 31.v.2011. MNRJ 10941 (4, 24.2–27.0 mm SL), tributary to rio Macaé, Macaé (22°19'50"S, 42°0'38"W), 01.xi.1981. MNRJ 11222 (15 of 25, 18.3–27.1 mm SL), tributary to rio Macaé, Macaé (22°19'50"S, 42°0'38"W), 20.vii.1980. MNRJ 17701 (14, 21.2–27.8 mm SL), rio Suruí, Magé (22°36'49"S, 43°6'16"W), 6.viii.1998. MNRJ 24377 (3, 25.7–30.2 mm SL), rio Barreiras BR-111 road (= rio Ana Felícia), tributary to rio Tinguá, rio Iguaçu drainage, Nova Iguaçu (22°36'48"S, 43°24'39"W), 23.iv.2002. MNRJ 26650 (4, 13.7–28.4 mm SL), tributary to rio Guapiaçu at fazenda São José de Guapiaçu, Cachoeiras de Macacu, 15.iv.2004. MZUSP 37938 (1, 23.6 mm SL), Tinguá, Nova Iguaçu (22°45'59"S, 43°26'00"W), 23.ix.1979. MZUSP 80211 (5, 22.0–26.3 mm SL), rio São João, 17.5 km from Boqueirão-Jupuiba road, in Gaviões district, Silva Jardim (22°34'00"S, 42°33'59"W), 12.x.2002. MZUSP 80213 (2, 21.7–22.4 mm SL), tributary to rio São João, 30 km from Boqueirão-Jupuiba road, in Gaviões district, Silva Jardim (22°34'00"S, 42°33'59"W), 12.x.2002.

Diagnosis: *Pseudotothyris janeirensis* differs from all congeners by having dorsal-fin spinelet (Fig. 11A) [vs. absent (Fig. 11B)]; transverse dark saddles on the dorsum absent (vs. present); subocular cheek plate always absent (Fig. 12B) [vs. generally present (Fig. 12A)]; and odontodes on lateral plates aligned in well-defined series (vs. randomly distributed).

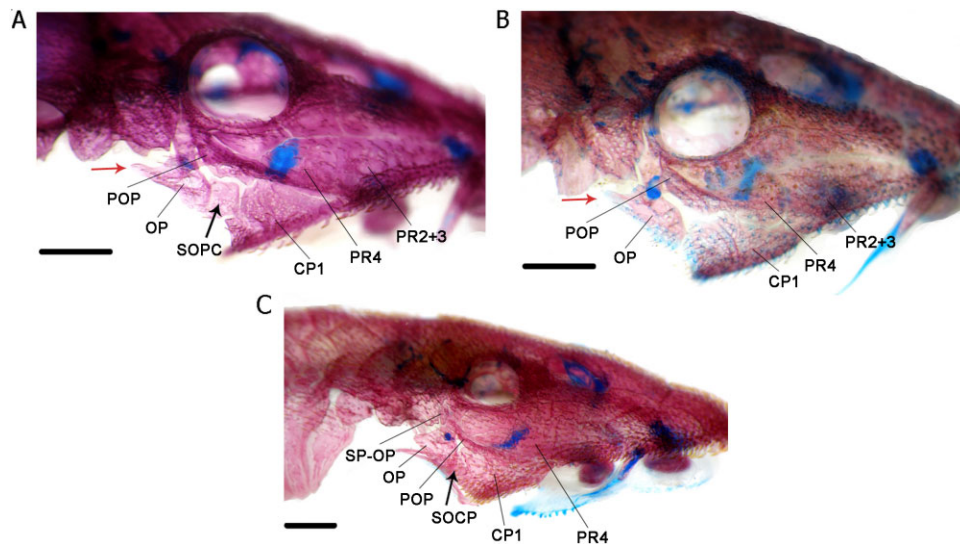


Figure 12. Skull in lateral view (right side). A, *Pseudotothyris obtusa*, MCP 31726, 24.2 mm standard length (SL), female. B, *Pseudotothyris janeirensis*, DZSJRP 12518, 23.1 mm SL, female. C, *Hisonotus piraicanjuba*, DZSJRP 13233, 23.7 mm SL, female. Arrows show the subocular cheek plate, and posterior extension of opercle. Abbreviations: CP1, canal-bearing plate 1; OP, opercle; POP, preopercle; PR2–4, postrostral plate 2–4; SOCP, subocular cheek plate; SP-OP, suprapreopercle. Scale bars = 1 mm.



Figure 13. *Pseudotothyris janeirensis*, DZSJRP 12518, 33.0 mm standard length, female, Brazil, Rio de Janeiro state, Engenheiro Paulo de Frontin municipality, rio Guandú drainage.



Figure 14. *Pseudotothyris janeirensis*, MNRJ 10278, holotype, 33.9 mm standard length, female, Brazil, Rio de Janeiro state, Engenheiro Paulo de Frontin municipality, rio Guandú drainage.

Additionally, *Pseudotothyris janeirensis* can be distinguished from *Pseudotothyris obtusa* by having abdomen almost entirely naked, except for one to three lateral abdominal plates and one to two preanal plates (vs. abdomen partially or totally covered by scattered plates); upper pharyngeal toothplate bearing 31–35 teeth (Fig. 9B) [vs. 20–30 (Fig. 9A, C)]; and ceratobranchial 5 bearing 18–23 teeth (Fig. 9B) [vs. 12–15 (Fig. 9A, C)]. Finally, *Pseudotothyris janeirensis* differs from *Pseudotothyris ignota* by having the anterior margin of snout completely covered by odontodes (Fig. 7B, E) [vs. anterior margin of snout with an odontode-free band (Fig. 7A, D)].

Description: Morphometric and meristic data in Tables 3 and 4. Dorsal body profile convex from tip of snout to dorsal-fin origin; descending posteriorly at dorsal-fin base; almost straight from end of dorsal-fin base to caudal-fin origin. Ventral body profile almost straight; ascending at pelvic-fin base; straight to caudal-fin origin. Greatest body depth variable, at dorsal-fin origin or at parietosupraoccipital tip. Greatest body width at pectoral girdle, gradually tapering towards snout and caudal fin. Caudal peduncle almost ellipsoid in transverse section. Head deep; compound pterotic and parietosupraoccipital with longitudinal crests; tuft of well-developed odontodes at parietosupraoccipital tip. Anterior margin of snout

rounded to slightly pointed in dorsal view; tip of snout with four elongate plates, their length greater than their width; well-developed odontodes restricted to dorsal portion of snout; other odontodes equal in size on remainder of head, and forming well-defined rows on body. Poorly developed keels in median and midventral plate series. Eye small, dorsolaterally placed, not visible in ventral view. Iris operculum absent. Elongate posterior extension on compound pterotic, forming dorsal part of broad swimbladder opening; large irregular fenestrae on posteroventral margin; infraorbital canal entering infraorbital series generally via compound pterotic, occasionally via sphenotic. Parietosupraoccipital forming part of dorsal wall of swimbladder capsule.

Body entirely covered by dermal plates, except on ventral part of head and region overlying opening of swimbladder capsule. Abdomen almost naked, except for one to three lateral abdominal plates and one to two preanal plates.

Lips oval, papillose; lower lip larger than upper, never reaching pectoral girdle; papillae gradually small and more spaced to lip edge. Maxillary barbel reduced, free from oral disk. Teeth slender and bifid; median cusp larger and rounded, lateral smaller and pointed. Premaxillary teeth 7–30 (23). Dentary teeth 7–27 (19/20). Premaxillary and dentary accessory teeth present only in juveniles.

Dorsal fin, ii,6–7 (7); originating approximately at vertical through end of pelvic-fin base; tip of adpressed rays reaching or surpassing vertical line passing end of anal-fin base; spinelet small, ellipsoid to rectangular; locking mechanism nonfunctional. Anterior portion of compound supraneural first dorsal-fin proximal radial contacting neural spine of seventh vertebra. Pectoral fin i,5–7 (6); originating immediately behind opercular opening; tip of adpressed rays surpassing vertical through end of pelvic-fin base; well-developed odontodes on unbranched ray, gradually enlarged toward tip. Cleithrum and coracoid totally exposed, sometimes a small median area without odontodes, covered only by skin. Arrector fossae partially enclosed by ventral lamina of coracoids in juveniles, opening restricted to a small area near midline; completely closed in adults. Pectoral axillary slit present in juveniles and adults, about 2–2.5 times the orbital diameter, at an angle of 45° with body axis. Pelvic fin i,5; unbranched ray shorter than branched ones. Anal fin i,4–5 (5); first proximal radial contacting haemal spine of 12th or 13th vertebra. Caudal fin i,13–14 (14),i; concave, lobes equal in size; five to six dorsal and four to six ventral procurrent rays. Adipose fin and azygous plates absent. Median lateral plate series 18–24, usually complete from compound pterotic to caudal-fin base; sometimes truncated, ending anteriorly to caudal-fin origin, one to two plates of dorsal and

Table 3. Morphometric data for *Pseudotothyris janeirensis*; holotype (H), ten paratypes, and 53 nontype specimens

Character	H	Paratypes				Types and nontypes			
		Minimum	Maximum	Mean	SD	Minimum	Maximum	Mean	SD
Standard length (mm)	33.9	28.34	32.34	30.0	–	21.2	33.9	36.3	–
Per cent of standard length									
Predorsal length	47.4	45.4	49.6	46.7	1.4	45.4	51.4	48.1	1.4
Preanal length	63.0	57.6	63.4	61.0	1.7	57.6	66.2	62.3	1.9
Prepectoral length	26.0	24.8	27.3	25.9	0.8	24.7	28.7	26.5	0.9
Prepelvic length	42.7	39.6	42.7	41.2	0.9	39.2	44.5	42.1	1.3
Postanal length	32.6	32.5	36.2	34.2	1.2	31.0	36.3	33.8	1.4
Thoracic length	21.4	18.9	21.9	20.5	0.9	16.5	21.9	18.8	1.4
Abdominal length	22.0	18.9	21.1	20.0	0.7	17.5	23.5	20.3	1.2
Caudal-peduncle depth	9.9	9.1	10.3	9.6	0.3	8.2	10.3	9.4	0.5
Head length	37.0	34.9	38.2	36.5	1.0	34.9	41.2	38.1	1.3
Cleithral width	29.7	26.5	31.7	28.2	1.5	26.0	31.7	27.8	1.0
Base of dorsal fin length	13.8	12.5	14.8	13.5	0.8	11.2	14.8	13.0	0.9
Dorsal-fin unbranched ray length	–	22.1	25.1	23.4	1.3	18.5	27.4	23.1	1.6
Pectoral-fin unbranched ray length	28.3	26.5	28.8	27.8	0.7	24.5	32.1	27.7	1.4
Pelvic-fin unbranched ray length	16.3	15.9	18.8	17.5	1.1	14.7	20.2	17.3	1.3
Dorsal to anal fin length	26.1	22.8	28.0	24.9	1.4	22.8	28.0	24.6	0.9
Snout–opercle length	24.8	23.7	25.2	24.6	0.6	23.7	28.6	26.0	1.1
Body depth	20.0	18.0	21.1	19.7	1.1	16.7	22.9	19.8	1.3
Per cent of head length									
Head width	67.4	66.7	70.3	68.6	1.3	60.4	73.6	66.9	2.1
Head depth	55.3	51.8	58.1	54.3	1.8	47.5	58.1	52.0	2.2
Snout length	44.9	44.5	47.8	46.0	1.2	43.7	48.7	45.9	1.1
Orbital diameter	13.6	14.2	17.6	16.4	1.2	12.5	19.7	15.5	1.6
Interorbital length	39.6	38.4	42.2	39.7	1.2	34.5	45.1	39.7	2.0
Maxillary barbel length	5.2	3.1	6.0	4.6	1.3	2.7	8.1	5.6	1.2
Prenasal length	29.3	26.3	30.7	28.2	1.3	26.3	32.0	29.3	1.4
Internasal length	10.2	11.1	13.2	12.3	0.7	8.4	13.9	11.5	1.1
Nasal chamber width	9.6	9.0	12.4	10.1	0.9	6.7	13.8	9.6	1.4
Females	–	9.9	10.6	10.2	0.5	6.7	10.6	8.9	0.8
Males	–	9.0	10.5	9.7	0.5	7.5	12.8	10.5	1.2
Nasal chamber length	15.6	13.8	17.5	15.8	1.2	9.4	18.9	14.9	2.0
Suborbital depth	25.2	21.4	25.0	23.0	1.3	17.1	25.2	21.6	1.7

SD, standard deviation.

ventral series contacting each other on midline of body; zero to three nonperforated plates near caudal-fin origin. Vertebrae 28.

Coloration in alcohol: Ground colour of dorsal surface brown. Dorsal portion of head until parietosupra-occipital tip dark brown; a clear area between anterior margin of snout to nasal chamber edge. Lateral portion of body brown, with a dark longitudinal stripe from compound pterotic to caudal-fin origin, sometimes inconspicuous posterior to dorsal fin. Ventral surface and lateroventral portion of body and head yellowish coloured.

Dorsal-, anal-, pectoral-, and pelvic-fin membranes hyaline; rays weakly pigmented; some specimens

with transverse bands, more evident on dorsal fin and first pectoral-fin ray. Anal-fin base with an anterolateral dark spot. Caudal fin densely pigmented, except for its tip and a circular unpigmented area on each lobe. Procurrent rays circular yellowish coloured, sometimes extending to lateral portion of caudal peduncle.

Sexual dimorphism: Males with conspicuous urogenital papilla immediately posterior to anus; expanded flap of skin on dorsal surface of the first pelvic-fin ray; tip of adpressed pelvic fin generally reaching anal-fin origin; nasal chamber frequently wider than in females [7.5–12.8% HL (mean 10.5%) in males; 6.7–10.6% HL (mean 8.9%) in females].

Table 4. Frequency distribution of meristic data for *Pseudotothyris janeirensis*; holotype, ten paratypes, and 53 nontype specimens. Plate (counted on both sides whenever possible), procurent ray, and vertebrae counts were carried out only for cleared and stained specimens. Holotype values are marked with an asterisk

Character	Frequency distribution	Range	Mode
Dorsal plates	22(1), 23(3)	22–23	23
Mid-dorsal plates	11(1), 13(1), 15(2)	11–15	15
Median plates	18(1), 20(1), 23(1), 24(1)	18–24	18/20/23/24
Anterior field plates	4(1), 5(1), 6(2)	4–6	6
Gap field plates	2(2), 4(2)	2–4	2/4
Posterior field plates	10(1), 11(1), 15(1), 16(1)	15–16	10/11/15/16
Nonperforated plates at caudal-peduncle end	0(2), 2(1), 3(1)	0–3	0
Midventral plates	13(1), 14(1), 17(1) 18(1)	13–18	13/14/17/18
Ventral plates	18(3), 20(1)	18–20	18
Lateral abdominal plates	1(4), 2(7), 3(6), 4(5)	1–5	2
Premaxillary teeth	7(2), 13(1), 16(1), 17(1), 18(2), 19(2), 20(5), 21(7), 22(13), 23(17), 24(12), 25(11), 26(10), 27(7), 28(2), 29(1), 30(3)	7–30	23
Dentary teeth	7(1), 8(1), 9(1), 10(1), 14 (1), 16(4), 17(10)*, 18(13), 19(17), 20(17), 21(15), 22(5), 23(8), 24(3), 26(1), 27(1)	7–27	19–20
Upper pharyngeal plate teeth	31(1), 34 (1), 35(1), 36(1)	31–36	31/34/35/36
Ceratobranchial 5 teeth	18(3), 23(1)	18–23	18
Dorsal-fin branched rays	6(1), 7(62)*, 8(1)	6–8	7
Pectoral-fin branched rays	5(2), 6(60)*, 7(2)	5–7	6
Pelvic-fin unbranched rays	5(63)*, 6(1)	5–6	5
Anal-fin unbranched rays	4(2), 5(62)*	4–5	5
Caudal-fin unbranched rays	13(3), 14(60)*	13–14	14
Dorsal procurent rays	5(1), 6(1)	5–6	5/6
Ventral procurent rays	4(1), 6(1)	4–6	4/6
Vertebrae	28(2)	–	28

Distribution: Restricted to coastal drainages in Rio de Janeiro state, from Engenheiro Paulo de Frontin to Macaé (Fig. 6).

Comments: Based on the original registration data, the type specimens of *Pseudotothyris janeirensis* were sampled in a lentic environment, regionally called *açude*, a kind of water reservoir. It is not common for *Pseudotothyris*, and for the majority of other Hypoptopomatinae species, to occur in this kind of habitat. *Pseudotothyris* species prefer habitats characterized by a moderate to rapid flow, rich in marginal vegetation.

PSEUDOTOTHYRIS OBTUSA (MIRANDA-RIBEIRO, 1911)
(FIGS 15, 16; TABLES 5, 6)

Otocinclus obtusus Miranda-Ribeiro, 1911: 91 (identification key), 95 (original description; type locality: originally unknown), 497 (index); Gosline, 1945:100 (catalogue); Miranda-Ribeiro, 1953: 401 (designation of types); Fowler, 1954:131 (catalogue).

Otocinclus obtusos (lapsus): Miranda-Ribeiro, 1911: 95 (name preceding description), 498 (index).

Pseudotothyris obtusa: Britski & Garavello, 1984: 232–235, figs 7, 8 (photographs) (holotype; *partim* material examined from São Paulo state; recombination in *Pseudotothyris*); Eschmeyer, 1998: 1218 (catalogue); Schaefer, 2003a: 327 (catalogue); Reis & Carvalho, 2007: 87 (catalogue); Ferraris, 2007: 290 (catalogue).

Holotype: Brazil: unknown locality [Atlantic South America; as written on the label of the holotype]: MNRJ 1026, specimen lost.

Material examined

All from Brazil: Neotype. São Paulo state: MZUSP 79939 (30.2 mm SL), Fonte Grande, seedling nursery, Pedrinhas, Ilha Comprida (24°53'56"S, 47°47'49"W), Oyakawa *et al.*, 07.xii.2002. Present designation. Nontypes. DZSJRP 2298 (3, 19.6–31.9 mm SL), S.E.A.R.A. farm, stream inside the forest, Jacupiranga, 23.viii.1985. DZSJRP 3141 (1, 22.4 mm



Figure 15. *Pseudotothyris obtusa*, MZUSP 79939, 30.2 mm standard length, female, Brazil, São Paulo state, Ilha Comprida municipality, rio Ribeira de Iguape drainage.

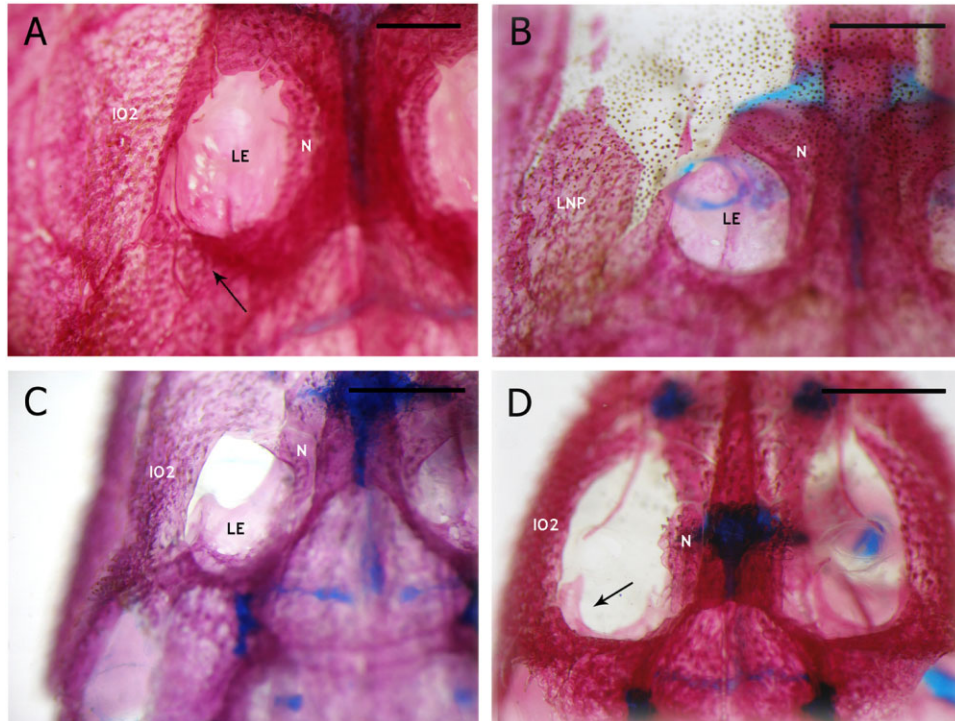


Figure 16. Nasal capsule in dorsal view. A, completely closed, *Neoplecostomus microps*, DZSJRP 2144, 62.8 mm standard length (SL), female. B, completely closed, *Gymnotocinclus anosteos*, UFRGS 11296, 43.7 mm SL, male. C, partially closed, *Schizolecis guntheri*, DZSJRP 6525, 32.9 mm SL. D, partially closed, *Otothyropsis* sp. nov., DZSJRP 2907. Arrows show exposed lateral ethmoid (A), and the lateral ethmoid surrounding less than 50% of nasal capsule (D). Abbreviations: IO2, infraorbital 2; LE, lateral ethmoid; LNP, lateronasal plate; N, nasal. Scale bars = 1 mm.

SL), rio Jacupiranga, Jacupiranga, 19.viii.1985. DZSJRP 3152 (5 + 1 c&s, 24.1–30.1 mm SL), S.E.A.R.A. farm, stream inside the forest, Jacupiranga, 16.viii.1985. DZSJRP 3163 (4, 21.4–27.3 mm SL), Sombrio-Moreira farm, unnamed stream, Jacupiranga, 14.viii.1985. DZSJRP 3199 (8, 20.0–30.7 mm SL), S.E.A.R.A farm, Km 467 by BR-116 road, Pariquera-Açu, 7.x.1987. MCP 12237 (4, 16.8–20.0 mm SL), stream by SP-079 road to Tapirai, tributary to rio Juquiá (24°11'S, 47°37'W), 27.vii.1988. MZUSP 69411 (7 + 1 c&s, 23.7–28.4 mm SL), ribeirão Poço Grande on SP-079, 15 km from Juquiá, Juquiá (25°15'14"S, 47°37'12"W), 14.v.2001. MZUSP 70017 (6, 22.5–29.4 mm SL), stream by dirt road to Parque Estadual Campina do Encantado, about 5 km from road to Iguape, Pariquera-Açu (24°24'47"S, 47°48'17"W), 15.iv.2001. MZUSP 79658 (1, 23.3 mm SL), tributary to rio São Lourenço, Oliveira Barros, Miracatu (24°16'59"S, 47°27'00"W), 30.i.1988. MZUSP 83024 (15 of 117, 19.1–25.8 mm SL), tributary to rio Momuna, near Momuna district, Iguape (24°42'57"S, 47°41'27"W), 28.v.2003. MZUSP 101333 (8 + 1 c&s, 21.5–27.3 mm SL), Sete Barras. UFRGS, 10180 (8, 24.3–31.6 mm SL), Km 208 by Rio-Santos road, tributary to rio Vermelho (23°46'46"S,

46°00'11"W). Additional drainages: MCP 31726 (6 + 1 c&s, 20.3–27.2 mm SL), 3 km from the SP-055 road, Mongaguá (24°7'1"S, 46°43'58"W), 21.ix.2002. MZUSP 42401 (16, 17.3–28.4 mm SL), Itanhaém (24°10'48"S, 46°46'48"W). MZUSP 53682 (13, 23.9–29.1 mm SL), stream at Km 28 by Rio-Santos road, Bertioga (23°51'S, 46°13'W), 01.v.1998. MZUSP 53686 (5, 19.2–25.1 mm SL), tributary to rio Una, Barra do Una beach, Km 182 by Rio-Santos road, São Sebastião (23°45'36"S, 45°24'36"W), 29.i.1998. MZUSP 110995 (14, 15.3–29.9 mm SL), collected with neotype. Paraná: MCP 26026 (4, 24.4–30.1 mm SL), Barra do rio Ararapira, ilha do Superagüi, Guaraqueçaba (25°14'1"S, 48°2'16"W), 30.viii.1991.

Diagnosis: *Pseudotothyris obtusa* differs from all congeners by having the upper pharyngeal toothplate bearing 20–30 teeth (Fig. 9C) [vs. 32–47 in *Pseudotothyris ignota* (Fig. 9A), 31–36 in *Pseudotothyris janeirensis* (Fig. 9B)]; ceratobranchial 5 bearing 12–15 teeth (Fig. 9C) [vs. 15–31 in *Pseudotothyris ignota* (Fig. 9A), 18–23 in *Pseudotothyris janeirensis* (Fig. 9B)]. Additionally, *Pseudotothyris obtusa* can be distinguished from *Pseudotothyris ignota* by having the anterior margin of snout completely covered by

Table 5. Morphometric data for *Pseudotothyris obtusa*; neotype (N) and 85 nontype specimens; range includes neotype

Character	N	Minimum	Maximum	Mean	SD
Standard length (mm)	30.2	16.8	31.9	25.1	–
Per cent of standard length					
Predorsal length	46.6	44.7	50.4	47.5	1.2
Preanal length	61.6	59.3	65.0	62.5	1.3
Prepectoral length	25.4	24.8	29.7	26.8	1.2
Prepelvic length	41.8	39.5	45.7	42.8	1.2
Postanal length	33.0	30.6	36.7	33.6	1.2
Thoracic length	20.2	16.1	22.2	19.4	1.0
Abdominal length	18.5	18.0	23.4	20.0	1.1
Caudal-peduncle depth	8.6	7.5	10.2	8.8	0.6
Head length	39.1	36.3	41.9	39.4	1.1
Cleithral width	28.4	25.2	29.1	27.3	0.9
Base of dorsal fin length	12.3	10.4	14.5	12.6	0.8
Dorsal-fin unbranched ray length	23.5	20.7	27.5	23.5	1.3
Pectoral-fin unbranched ray length	29.2	24.3	31.8	28.1	1.6
Pelvic-fin unbranched ray length	16.4	14.4	20.9	17.4	1.4
Dorsal to anal fin length	24.4	21.1	25.1	23.4	1.0
Snout–opercle length	25.2	24.0	28.8	26.0	1.1
Body depth	20.2	15.6	21.0	18.4	1.2
Per cent of head length					
Head width	65.2	60.1	70.7	64.8	2.4
Head depth	51.8	46.6	54.1	50.5	1.9
Snout length	42.1	40.3	45.4	43.1	1.1
Orbital diameter	13.6	12.4	17.5	14.8	1.1
Interorbital length	39.1	35.0	40.9	37.9	1.3
Maxillary barbel length	6.4	3.1	9.0	6.5	1.3
Prenasal length	26.2	24.7	30.4	28.0	1.3
Internasal length	9.3	8.7	13.4	10.9	1.1
Nasal chamber width	9.7	7.8	13.3	10.4	1.4
Females	–	7.8	11.0	9.4	0.8
Males	–	11.1	13.3	12.0	0.6
Nasal chamber length	15.4	12.2	18.9	15.2	1.7
Suborbital depth	22.2	18.2	24.9	21.7	1.4

SD, standard deviation.

odontodes (Fig. 7C, F) [vs. anterior margin of snout with an odontode-free band (Fig. 7A, D)]; first anal-fin pterygiophore contacting the 12th vertebra (vs. 13th); and metapterygoid-hyomandibula suture reduced, the bones not contacting each other dorsally to the suture (Fig. 10E) [vs. metapterygoid and hyomandibula contacting each other dorsally to the suture (Fig. 10F)]. Finally, *Pseudotothyris obtusa* differs from *Pseudotothyris janeirensis* by having scattered plates covering the abdomen partial or totally (vs. abdomen almost naked, except for one to three lateral abdominal plates and one to two preanal plates); spinelet absent (Fig. 11B) [vs. present (Fig. 11A)]; three transverse dark saddles on the dorsum (vs. transverse dark saddles on the dorsum absent); subocular cheek plate generally present (Fig. 12A) [vs. always absent (Fig. 12B)]; and

odontodes on lateral plates randomly distributed (vs. odontodes aligned in well-defined series).

Description: Morphometric and meristic data in Tables 5 and 6. Dorsal body profile convex from tip of snout to dorsal-fin origin; descending at dorsal-fin base; almost straight from end of dorsal-fin base to caudal-fin origin. Ventral body profile almost straight; ascending at pelvic-fin base; straight to caudal-fin origin. Greatest body depth at parietosupraoccipital tip. Greatest body width at pectoral girdle, gradually tapering towards snout and caudal fin. Caudal peduncle almost ellipsoid in transverse section. Head deep; compound pterotic and parietosupraoccipital with longitudinal crests; tuft of well-developed odontodes at parietosupraoccipital tip. Anterior margin of snout rounded to slightly pointed, in dorsal view; tip of

Table 6. Frequency distribution of meristic data for *Pseudotothyris obtusa*; neotype and 85 nontype specimens. Plate (counted on both sides whenever possible), procurent ray, and vertebrae counts were carried out only for cleared and stained specimens. Neotype values are marked with an asterisk

Character	Frequency distribution	Range	Mode
Dorsal plates	22(2), 23(2), 24(4)	22–24	24
Mid-dorsal plates	14(2), 15(5), 16(1)	14–16	15
Median plates	18(1), 19(1), 23(5), 24(1)	18–24	23
Anterior field plates	4(3), 5(5)	4–5	5
Gap field plates	2(2), 3(1), 4(3), 5(2)	2–5	4
Posterior field plates	11(1), 12(1), 13(2), 14(1), 15(2), 17(1)	11–17	13/15
Nonperforated plates at caudal-peduncle end	0(2), 3(2), 4(3), 5(1)	0–5	4
Midventral plates	12(1), 14(2), 15(3)	12–15	15
Ventral plates	19(3), 20(1), 21(2)	19–21	19
Lateral abdominal plates	3(1), 4(4), 5(1) 6(2)	3–6	4
Premaxillary teeth	9(1), 12(2), 13(3), 14(3) 15(6), 16(10), 17(3), 18(14), 19(19), 20(17), 21(19), 22(16), 23(16), 24(9), 25(3), 26(7), 27(3), 28(1), 29(1)*	9–29	19/21
Dentary teeth	9(1), 10(1), 11(3), 12(3), 13(1), 14(8), 15(17), 16(23), 17(21), 18(30), 19(21), 20(14), 21(10), 22(3)*, 23(2), 24(2)	9–24	18
Upper pharyngeal plate teeth	20(1), 23(1), 24(1), 27(1), 29(1), 30(1)	20–30	–
Ceratobranchial 5 teeth	12(2), 14(3), 15(1)	12–15	14
Dorsal-fin branched rays	6(1), 7(83)*, 8(2)	6–8	7
Pectoral-fin branched rays	5(4), 6(82)*	5–6	6
Pelvic-fin unbranched rays	5(85)*, 6(1)	5–6	5
Anal-fin unbranched rays	5(85)*, 6(1)	5–6	5
Caudal-fin unbranched rays	13(5), 14(80)*	11–14	14
Dorsal procurent rays	5(2), 6(1), 7(1)	5–7	5
Ventral procurent rays	3(1), 4(2), 5(1)	3–5	4
Vertebrae	27(2), 28(1)	27–28	27

snout with four elongate plates, their length greater than their width; well-developed odontodes restricted to dorsal portion of snout; other odontodes equal in size and randomly distributed on remainder of head and body, not forming conspicuous rows. Poorly developed keels in median and midventral plate series. Eye small, dorsolaterally placed, not visible in ventral view. Iris operculum absent. Elongate posterior extension on compound pterotic, partially covering dorsal part of broad swimbladder opening; large irregular fenestrae on posteroventral margin; infraorbital canal entering infraorbital series via compound pterotic or sphenotic. Parietosupraoccipital forming part of dorsal wall of swimbladder capsule.

Body entirely covered by dermal plates, except on ventral part of head, region overlying opening of swimbladder capsule, and around pelvic-fin origin. Abdomen generally entirely covered by randomly distributed small plates; three to six lateral abdominal plates; one to three preanal plates.

Lips oval, papillose; lower lip larger than upper, not reaching pectoral girdle; papillae gradually small to lip edge. Maxillary barbel reduced, free from oral disk. Teeth slender and bifid; median cusp

larger and rounded, lateral smaller and pointed. Premaxillary teeth 9–29 (19/21). Dentary teeth 9–24 (18). Premaxillary and dentary accessory teeth present only in juveniles.

Dorsal fin, ii,6–8 (7); originating approximately at vertical through end of pelvic-fin base; tip of adpressed rays surpassing vertical line passing end of anal-fin base; spinelet absent. Anterior portion of compound supraneural first dorsal-fin proximal radial contacting neural spine of seventh vertebra. Pectoral fin i,5–6 (6); originating immediately behind opercular opening; tip of adpressed rays surpassing vertical through end of pelvic-fin base; well-developed odontodes on unbranched ray, gradually enlarged toward tip. Cleithrum and coracoid totally exposed, sometimes a small median area without odontodes, covered only by skin. Arrector fossae partially enclosed by ventral lamina of coracoids in juveniles, opening restricted to a small area near midline; completely closed in adults. Pectoral axillary slit present in juveniles and adults, about two to four times the orbital diameter, at an angle of 45° to body axis. Pelvic fin i,5–6 (5); unbranched ray shorter than branched ones. Anal fin i,5–6 (5); first proximal radial

contacting haemal spine of 12th vertebra. Caudal fin i,14,i; concave, lobes equal in size; 5–7 (5) dorsal and 3–5 (4) ventral procurrent rays. Adipose fin absent. Median lateral plate series 18–24 (23), usually complete from compound pterotic to caudal-fin base; sometimes truncated, ending anteriorly to caudal-fin origin, one to two plates of dorsal and ventral series contacting each other along midline; some specimens with single median plate after truncation. Vertebrae 27–28 (27).

Coloration in alcohol: Ground colour of dorsal surface brown with three transverse dark saddles connecting to dark longitudinal stripe on lateral of body; first bar near end of dorsal-fin base, incomplete at midline; second at vertical through end of anal-fin base; third preceding dorsal procurrent caudal rays. Mid-dorsal portion of head to parietosupraoccipital tip dark brown; area from anterior margin of snout to nasal chamber edge clear. Ventral surface and lateroventral portion of body and head yellowish coloured.

Dorsal-, anal-, pectoral-, and pelvic-fin membranes hyaline. Dorsal- and anal-fin rays with dark bands, sometimes entirely dark; some specimens with dorsal-fin base clear. Pectoral- and pelvic-fin unbranched rays entirely dark; some specimens with dark bands. Anal-fin base with an anterolateral dark spot. Caudal fin densely pigmented, except for its tip and a circular unpigmented area on each lobe. Procurrent rays region yellowish coloured, sometimes extending to lateral portion of caudal peduncle.

Sexual dimorphism: Males with conspicuous urogenital papilla immediately posterior to anus; expanded flap of skin on dorsal surface of the first pelvic-fin ray; tip of adpressed pelvic fin generally reaching anal-fin origin; nasal chamber wider than in females (11.1–13.3% HL in males; 7.8–11.0% HL in females).

Distribution: Coastal drainages from São Sebastião in São Paulo state to Ilha do Superagüi, Baía de Paranaguá, in Paraná state (Fig. 6).

Comments on type-series: The original description of *Otocinclus obtusus*, provided by Alípio de Miranda Ribeiro in 1911, gave no indication of the number of specimens examined; however, it was entirely written in the singular form, and, besides that, the author only referred to a single value for SL, as well as for all other measurements and counts presented. Based on this, we concluded that the original description was based on a single specimen, the holotype. Later, Paulo de Miranda Ribeiro (1953: 401), in a list of the type material described by Alípio de Miranda Ribeiro and deposited at MNRJ, cited five cotypes of *Otocinclus obtusus*, designating what he called as

cotype 'A' as the lectotype. The specimens mentioned by Paulo de Miranda Ribeiro (1953) were not found in the fish collection of MNRJ. Furthermore, in the paper of description of *Pseudotothyris*, Britski & Garavello (1984) analysed a single type specimen (MNRJ 1026), referred to by them as the holotype, and did not refer to any additional type specimen for *Otocinclus obtusus*. Thus, the absence of these supposed cotypes, in addition to the fact that the original description had been based on a single specimen, makes the type designation of Paulo de Miranda Ribeiro seem to us to be an error and must be considered as invalid.

Recently, one of us (F. O. M.) had access to the bottle under the catalogue number MNRJ 1026; however, the specimen was lacking, and only suspended particles and some minute fragments were found. These may have been the two pectoral spines and perhaps the two compound pterotic bones. These few parts do not allow an unequivocal identification of the species. After various other attempts the holotype was not located anywhere, so we have concluded that the type specimen analysed by A. de Miranda Ribeiro (1911) and by Britski & Garavello (1984) is indeed lost. Thus, we propose here the designation of a neotype for *Otocinclus obtusus* (MZUSP 79939, 30.2 mm SL).

General comments: Figure 3, indicated by A. de Miranda Ribeiro (1911) in the original description as *Otocinclus obtusus*, is obviously the holotype of *Otocinclus gibbosus*, another species described in the same paper (currently valid as *Lampiella gibbosa*).

PHYLOGENETIC ANALYSIS

Character descriptions

Data matrix in Table 7.

Mesethmoid

1. Mesethmoid projected anteriorly relative to the condyle [modified; Armbruster, 2004 (101)]: (0) absent or slightly projected; (1) present. Consistency index (CI) = 0.143; retention index (RI) = 0.400.

As in *Delturus carinotus* and some Neoplecostominae members, in *Otothyris* the mesethmoid condyle is positioned near the anterior margin of the bone (Fig. 5A, G, D). In *Pseudotothyris*, the mesethmoid is projected anteriorly relative to the condyle (Fig. 5B, D–F, H).

2. Mesethmoid anteroventral portion: (0) simple, without modification anterior to condyle (Fig. 5A–E, G, H); (1) with a process anterior to condyle (Fig. 5F). CI = 0.143; RI = 0.571.

3. Mesethmoid anterolateral margin [modified; Schaefer, 1998 (2)]: (0) expanded, its width equivalent to or wider than the width of the bone at the posterior end (Fig. 5A, E); (1) narrow (Fig. 5B, D, F–H); (2) bifurcate, with expanded lateral processes (Fig. 5C). CI = 0.286; RI = 0.444.
4. Mesethmoid anterior margin [modified; Schaefer, 1998 (3)]: (0) either straight or rounded; (1) slightly projected; (2) pointed to arrow-shaped; (3) concave. CI = 0.176; RI = 0.300.

In the plesiomorphic condition, found also in *Otothyris*, the mesethmoid anterior margin is straight or rounded (Fig. 5A, F, G). In the derived condition, the anterior margin of the mesethmoid is slightly projected (as in *Pseudotothyris obtusa* and *Pseudotothyris ignota*; Fig. 5B, D) or pointed (as in *Pseudotothyris janeirensis*; Fig. 5E, H). In addition, some taxa can have the anterior margin of bone concave (Fig. 5C).

5. Mesethmoid anterior margin with a cartilaginous process [Calegari, 2010 (5)]: (0) absent; (1) present. CI = 0.250; RI = 0.769.

In the plesiomorphic condition, the mesethmoid anterior margin is ossified. In the derived condition, shared by *Pareiorhaphis hystrix* and some relatively basal hypoptopomatines, there is a small cartilage in the anterior margin of the bone, even in adults (Fig. 5D).

6. Dorsal portion of mesethmoid [modified; Gauger & Buckup, 2005 (47)]: (0) partially covered by plates, except for the anterior margin; (1) partially covered by plates, exposed on the dorsal surface of head; (2) totally covered by plates (Fig. 3A–C). CI = 0.222; RI = 0.222.

Lateral ethmoid

7. Lateral ethmoid in dorsal view [modified; Gauger & Buckup, 2005 (49)]: (0) exposed without odontodes; (1) exposed, small triangular area, with a single series of odontodes (Fig. 16D); (2) exposed, large triangular area, with two or more odontode series (Fig. 16A); (3) not exposed (Fig. 3A–C). CI = 0.231; RI = 0.643.
8. Lateral ethmoid lateral strut [Schaefer, 1991 (6); 1998 (6)]: (0) short and broad, contacting third infraorbital just lateral to the edge of the nasal capsule; (1) elongate, contacting third infraorbital well lateral to the edge of the nasal capsule. CI = 0.500; RI = 0.667.
9. Nasal capsule [modified; Schaefer, 1991 (5); 1998 (5)]: (0) completely closed by lateral ethmoid from below (Fig. 16A, B); (1) partially closed, lateral ethmoid surrounding more than 50% of nasal capsule (Fig. 16C); (2) partially closed, lateral

ethmoid surrounding less than 50% of nasal capsule (Fig. 16D). CI = 0.143; RI = 0.368.

Compound pterotic

10. Compound pterotic shape [modified; Schaefer, 1991 (8); 1998 (8)]: (0) with a posterior process reaching or almost reaching the rib of the sixth vertebra; (1) with a very elongate posterior process, distinct from the rest of the bone, surpassing the rib of sixth vertebra; (2) roughly quadrangular, without posterior process, or if present far from rib of sixth vertebra. CI = 0.250; RI = 0.760.

All Neoplecostominae and many basal Hypoptopomatinae have the compound pterotic roughly quadrangular, without a posterior extension (Fig. 17A). Schaefer (1991, 1998), Gauger & Buckup (2005), and Ribeiro *et al.* (2005) considered the posterior extension of the compound pterotic as a single state. The latter work brought this feature as a synapomorphy to join the clade *Pseudotothyris*, *Otothyris*, and *Otothyropsis*. Here, we considered this state as two different states: the posterior extension may reach or almost reach the rib of sixth vertebra (state 0, Fig. 17B) or may surpass this rib (state 1, Figs 2A, B, 17C, D). A posterior extension very elongate, surpassing the rib of sixth vertebra, is exclusive for *Pseudotothyris* and *Otothyris* species amongst the Hypoptopomatinae, and constitutes a unique derived synapomorphy for this clade.

11. Compound pterotic fenestrae [modified; Schaefer, 1991 (9); 1998 (10)]: (0) all small and circular (Schaefer, 1997: fig. 9b); (1) non-uniform in shape and size, small and more circular in dorsal, and large and shapeless in ventral portion (Ribeiro *et al.*, 2005: fig. 7a); (2) all large and cavernous groove-shaped (Ribeiro *et al.*, 2005: fig. 7b–d). CI = 0.182; RI = 0.640.

Parietosupraoccipital

12. Parietosupraoccipital [Schaefer, 1991 (12), 1998 (12)]: (0) not contributing to the dorsal portion of swimbladder capsule; (1) forming part of the dorsal wall of the swimbladder capsule. CI = 0.100; RI = 0.471.

In the plesiomorphic condition, present in most Loricariidae, including the Neoplecostominae and many of the Hypoptopomatinae, the dorsal wall of the swimbladder capsule is formed only by the compound pterotic. In the derived condition, the parietosupraoccipital also contributes to forming the dorsal wall of this structure (Ribeiro *et al.*, 2005: fig. 8). Until now, this condition had only been observed for *Pseudotothyris*, *Otothyris*, and

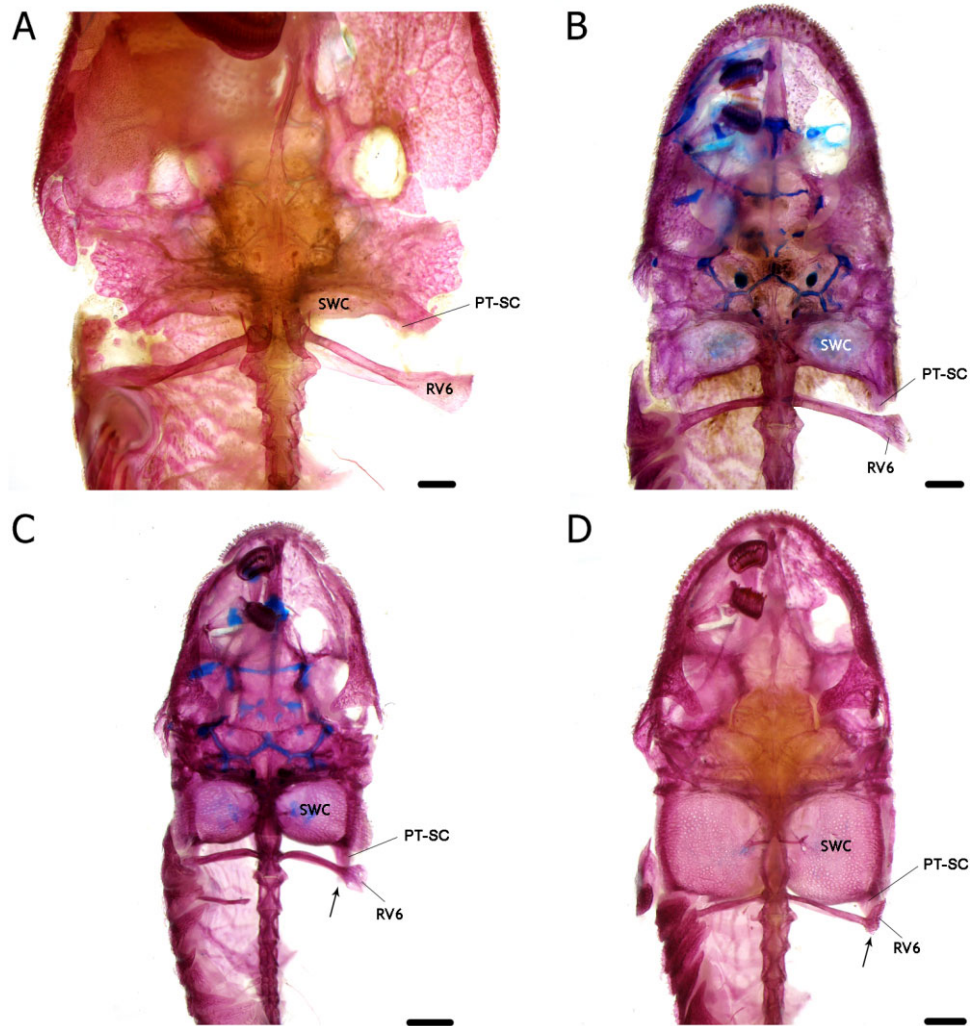


Figure 17. Skull in ventral view. A, *Isbrueckerichthys duseni*, DZSJRP 13670, 48.3 mm standard length (SL), sex undetermined. B, *Otothyropsis marapoama*, DZSJRP 9937, 26.3 mm SL, sex undetermined. C, *Pseudotothyris obtusa*, MCP 31726, 24.2 mm SL, female. D, *Otothyris rostrata*, MCN 18943, 23.6 mm SL, male. Arrows show the extension of the compound pterotic exceeding the rib of the sixth vertebra. Abbreviations: PT-SC, compound pterotic; RV6, rib of sixth vertebrae; SWC, swimbladder capsule. Scale bars = 1 mm.

Otothyropsis (Schaefer, 1998; Gauger & Buckup, 2005; Ribeiro *et al.*, 2005). However, this feature is more widely distributed than previously thought; we observed the parietosupraoccipital forming the swimbladder capsule in many Hypoptopomatinae species, appearing independently many times.

13. Swimbladder capsule in ventral view [modified; Schaefer, 1998 (11)]: (0) small, its posterior margin does not extend to the joint between the Weberian complex centrum and the sixth centrum; (1) enlarged, its posterior margin reaching or slightly surpassing the joint; (2) very enlarged, length and width equivalent in size,

reaching or almost reaching the rib of the sixth vertebra. CI = 0.154; RI = 0.450.

In the plesiomorphic condition, found in most of the Loricariidae, the swimbladder is small, its width larger than its length, and its posterior margin does not reach the joint between the Weberian complex centrum and the sixth centrum (state 0, Fig. 17A). In the apomorphic condition, the swimbladder is enlarged. This feature was considered as a single state by Schaefer (1998), but here it was subdivided into two different states: swimbladder reaching or slightly surpassing the joint, its width still larger than its length (state 1, Fig. 17B), and swimbladder reaching or almost reaching the rib of the sixth ver-

tebra, its width and length equivalent in size (state 2, Fig. 17C, D). This last condition was only observed in *Pseudotothyris*, *Otothyris juquiae*, and *Otothyris rostrata*.

Infraorbitals

14. Number of infraorbitals [modified; Armbruster, 2004 (91)]: (0) six; (1) five; (2) four. CI = 0.400; RI = 0.625.

Most of the Loricariidae have five to six infraorbitals. All the Neoplecostominae, except for *Isbrueckerichthys* and most of the Hypoptopomatinae, have five elements in infraorbital series (Fig. 4A, E). *Otothyris* and *Pseudotothyris* have only four infraorbitals, sharing the absence of infraorbital 1 (Fig. 4B, C). *Pseudotothyris janeirensis* is polymorphic for this character. Four infraorbitals were also observed for *Microlepidogaster* sp. nov., but as a consequence of the fusion between infraorbitals 3 and 4, rather than the absence of infraorbital 1 (Fig. 4D).

15. Infraorbital 1: (0) present, bearing canal; (1) present, without canal; (2) absent. CI = 1.000; RI = 1.000.

Most Neoplecostominae and Hypoptopomatinae have five infraorbitals bearing a branch of the laterosensory canal (Fig. 4A, E). Although *Otothyropsis piribebuy* has five infraorbitals, the first one does not bear the laterosensory canal. In *Otothyris*, *Pseudotothyris obtusa*, and *Pseudotothyris ignota*, the infraorbital 1 is absent (Fig. 4B, C). For *Pseudotothyris janeirensis*, we found a single specimen with infraorbital 1 present just on one side, and the species was considered polymorphic for this character.

16. Infraorbital 2 laterosensory canal: (0) present; (1) absent. CI = 0.500; RI = 0.667.

All Neoplecostominae and most Hypoptopomatinae have infraorbital 2 as a large plate bearing a branch of the laterosensory canal (Fig. 4 A, B, D, E). In the derived condition, observed for *Otothyris juquiae*, *Otothyris lophophanes*, *Otothyris rostrata*, *Otothyris travassosi*, and *Otothyropsis piribebuy*, the canal of infraorbital 2 is absent (Fig. 4C). Amongst *Otothyris* species, the canal is present only for some specimens of *Otothyris travassosi*.

17. Infraorbital 2 and nasal contact: (0) absent (Fig 3B); (1) present (Fig. 3A, C). CI = 0.100; RI = 0.471.

18. Shape of infraorbital 4 or correspondent [modified; Schaefer, 1991 (49); 1998 (37)]: (0) expanded ventrally below the canal, quadrangular to rec-

tangular; (1) expanded ventrally below the canal, triangular; (2) not expanded below the canal. CI = 0.200; RI = 0.500.

Schaefer (1991, 1998) considered only two states for this character: infraorbital quadrangular or ventrally expanded. Here, we redefined this character and established three states. Infraorbital 4 may be ventrally expanded, but rectangular (state 0, Fig. 4A) or triangular (state 1, Fig. 4B, C) in shape. *Gymnotocinclus*, *Otocinclus*, and *Oxyropsis* have infraorbital 4 reduced, restricted to laterosensory canal (state 2, Fig. 4E).

19. Last element of infraorbital series: (0) expanded ventrally below the canal (Fig. 4A, D); (1) not expanded below the canal (Fig. 4B, C, E). CI = 0.083; RI = 0.522.

Amongst the analysed taxa, only *Delturus carinotus*, *Hypostomus careopinnatus*, and *Isbrueckerichthys duseni* have six infraorbitals. The sixth element is very similar, in shape, size, and position, to the fifth one in the species that have only five infraorbitals. Thus, here these two elements were considered as homologous. This follows the homology hypothesis proposed by Armbruster (2004), who suggested numbering the infraorbital series from posterior to anterior, with the last infraorbital being IO6, as many Loricariidae species have lost the first infraorbital.

20. Entry of laterosensory canal in infraorbital series [Schaefer, 1991 (48)]: (0) via the sphenotic; (1) via the compound pterotic. CI = 0.500; RI = 0.500.

In most loricariids the infraorbital canal enters the infraorbital series via the sphenotic (Carvalho & Reis, 2009: fig. 3b). In the derived condition, entry occurs via the compound pterotic (Carvalho & Reis, 2009: fig. 3a). According to Schaefer (1991), amongst the Hypoptopomatinae only *Otothyris* has the derived condition. Gauger & Buckup (2005) also observed this state for *Corumbataia*. Here, we confirm the derived condition for *Corumbataia* (except for *Corumbataia veadeiros*, which according to the original description has the infraorbital canal entering via sphenotic). However, this character seems to be variable amongst *Otothyris* and *Pseudotothyris*. All specimens of *Otothyris juquiae* have the plesiomorphic condition and the laterosensory canal enters the infraorbital series via the sphenotic. The same condition is found in *Pseudotothyris janeirensis*. By contrast, *Otothyris lophophanes* has the canal entering the series via the compound pterotic. Finally, *Otothyris travassosi*, *Otothyris rostrata*, *Pseudotothyris obtusa*, and *Pseudotothyris*

ignota are polymorphic for this feature, even intraindividually, in different sides of the same specimen.

Mandibular arc and jaw suspensorium

21. Metapterygoid channel [modified; Schaefer, 1998 (13)]: (0) absent (Fig. 10A); (1) present, shallow, its depth much less than 50% of its length (Fig. 10D); (2) present, deep, its depth about 50% of its length (Fig. 10B, C, E–H). CI = 0.500; RI = 0.667.
22. Metapterygoid–hyomandibula contact [Schaefer, 1991 (16); 1998 (15)]: (0) restricted, bones not contacting one another dorsally to suture; (1) complete, extending dorsally beyond the suture. CI = 0.067; RI = 0.125.

In the plesiomorphic condition, the metapterygoid–hyomandibula contact is restricted, the bones do not contact each other dorsally to the suture (Fig. 10E). It seems to be a result of separation of the bones (as in *Otothyropsis* sp. nov.) or as a consequence of the concavity present in the hyomandibula (as in *Pseudotothyris obtusa*). In the derived condition, the contact between these bones is complete until the dorsal margin (Fig. 10A–D, F–H). This character may be used to distinguish *Pseudotothyris obtusa* and *Pseudotothyris ignota*.

23. Hyomandibula posterior margin [modified; Armbruster, 2004 (34)]: (0) not sutured to compound pterotic; (1) sutured to compound pterotic. CI = 0.111; RI = 0.556.
24. Levator arcus palatini crest [modified; Schaefer, 1991 (15); 1998 (14)]: (0) present, low, poorly developed; (1) present, high, well-developed between the adductor crest to the anterior margin of hyomandibula; (2) absent. CI = 0.133; RI = 0.536.

In most loricariids, the hyomandibula has a well-developed crest running anteroposteriorly from the anterodorsal margin to the adductor crest, called the levator arcus palatini crest (Fig. 10A, B, E–H). According to Schaefer (1991, 1998), this crest is absent in *Acestridium*, *Hisonotus*, *Hypoptopoma*, *Microlepidogaster*, *Nannoptyopoma*, *Oxyropsis*, *Otocinclus*, and *Niobichthys*. The absence of the levator crest was confirmed only for *Hypoptopoma*, *Niobichthys*, *Otocinclus*, and *Oxyropsis*, and also observed for *Otothyropsis marapoama* (Fig. 10D). All examined species of *Microlepidogaster* and *Hisonotus* have the crest, although it is sometimes poorly developed (Fig. 10C).

25. Accessory teeth on premaxilla and dentary in adults [modified; Schaefer, 1998 (44); 2003b (7)]: (0) absent; (1) present. CI = 0.333; RI = 0.333.

Accessory teeth are small conical teeth on the posterior portion of the premaxilla and dentary, easily distinguished from the bifid replacement teeth. Accessory teeth are shared by Astroblepidae and Loricariidae. These teeth were first observed by Reis & Schaefer (1992) in *Eurycheilichthys* and *Parotocinclus collinsae*. Later, these teeth were also observed by many authors (Reis & Schaefer, 1998 in *Epactionotus*; Schaefer & Provenzano, 1998 in *Niobichthys*; Gauger & Buckup, 2005 in *Parotocinclus bidentatus* and *Parotocinclus muriaensis*; Schaefer, 2003b in *Lithogenes villosus*; Provenzano *et al.*, 2003 in *Lithogenes valencia*; and Martins & Langeani, 2011b in *Rhinolekos schaeferi*). Lehmann (2006) verified the presence of accessory teeth in *Parotocinclus maculicauda*, *Hemipsilichthys gobio*, and *Hemipsilichthys papillatus*, but only for juvenile specimens. We think that the presence of accessory teeth is common amongst Loricariidae species, being also observed by us in juveniles of *Pareiorhina rudolphi*, *Neoplecostomus microps*, *Neoplecostomus paranensis*, *Microlepidogaster arachas*, *Microlepidogaster longicolla*, *Pseudotothyris ignota*, *Pseudotothyris janeirensis*, *Pseudotothyris obtusa*, *Schizolecis guntheri*, *Rhinolekos britskii*, and *Rhinolekos garavelloii*. The presence of accessory teeth is probably plesiomorphic for Loricariidae, as they are present in *Lithogenes* (except *Lithogenes wahari*, for which accessory teeth were not observed in the types in the original description). The loss of these teeth, only in adults or in both adult and juveniles, is considered here a derived condition for the Loricariidae. The presence of accessory teeth in adults of the Hypoptopomatinae, such as *Epactionotus* and *Eurycheilichthys*, should then be considered a reversal, maintaining a paeodomorphic feature.

Opercular series

26. Opercular posterior margin: (0) straight, so that the opercle is trapezoidal (Fig. 18B, C); (1) strongly concave, so that the posterior portion of the opercle is elongated posteriorly, distinct from the main body of the bone (Fig. 18A, D). CI = 0.125; RI = 0.632.
27. Opercular crest: (0) absent or restricted to an elevation near opercular condyle; (1) present, well developed. CI = 0.200; RI = 0.500.

Near the opercle–hyomandibula articulation there is a bone elevation, named here as the opercular crest. In most Hypoptopomatinae and Neoplecostominae, the opercular crest is well developed and long, almost reaching the posterior margin of the opercle (Fig. 18A, D). In *Delturus carinotus*, *Harttia kronei*, *Hypostomus careopinatus*, *Pareiorhaphis hystrix*, and some Hypoptopomatinae, this crest is completely absent or

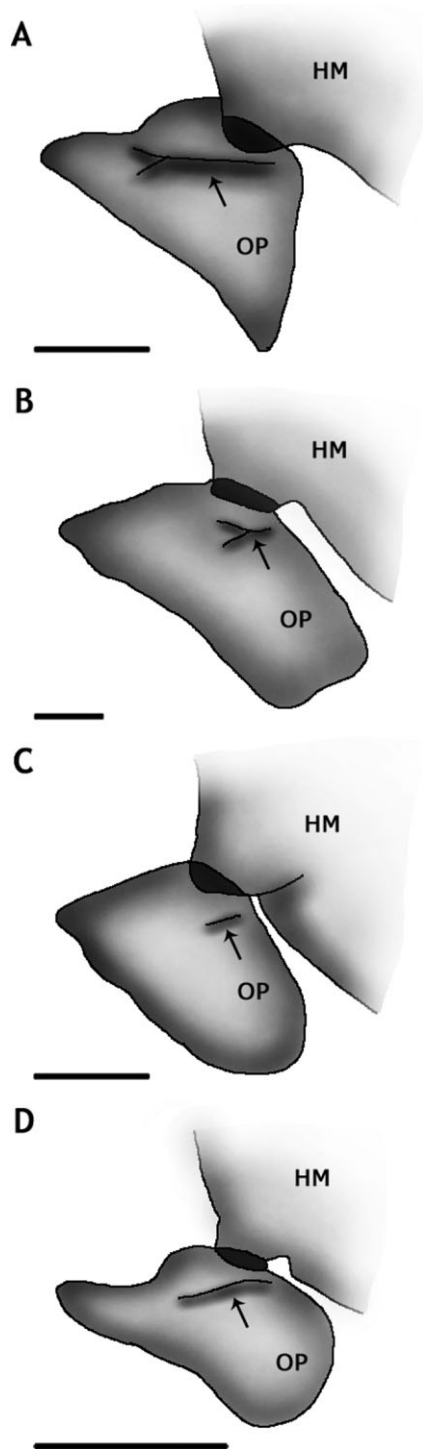


Figure 18. Opercle in mesial view. A, *Schizolecis guntheri*, DZSJRP 6525, 32.9 mm standard length (SL), sex undetermined. B, *Gymnotocinclus anosteos*, UFRGS 11296, 43.7 mm SL, male. C, *Corumbataia cuestae*, DZSJRP 7947, unmeasured, sex undetermined. D, *Pseudotothyris obtusa*, MCP 31726, 24.4 mm SL, female. Arrows show the opercular crest. Abbreviations: HM, hyomandibula; OP, opercle. Scale bars = 1 mm.

poorly developed, restricted to a small elevation (Fig. 18B, C).

28. Preopercle: (0) exposed, emergent to skin surface (Fig. 12A–C); (Ribeiro *et al.*, 2005: fig. 3b); (1) not exposed (Schaefer, 1997: fig. 9b). CI = 0.500; RI = 0.667.

29. Preopercular ventral margin [Schaefer, 1991 (20); 1998 (18)]: (0) not deflected medially; (1) deflected medially, forming a laminar shelf medial to the canal-bearing cheek plate (cp1). CI = 0.250; RI = 0.769.

30. Preopercular canal [Schaefer, 1991 (22); 1998 (20)]: (0) present; (1) absent. CI = 0.500; RI = 0.750.

Except for Scoloplacidae and Trichomycteridae, all other Loricarioidea have the preopercle bearing a branch of the laterosensory canal. In the derived condition, the laterosensory canal in the preopercle is absent. *Otocinclus affinis*, *Acestridium martini*, *Oxyropsis acutirostra*, *Otothyris juquiae*, *Otothyris rostrata*, and *Otothyris travassosi* share the absence of the preopercular canal. However, as already evidenced by Schaefer (1998), the genus *Otothyris* is polymorphic for this character. Some specimens of *Otothyris travassosi* and *Otothyris lophophanes* have a branch of the laterosensory canal in the preopercle. In species with the preopercle canal, after the preopercle, the canal enters canal-bearing plate 1 (cp1). Schaefer (1998: char. 38) did not observe any branch of the laterosensory canal in cp1 for *Otothyris* species; however, all specimens of *Otothyris* examined here have a branch of laterosensory canal in cp1, even in those specimens that do not have a preopercular canal.

31. Suprapreopercle [Armbruster, 2004 (80)]: (0) present; (1) absent. CI = 0.333; RI = 0.750.

The laterosensory canal that exits the compound pterotic may either enter the preopercle directly or may pass first into a small plate, called the suprapreopercle. In *Delturus carinotus*, *Harttia kronei*, and all examined Neoplecostominae (except for *Pareiorhina rudolphi*, polymorphic for this feature), the suprapreopercle is present. In the derived condition, shared by most of the Hypoptopomatinae and *Hypostomus careopinnatus*, the suprapreopercle is absent. *Hisonotus insperatus*, *Hisonotus luteofrenatus*, and *Hisonotus piraicanjuba* are the only species amongst hypoptopomatines with a suprapreopercle, a useful character with which to diagnose these species from the other subfamily members. This character is polymorphic in *Microlepidogaster dimorpha*.

32. Subocular cheek plate (socp) [Schaefer, 1991 (19); 1998 (17)]: (0) absent; (1) present. CI = 0.167; RI = 0.286.

Between the opercle and the canal-bearing plate (cp1) there may be one or more additional plates without a branch of the laterosensory canal. One of these plates was originally called subocular cheek plates by Schaefer (1997) or occasionally subopercular cheek plates (Fig. 12A, C). Although Schaefer (1997) assigned the abbreviation 'cp2' to designate this plate (see Schaefer, 1997: fig. 9b), here we preferred to indicate this plate as 'sopc' to avoid confusion with the plate 'cp2' in Armbruster (2004) that bears a branch of the laterosensory canal and is located between the preopercle and canal-bearing plate 1. In the derived condition, found in most Loricariidae, the subocular plate is present. Amongst the Neoplecostominae, only *Pareiorhaphis hystrix* does not have the subocular cheek plate, and amongst the Hypoptopomatinae this plate is absent only in *Acestridium martini*, *Gymnotocinclus*, *Otocinclus affinis*, *Oxyropsis acuti-rostra*, and *Pseudotothyris janeirensis* (Fig. 12B). *Otothyropsis marapoama*, *Pseudotocinclus parahybae*, and the other two species of *Pseudotothyris* are polymorphic for this character, although the presence of socp is considerably more common. Schaefer (1998) did not observe the subocular cheek plate (referred to as the subopercular plate) for *Pseudotothyris janeirensis* and *Pseudotothyris obtusa*, proposing this feature as the single synapomorphy for the genus. Here, we confirmed the absence of the subocular cheek plate only for *Pseudotothyris janeirensis*, but this plate was observed for most specimens of *Pseudotothyris obtusa* and *Pseudotothyris ignota*. Thus, this feature is not optimized as a synapomorphy for the genus and should not be used to distinguish the genus within the Hypoptopomatinae.

33. Canal-bearing plate 2, between the canal-bearing plate (cp1) and preopercle [Armbruster, 2004 (83)]: (0) absent; (1) present, receiving the canal before the canal plate. CI = 0.250; RI = 0.000.

In *Delturus carinotus*, *Harttia kronei*, *Hypostomus careopinnatus*, *Neoplecostomus microps*, and almost all the Hypoptopomatinae species, the laterosensory canal exits the preopercle and enters directly into cp1. In most Neoplecostominae and in *Eurycheilichthys pantherinus* there is a plate that receives the branch of the laterosensory canal before cp1. This plate was called canal plate 2 (cp2) by Armbruster (2004: fig. 13b), and as detailed above it is distinct from cp2 in Schaefer (1997).

Hyoid arc and branchial skeleton

34. Upper pharyngeal toothplate size [modified; Schaefer, 1991 (23); 1998 (23)]: (0) small, its length less than 50% of the length of

ceratobranchial 5; (1) large, equal to or greater than 50% of the length of ceratobranchial 5. CI = 0.067; RI = 0.440.

Siluriformes have the upper pharyngeal toothplate associated with the fourth infrapharyngobranchial (Fink & Fink, 1981). As suggested by Schaefer (1991, 1998), the size of the upper pharyngeal toothplate is variable amongst the Loricariidae compared to the size of the fourth infrapharyngobranchial. However, we observed that the size of the fourth infrapharyngobranchial is also variable. Thus, we preferred to compare the size of the upper pharyngeal toothplate with the size of ceratobranchial 5.

35. Upper pharyngeal toothplate shape: (0) wedge-shaped, with a well-developed anterior projection; (1) rounded, without an anterior projection; (2) triangular; (3) straight, blade-shaped; (4) curved, blade-shaped. CI = 0.333; RI = 0.467.

Schaefer (1991, 1998) analysed the shape and the size of the upper pharyngeal toothplate in the same character. Here, we preferred to consider the shape of upper pharyngeal toothplate independently of its size. In *Delturus carinotus*, *Harttia kronei*, *Hypostomus careopinnatus*, most of the Neoplecostominae (except for *Neoplecostomus microps*), and most of the Hypoptopomatinae, the upper pharyngeal toothplate is wedge-shaped, with a well-developed anterior projection (Fig. 19C). In *Neoplecostomus microps* and some Hypoptopomatinae, the upper pharyngeal toothplate is rounded to kidney-shaped, not having any kind of projection (Fig. 19A). In *Parotocinclus jumbo* the upper pharyngeal toothplate has a peculiar shape, roughly triangular with small teeth (Fig. 19D). Finally, the toothplate is blade-shaped with a reduced area bearing small teeth in *Otocinclus affinis* and *Nannoplecostomus eleonora*, being straight in the first species (Fig. 19B) and curved in the second one.

36. Length of accessory process of ceratobranchial 1 [modified; Schaefer, 2003b (23); Armbruster, 2004 (7)]: (0) short, about 50% or less of ceratobranchial length (Fig. 20B, D); (1) long, sometimes same length as ceratobranchial (Fig. 20A, C). CI = 0.100; RI = 0.500.

An accessory process in ceratobranchial 1 is exclusive for the Loricariidae (Schaefer, 1987), even though it is not present in all of them, for example in *Lithogenes* (Schaefer, 2003b). According to Schaefer (1987), the accessory process bears modified gill rakers that optimize the capture of food particles. Armbruster (2004) suggested that the greater size of the accessory process increases the ability of the

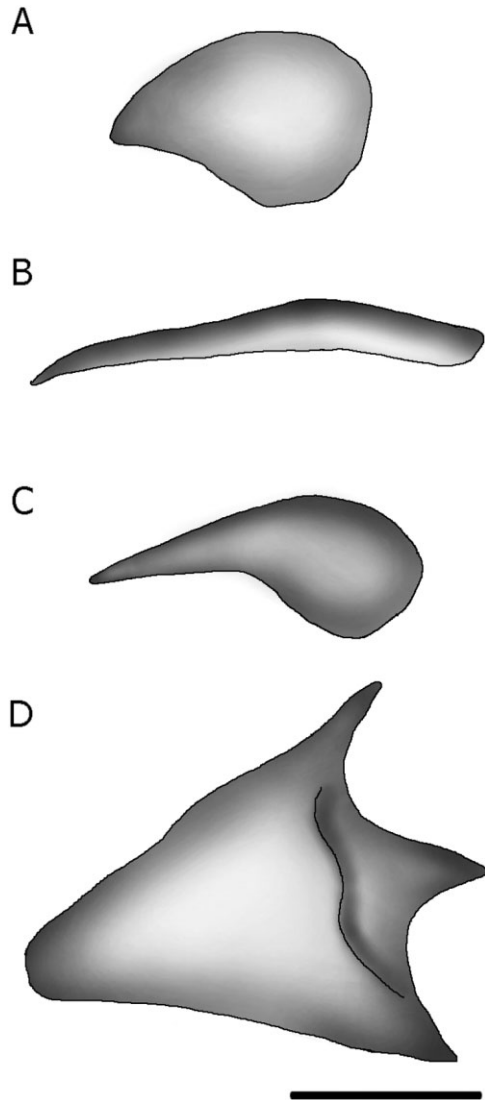


Figure 19. Upper pharyngeal toothplate. A, *Pseudotothyris janeirensis*, MZUSP 80211, 24.9 mm standard length (SL), female. B, *Otocinclus affinis*, DZSJRP 7610, 31.5 mm SL, sex undetermined. C, *Ootothyropsis marapoama*, DZSJRP 9937, 26.3 mm SL, sex undetermined. D, *Parotocinclus jumbo*, MZUSP 69514, unmeasured, sex undetermined. Scale bar = 0.5 mm.

fishes to strain food; thus, it is expected that the process has expanded through evolution. However, many derived hypoptopomatines, such as *Pseudotothyris*, *Ootothyris*, and many *Hisonotus* species have the accessory process reduced, which seems to be a reversal to small size.

37. Accessory element of ceratobranchial 4: (0) absent; (1) present, L-shaped; (2) present, stick-shaped; (3) present, T-shaped. CI = 0.158; RI = 0.407.

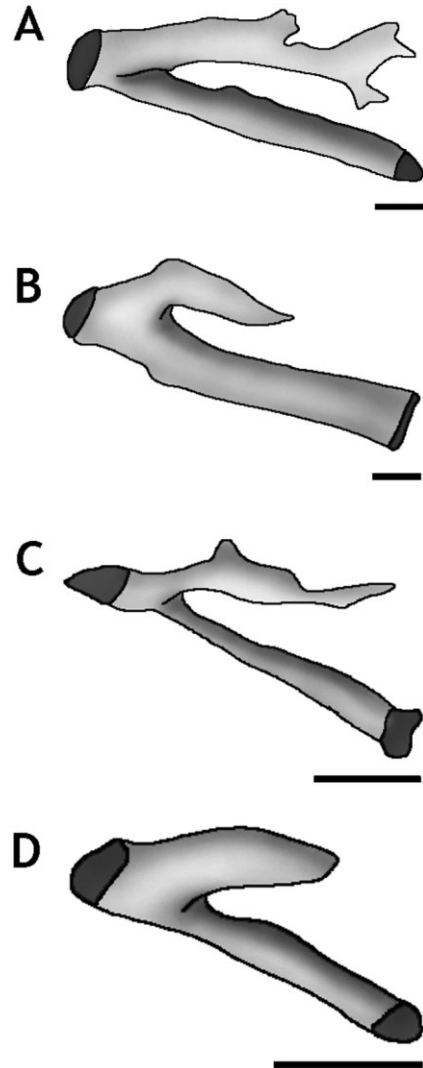


Figure 20. Ceratobranchial 1 in ventral view (left side). A, *Pareiorhaphis hystrix*, DZSJRP 13714, 49.8 mm standard length (SL), sex undetermined. B, *Neoplecostomus microps*, DZSJRP 2768, unmeasured, sex undetermined. C, *Schizolecis guntheri*, DZSJRP 6526, 32.9 mm SL, male. D, *Pseudotothyris obtusa*, MCP 31726, 24.2 mm SL, female. Scale bars = 0.5 mm.

Amongst the analysed taxa, the accessory element of ceratobranchial 4 is a cartilaginous element, situated near the contact surface between ceratobranchial 4 and epibranchial 4. This element articulates with the posteroventral end of epibranchial 4, and seems to be linked to the cartilaginous distal tip of ceratobranchial 5. A few species do not have the accessory element of ceratobranchial (state 0); however, when present its shape is quite variable and can be L-shaped (state 1), stick-shaped (state 2) or T-shaped (state 3).

38. Ceratobranchial 5 teeth: (0) in more than one series; (1) aligned in a single series near the edge. CI = 0.143; RI = 0.250.
39. Ceratobranchial 5 dorsal process: (0) absent (Fig. 21A); (1) present (Fig. 21B, C). CI = 0.077; RI = 0.294.

In *Delturus carinotus*, *Hartia kronei*, and *Hypostomus careopinnatus*, the dorsal margin of ceratobranchial 5 is straight. In most neoplecostomines and hypoptopomatines there is a pointed process, variable in size, at the dorsal margin of ceratobranchial 5.

40. Accessory process on epibranchial 1 [modified; Schaefer, 1997 (9); Armbruster, 2004 (14)]: (0) present, not reaching epibranchial margin; (1) absent. CI = 0.167; RI = 0.643.
41. Infrapharyngobranchial 3 dorsomesial process [modified; Lehmann, 2006 (82)]: (0) absent; (1) present. CI = 0.077; RI = 0.333.
42. Ossification of basibranchial 2: (0) present, ossified; (1) absent, cartilaginous. CI = 0.500; RI = 0.000.
43. Basibranchial 2 size: (0) large; (1) small, smaller than the hypobranchial. CI = 0.111; RI = 0.200.

Weberian apparatus

44. Lateroventral expansion of complex centrum ventral process [Armbruster, 2004 (136)]: (0) absent or short; (1) long. CI = 0.067; RI = 0.263.
45. Remaining portion of parapophysis of vertebrae 4 and 5: (0) laterally exposed, without odontodes; (1) laterally exposed, bearing odontodes; (2) not exposed laterally. CI = 0.167; RI = 0.231.
46. Exposed area of remaining portion of parapophysis of vertebrae 4 and 5: (0) thin, its width approximately equal to the width of distal end of sixth vertebra rib; (1) wide; (2) very wide, occupying approximately two thirds of compound pterotic length. CI = 0.250; RI = 0.714.

The swimbladder capsule opening is formed dorsally by the compound pterotic and ventrally by the remaining portions of the parapophysis of vertebrae 4 and 5. In Neoplecostominae and basal Hypoptopomatinae, the lateral exposed part of the remaining portion of the parapophysis is narrow and the width of its tip is similar to the distal portion of the rib of the sixth vertebra (state 0). In derived hypoptopomatines, the remaining portion of the parapophysis of vertebrae 4 and 5 is wider (states 1 and 2), occupying about two thirds of the compound pterotic length in *Otothyris* species. The width of the remaining portion of the parapophysis of vertebrae 4 and 5 is proportional to the length of the swimbladder capsule and to its opening. The character was not coded for *Hartia kronei*,

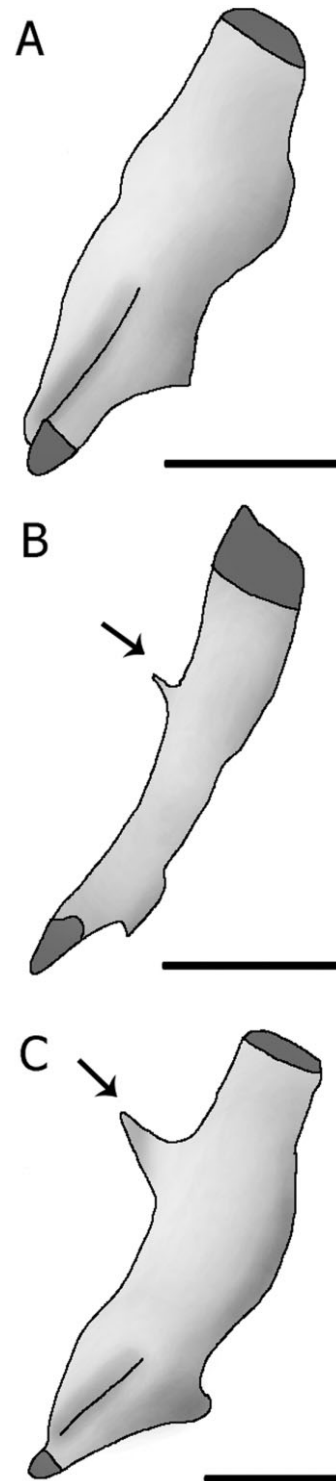


Figure 21. Ceratobranchial 5 in ventral view (right side). A, *Pseudotothyris ignota* sp. nov., UFRGS 9057, 32.0 mm standard length (SL), female. B, *Corumbataia tocantinensis*, MZUEL 4998, 27.6 mm SL, sex undetermined. C, *Lampiella gibbosa*, DZSJRP 13621, 33.8 mm SL, female. Arrows show the dorsal process. Scale bars = 0.5 mm.

Hypostomus careopinnatus, and *Hypoptopoma inexpectata*, which do not have a laterally exposed part of the remaining portion of the parapophysis of vertebrae 4 and 5.

Axial skeleton

47. Number of vertebrae: (0) 27–29; (1) 30–32; (2) 34; (3) 25; (4) 26. CI = 0.308; RI = 0.667.

A tendency observed in the Hypoptopomatinae is a decrease in the number of vertebrae. Except for *Delturus carinotus* (with 29 vertebrae) and *Pareiorhaphis hystrix* (with 34 vertebrae), *Harttia kronei*, *Hypostomus careopinnatus*, and all other Neoplecostominae have 32 vertebrae. Amongst the Hypoptopomatinae species, except for some species of *Rhinolekos* (that also have 32 vertebrae) and *Pseudotocinclus* (with 34 vertebrae), all other species have few vertebrae. The loss of vertebrae was apparently gradual, and the more inclusive clades have greater reductions (except for most of the Hypoptopomatini members, which have a reversion, with an increase in the number of vertebrae).

48. Number of bifid neural spines posterior to seventh vertebra [Schaefer, 1987 (11)]: (0) more than nine; (1) six to nine (Fig. 22A–C); (2) fewer than five. CI = 0.182; RI = 0.100.

49. Central neural spine of seventh vertebra (only for species with an anterior dorsal fin): (0) poorly developed, far from the dorsal series of plates (Fig. 22B, C); (1) well developed, reaching or almost reaching the dorsal series of plates (Fig. 22A). CI = 0.100; RI = 0.526.

Most of the species analysed here have the anterior portion of the compound supraneural–first dorsal fin proximal radial contacting the neural spine of the seventh vertebra. In some hypoptopomatines, such as *Rhinolekos*, *Microlepidogaster*, and *Epactionotus*, the dorsal fin is shifted posteriorly, the articulation occurring with the eighth to 11th vertebrae. Owing to imprecision in the establishment of homology of the number of vertebrae, this character was coded as inapplicable for those species with the dorsal fin shifted posteriorly. This is also true of characters 50 and 51.

50. Bifid neural spines of seventh vertebra (only for species with anterior dorsal fin) [modified; Lehmann, 2006 (107)]: (0) laminar, dorsolaterally projected; (1) absent or poorly developed; (2) process-shaped, anteriorly projected; (3) antero-dorsally fused. CI = 0.273; RI = 0.429.

Harttia kronei, *Hypostomus careopinnatus*, all analysed Neoplecostominae (except for *Kronichthys heylandi*), and most of the Hypoptopomatinae do not

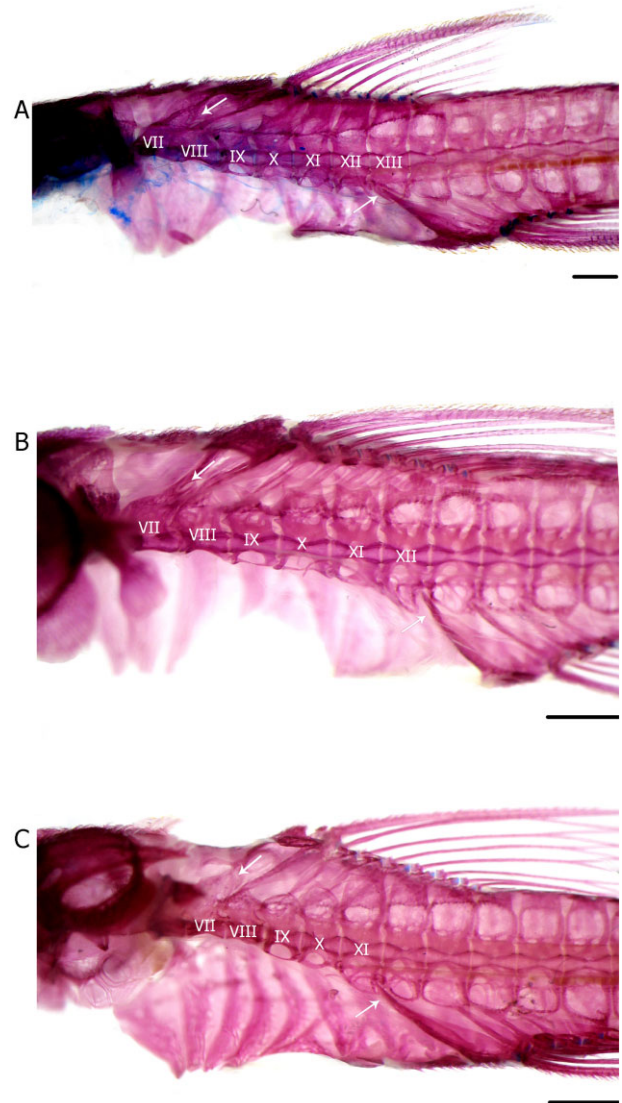


Figure 22. Axial skeleton in lateral view (left side). A, *Schizolecis guntheri*, DZSJRP 6525, 32.9 mm standard length (SL), male. B, *Pseudotothyris obtusa*, MCP 31726, 24.2 mm SL, female. C, *Otothyris lophophanes*, MNRJ 22985, 20.0 mm SL, female. Numbers indicate the vertebrae. Arrows show the articulation of the dorsal and anal fin with the vertebral column. Scale bars = 1 mm.

have bifid neural spines on the seventh vertebra, or if present they are reduced. Bifid neural spines antero-dorsally fused are shared by all *Otothyris* species and are not found in any other Hypoptopomatinae, being an exclusive synapomorphy for the genus.

51. Central neural spine of eighth vertebra (only for species with anterior dorsal fin): (0) absent or reduced (Fig. 22A, C); (1) present (Fig. 22B). CI = 0.091; RI = 0.231.

52. Connecting bone in adults [modified; Lehmann, 2006 (115)]: (0) distinguishable, although fused to lateral plates; (1) absent or not distinguishable. CI = 0.143; RI = 0.500.
53. Intervertebral sutures [modified; Schaefer, 1991 (30); 1998 (25)]: (0) occupying half of the distance between the vertebral centrum and the vertebral distal margin; (1) extending to or almost reaching the vertebral distal margin (Calegari *et al.*, 2011: fig. 1); (2) reduced, restricted to the more proximal portions. CI = 0.105; RI = 0.292.

Median fins

54. Anterior portion of the compound supraneural–first dorsal fin proximal radial contacting neural spine of [modified; Schaefer, 1998 (26)]: (0) seventh vertebra; (1) eighth vertebra; (2) ninth vertebra; (3) tenth vertebra; (4) 11th vertebra. CI = 0.571; RI = 0.625.

In the plesiomorphic condition, observed in *Delturus carinotus*, *Harttia kronei*, *Hypostomus careopinatus*, all the Neoplecostominae, and most of the Hypoptopomatinae, the anterior portion of the compound supraneural–first dorsal fin proximal radial (SN + PX1) contacts the neural spine of the seventh vertebra (Fig. 22A–C). In the derived condition, observed for some Hypoptopomatinae, the contact occurs posteriorly (eighth for *Epactionotus* and *Microlepidogaster perforatus*; ninth for *Microlepidogaster arachas*, *Microlepidogaster* sp. nov., *Rhinolekos britskii*, *Rhinolekos* sp. nov. 1 and 2; tenth for *Rhinolekos garavelloii*, *Rhinolekos schaeferi*, and *Microlepidogaster longicolla*; and 11th for *Acestridium martini*) (see Calegari & Reis, 2010: fig. 3; and Martins & Langeani, 2011b: fig. 1). Schaefer (1998) referred to *Microlepidogaster perforatus* as having the contact in the ninth vertebra. The derived condition is more common than previously thought, and it may be related to the increase in the number of vertebrae anteriorly to the dorsal-fin insertion, or because of a shift of the fin itself, thus we are unable to suggest reasons why the dorsal fin is positioned posteriorly in the body.

55. Spinelet [Schaefer, 1991 (36); 1998 (27)]: (0) present, locking mechanism functional; (1) present, reduced, locking mechanism nonfunctional (Fig. 11A); (2) absent (Fig. 11B). CI = 0.167; RI = 0.091.
56. Exposed area of nuchal plate [modified, Lehmann, 2006 (152)]: (0) reduced, not dorsally exposed; (1) its width greater than its length; (2) its length greater than its width; (3) quadrangular, length and width equivalent. CI = 0.250; RI = 0.400.

57. Longitudinal crest of compound supraneural–first dorsal fin proximal radial: (0) present, well developed; (1) present low, poorly developed; (2) absent. CI = 0.125; RI = 0.418.

In loricariids, the supraneural is fused to the first dorsal fin proximal radial (SN + PX1). This compound element can have a bony elevation, named the longitudinal crest here, running from the nuchal plate to the mid-anterior margin of the first dorsal fin proximal radial. In *Delturus carinotus*, all Neoplecostominae, and some Hypoptopomatinae, the crest is well developed (state 0). In *Harttia kronei*, *Hypostomus careopinatus*, and many Hypoptopomatinae species, the crest is low and poorly developed (state 1). In *Acestridium martini*, *Hisonotus piracanjuba*, *Otothyris lophophanes*, *Otothyris rostrata*, *Otothyris travassosi*, and *Microlepidogaster* sp. nov., the crest is completely absent (state 2).

58. Transverse process of first dorsal-fin pterygiophore exposed and bearing odontodes [Lehmann, 2006 (153)]: (0) absent; (1) present. CI = 0.500; RI = 0.800.

In *Delturus carinotus*, *Harttia kronei*, *Hypostomus careopinatus*, all Neoplecostominae, and most Hypoptopomatinae, the transverse process of the first dorsal-fin pterygiophore is covered by the dorsal plate series (state 0). An exposed transverse process (state 1) is exclusive for *Pseudotothyris*, *Otothyris*, and *Pseudotocinclus tietensis* (Fig. 11). Occasionally, some specimens of *Otothyris rostrata* and *Pseudotothyris obtusa* may have the plesiomorphic condition.

59. Adipose fin and azygous plates [modified; Gauger & Buckup, 2005 (52)]: (0) present; (1) absent; (2) only azygous plates; (3) only adipose fin. CI = 0.429; RI = 0.556.
60. First anal-fin pterygiophore contact [modified; Schaefer, 1987 (17)]: (0) 14th vertebra; (1) 13th vertebra (Fig. 22A); (2) 12th vertebra (Fig. 22B); (3) 11th vertebra (Fig. 22C); (4) 16th vertebra; (5) 15th vertebra. CI = 0.294; RI = 0.600.

As stated by Schaefer (1987), anterior displacement of the anal fin insertion seems to be a tendency in Loricariidae. In Astroblepidae, the articulation of the first anal-fin pterygiophore occurs at the 18th or posterior vertebrae (Schaefer, 1987). In *Lithogenes* the articulation occurs with the 19th or 20th vertebra (Schaefer, 2003b). *Delturus carinotus* has the anterior portion of the first anal-fin pterygiophore contacting the 14th vertebra. In all Neoplecostominae the contact is with the 15th vertebra (except for *Pareiorhaphis*, in which the contact is with the 16th vertebra). In the Hypoptopomatinae the contact

varies from the 11th to 16th. The most basal species of the Hypoptopomatinae have the anal fin articulating with the 14th vertebra, a lower number compared with the Neoplecostominae members. It is probably a consequence of loss of vertebrae between the anal and dorsal-fin insertions, resulting simultaneously in the anterior displacement of the anal fin and reduction in the number of vertebrae (see comments on character 46 for more details on vertebrae loss). This probably happened repeated times within the subfamily as many derived species have the anal articulation more forward and also a more reduced number of vertebrae.

61. Pterygiophore anterior to anal-fin base [Lehmann, 2006 (157)]: (0) covered by skin; (1) partially or totally covered by central or lateral plates, not bearing odontodes; (2) single central plate fused to the pterygiophore, bearing odontodes. CI = 0.200; RI = 0.667.
62. Number of caudal-fin branched rays [Schaefer, 1991 (35)]: (0) 14; (1) 12; (2) ten. CI = 0.667; RI = 0.750.
63. Pectoral spine medial serrae [modified; Schaefer, 1991 (39); 1998 (29)]: (0) absent; (1) present only in juveniles; (2) present in juveniles and adults. CI = 0.222; RI = 0.650.

The species with juveniles not examined, but whose adults always had the medial serrae absent were coded as polymorphic (0, 1), because we know that these are the only codification possibilities.

64. Arrector fossae in pectoral skeleton in adults [modified; Schaefer, 1991 (41); 1998 (30); Gauger & Buckup, 2005 (30)]: (0) totally opened, arrector ventralis muscle totally exposed; (1) partially closed, opening relatively large, extending laterally halfway towards the base of the pectoral fin; (2) partially closed, opening restricted to a small area near the ventral midline; (3) partially closed, opening represented only by a small fenestra in the middle half of the pectoral girdle; (4) totally closed. CI = 0.308; RI = 0.743.

Schaefer (1991, 1998) suggested the pectoral girdle morphology as a diagnostic feature for the Hypoptopomatinae, which is characterized by the ventral laminar extensions of the cleithrum and coracoid partially or totally covering the arrector fossae [char. 40 (39), 1991 (1998)]. Furthermore, the ventral surface of the pectoral girdle can be variably exposed, bearing few to many odontodes. In Neoplecostominae, the cleithrum and coracoid do not have any ventral laminar expansion and consequently the arrector fossae are completely opened and do not bear odontodes ventrally; thus, the pectoral girdle is not exposed (Fig. 23A). In most basal hypoptopomatines,

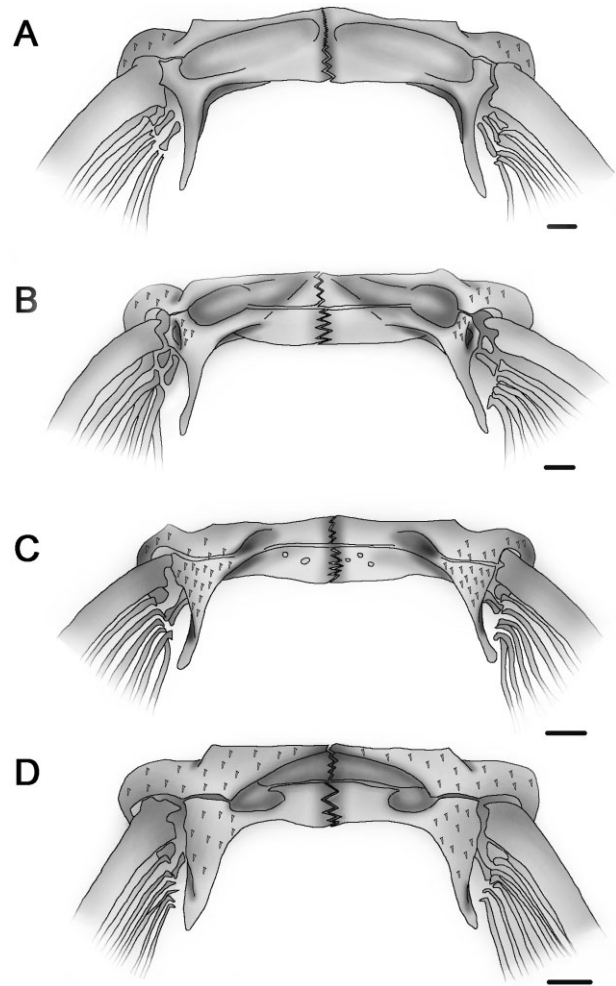


Figure 23. Pectoral girdle in ventral view. A, *Kronichthys heylandi*, DZSJRP 12498, 49.4 mm standard length (SL), male. B, *Plesioptopoma curvidens*, DZSJRP 16133, 51.4 mm SL, female. C, *Rhinolekos britskii*, DZSJRP 6983, 36.0 mm SL, female. D, *Pseudotocinclus tietensis*, LBP 2964, 53.3 mm SL, female. Scale bars = 1 mm.

the ventral laminar expansions are restricted to the most lateral portions, near ray insertions, covering the arrector fossae only partially (Fig. 23B, C), such that the pectoral girdle is exposed only laterally. Within the Hypoptopomatinae, laminar expansions of the cleithrum and coracoid tend to increase toward the midline of the pectoral girdle, restricting or completely closing the arrector fossae (Figs 23D, 24A, B), and increasing the exposed area of the pectoral girdle. Ontogenetically, it is possible to observe the gradual closing of the arrector fossae. In *Pseudotocinclus*, the juveniles have the arrector fossae partially closed, restricted to small portions near to the pectoral-fin suture. In adults, the development of laminar expansions is complete, and the arrector fossae are completely closed.

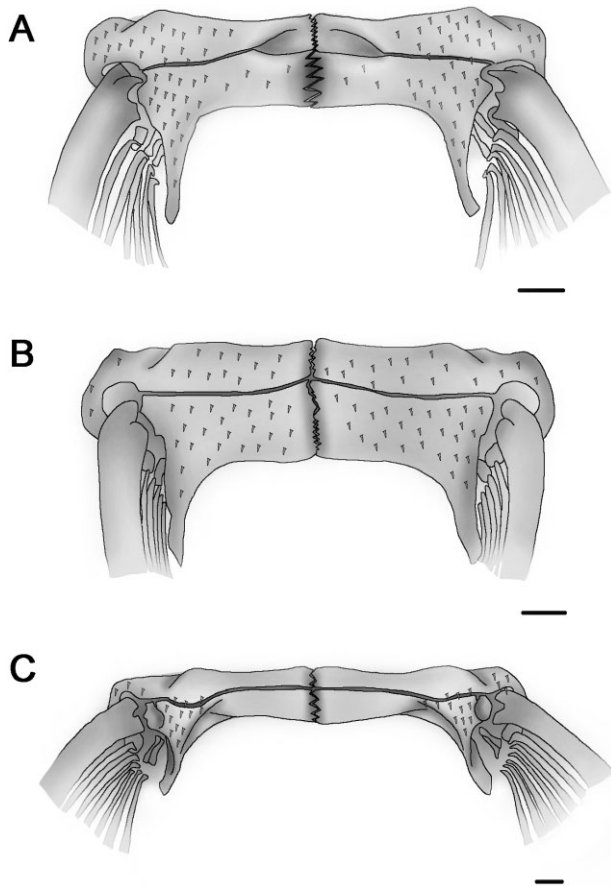


Figure 24. Pectoral girdle in ventral view. A, *Epactionotus bilineatus*, DZSJRP 11358, 32.9 mm standard length (SL), female. B, *Pseudotothyris obtusa*, MCP 31726, 24.2 mm SL, female. C, *Gymnotocinclus anosteos*, UFRGS 11296, 43.7 mm SL, male. Scale bars = 1 mm.

Gymnotocinclus, *Microlepidogaster* sp. nov., and *Nannoplecostomus* have a different condition, with a peculiar morphology of the pectoral girdle (state 3). In these taxa, the cleithrum and coracoid have laminar expansions only laterally; however, the arrector fossae are almost completely closed as the muscle is exposed ventrally only by a small fenestra in the middle half of the pectoral girdle (Carvalho, Lehmann & Reis, 2008: fig. 6). Occasionally the arrector fossae are completely closed, as occurs in some specimens of *Gymnotocinclus* (Fig. 25C).

65. Pectoral girdle exposure [Gauger & Buckup, 2005 (53)]: (0) not exposed ventrally (Fig. 23A); (1) exposed only laterally, with many odontodes on a thin skin (Figs 23C, D, 24C); (2) totally exposed, sometimes with a median area covered by skin (Fig. 24A, B); (3) exposed only laterally, with few odontodes immersed in a thick skin (Fig. 23B). CI = 0.273; RI = 0.652.

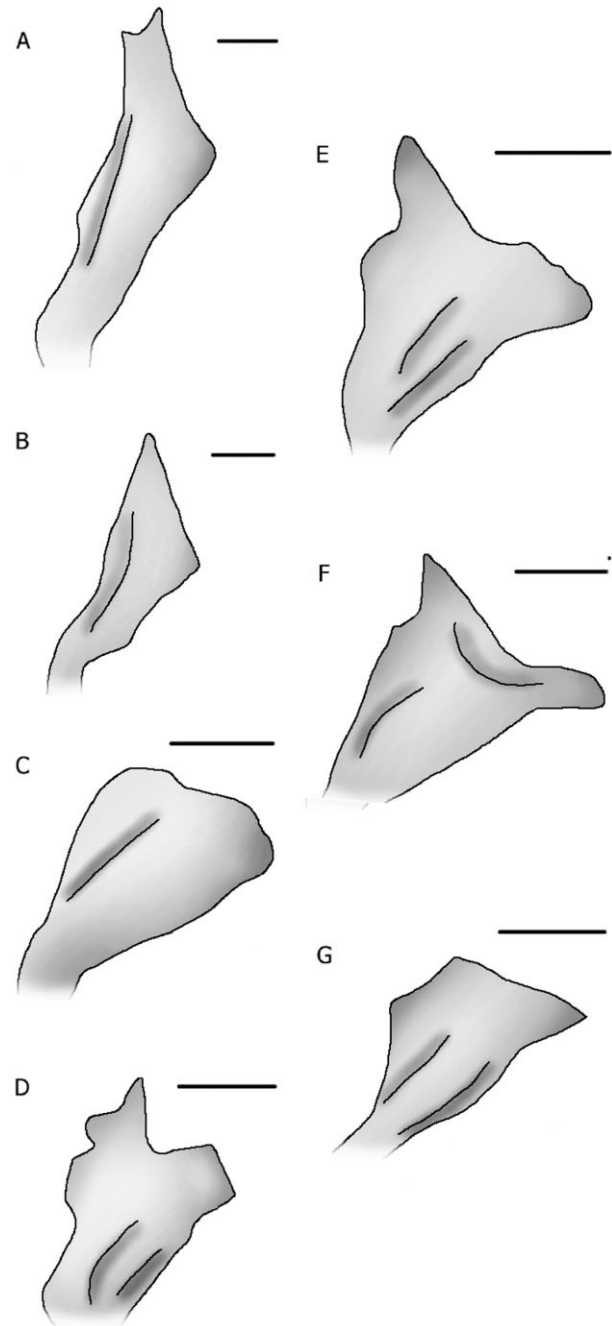


Figure 25. Cleithrum humeral process in lateral view. A, *Neoplecostomus microps*, DZSJRP 2144, 62.8 mm standard length (SL), female. B, *Gymnotocinclus anosteos*, UFRGS 11296, 43.7 mm SL, male. C, *Ootothyropsis marapoama*, DZSJRP 9937, 26.3 mm SL, sex undetermined. D, *Hisonotus piracanjuba*, DZSJRP 13233, 23.7 mm SL, female. E, *Schizolecis guntheri*, DZSJRP 6525, 32.9 mm SL, sex undetermined. F, *Pseudotothyris obtusa*, MZUSP 69411, 23.1 mm SL, male. G, *Ootothyris travassosi*, MNRJ 22947, 22.3 mm SL, female. Scale bars = 1 mm.

See comments for character 63.

66. Cleithrum humeral process, in lateral view [modified; Lehmann, 2006 (124)]: (0) not projected posteriorly; (1) posteriorly projected, with truncated to rounded ending; (2) posteriorly projected, with pointed ending. CI = 0.154; RI = 0.560.

Delturus carinotus, *Harttia kronei*, *Isbrueckerichthys duseni*, *Neoplecostomus microps*, and *Pareiorhina rudolphi* have the humeral process of cleithrum not posteriorly projected (state 0, Fig. 25A, B), resulting in a naked area between the cleithrum and body lateral plates. Amongst the Hypoptopomatinae, this state is also shared by *Gymnotocinclus anosteos*, *Lampiella gibbosa*, *Nannoplecostomus eleonora*, and *Parotocinclus jumbo*. In all other analysed taxa, the humeral process of cleithrum is posteriorly projected, with its ending either truncated (state 1, Fig. 25C, D) or pointed (state 2, Fig. 25E, F). *Pseudotothyris* shares with *Otothyris*, and also with *Acestridium martini*, *Epactionotus*, *Hisonotus chromodontus*, *Niobichthys*, *Otocinclus affinis*, and *Schizolecis guntheri*, the presence of a humeral process with a pointed ending.

67. Basipterygium [modified; Schaefer, 1991 (43); 1998 (31)]: (0) anteriorly opened, presence of fenestrae posterior to anterior margin; (1) anteriorly solid, without fenestrae. CI = 0.911; RI = 0.500.

Dermal plates

68. Median plate series: (0) without nonperforated or missing plates through the series (Schaefer, 1997: fig. 3b); (1) one to three nonperforated or missing plates through the series (Schaefer, 1997: fig. 3a); (2) four or more nonperforated or missing plates through the series (Schaefer, 1997: fig. 3e–h); (3) compound only by five or fewer perforated plates right after compound pterotic (Schaefer, 1997: fig. 3c, d). CI = 0.267; RI = 0.389.
69. Mid-dorsal plate series [modified; Schaefer, 1998 (32)]: (0) complete; (1) truncated very posteriorly, plates surpassing the dorsal-fin length; (2) truncated posteriorly, plates reaching no more than the dorsal-fin length; (3) truncated anteriorly, with only six or fewer plates; (4) truncated in the middle of the series, approximately seven to ten plates missing; (5) totally absent. CI = 0.313; RI = 0.313.

Most loricariids have five series of plates laterally (except for *Lithogenes*, with only three lateral plate series: dorsal, median, and ventral; and some Delturinae, such as *Delturus carinotus* and *Hemipisilichthys gobio*, that have six lateral plate series as there are two dorsal series). In most Hypostominae,

all lateral plates series are complete until the end of the caudal peduncle (state 0). The same occurs amongst the Delturinae, except for the extra dorsal series, which is truncated. In the Neoplecostominae (except for *Isbrueckerichthys duseni*, which is polymorphic for this feature), Hypoptopomatinae, and the Loricariinae, only the dorsal, median and ventral series reach the end of the caudal peduncle. In *Harttia kronei*, all Neoplecostominae and most Hypoptopomatinae, the mid-dorsal series is truncated very posteriorly in the body, surpassing the addressed dorsal fin, however it never reaches the caudal-peduncle end (state 1; Schaefer, 1997: fig. 3c–h). In some *Hisonotus*, some *Microlepidogaster*, *Nannoplecostomus*, *Niobichthys*, *Otothyris*, and *Oxyropsis*, the decrease in number of plates is greater, and the mid-dorsal series may either reach, but never surpass, the addressed dorsal fin (state 2; Schaefer, 1997: fig. 3a), or it may be restricted to six or fewer plates in the anterior portion of the body (state 3; Schaefer, 1997: fig. 3b). In *Parotocinclus maculicauda* and *Hisonotus notatus* there is a gap in the middle of the series (state 4), and in *Acestridium martini* the mid-dorsal series is completely absent (state 5). Amongst the five lateral series of plates, the mid-dorsal and midventral series are the last to ossify during ontogenetic development. Opposite to the other three series (dorsal, ventral, and median), these series become ossified from the anterior to the posterior portion of the body. Based on this, the reduction in mid-dorsal series found in some Hypoptopomatinae, such as *Otothyris* and *Acestridium martini*, can be interpreted as retention of a juvenile feature in adults. This character was coded as inapplicable for *Gymnotocinclus anosteos* because of the generalized loss of plates in this species. This is also true of characters 69 and 70.

70. Ventral plates contacting or almost contacting at the midline anterior to anal-fin origin: (0) absent, plates very far from each other; (1) present. CI = 0.250; RI = 0.667.
71. Postanal ventral plates contacting at the midline (Gauger & Buckup, 2005 [51]): (0) present, one or more plates contacting; (1) absent. CI = 1.000; RI = 1.000.
72. Odontodes on lateral plates [modified; Schaefer, 1998 (41)]: (0) aligned, forming conspicuous series; (1) enlarged odontodes concentrated along posterior plate margin; (2) randomly distributed. CI = 0.167; RI = 0.375.
73. Abdominal covering [Gauger & Buckup, 2005 (56)]: (0) completely naked; (1) partially covered by dermal plates, with naked areas; (2) completely covered. CI = 0.143; RI = 0.571.
74. Abdominal dermal plate size [Gauger & Buckup, 2005 (55)]: (0) small, generally irregularly

distributed; (1) large, generally distributed in longitudinal series. CI = 0.167; RI = 0.643.

75. Lateral abdominal plates: (0) absent; (1) present, easily distinguishable from other abdominal plates (Calegari *et al.*, 2011: fig. 5). CI = 1.000; RI = 1.000.
76. Anterodorsal portion of snout [modified; Schaefer, 1991 (51); 1998 (34)]: (0) naked or bearing numerous small plates (Martins & Langeani, 2011b: fig. 2); (1) with four long plates (Fig. 3A, C); (2) with two plates (Fig. 3B); (3) with a single rostral plate (Ribeiro *et al.*, 2005: fig. 3). CI = 0.273; RI = 0.750.

Schaefer (1998) considered as apomorphic the presence of a paired or a single median rostral plate, and as plesiomorphic the anterior margin of snout naked or comprised of numerous plates. Here, we preferred to subdivide this character into four different states. Most Loricariidae have the anterior portion of the snout naked or bearing many small plates (state 0), a feature shared by *Delturus carinotus*, *Harttia kronei*, *Hypostomus careopinnatus*, all Neoplecostominae, and some basal Hypoptopomatinae. In other Hypoptopomatinae, although the snout is completely covered, there is a decrease in the number of plates present in the region. In *Pseudotothyris* and *Schizolecis*, four medium-sized elongate plates are present (state 1). In *Corumbataia tocantinensis*, homoplatically there are also four plates; however, they are small and quadrangular in shape. In *Otothyris*, there are only two medium-sized plates (state 2) because of the loss of two plates compared with the pattern observed in *Pseudotothyris* and *Schizolecis*. *Hisonotus luteofrenatus*, *Hisonotus insperatus*, and *Hisonotus piracanjuba* also have two plates on the anterior portion of the snout, which are distinct from and not homologous with those of *Otothyris*; this state was suggested as a synapomorphy uniting these three *Hisonotus* species by Martins & Langeani (2012). By contrast, the other species of *Hisonotus*, as well as *Epactionotus*, *Hypoptopoma*, *Lampiella*, *Nannoplecostomus*, *Otocinclus*, *Otothyropsis*, and most *Parotocinclus* species have a single large plate on the anterior-most portion of the snout (state 3).

77. Posterior margin of rostral plate (only for species with one or two rostral plates): (0) straight; (1) with a U- or V-shaped concavity (Calegari *et al.*, 2011: fig. 6). CI = 0.167; RI = 0.500.
78. Ventral projection of snout anterior plates (only for species with one to four rostral plates): (0) absent (Fig. 26A); (1) present (Fig. 26B–D). CI = 0.300; RI = 0.818.
79. Ventromesial margin of rostral plate(s) (only for species with rostral plate(s) ventrally projected)

[modified; Schaefer, 1998 (35)]: (0) without or with a small notch (Fig. 26B); (1) with a notch articulating with the mesethmoid (Fig. 26C); (2) with a rectangular projection (Fig. 26D). CI = 0.222; RI = 0.125.

80. Nasal size: (0) small, restricted to the laterosensory canal (Fig. 3A); (1) medium-sized, expanded mesially to laterosensory canal; however, clearly smaller than infraorbital 2 (Fig. 3B, C); (2) large, size comparable to infraorbital 2. CI = 0.154; RI = 0.083.
81. Lateronasal plate: (0) present, between infraorbital 2 and lateral edge of nasal chamber (Fig. 4A, E); (1) absent, infraorbital 2 forming the lateral edge of nasal chamber (Fig. 4B–D). CI = 0.167; RI = 0.444.

Most Loricariidae have infraorbital 2 surrounding the nasal chamber. Recently, Martins & Langeani (2011b) described *Rhinolekos* as having a large plate between infraorbital 2 and the nasal chamber, the lateronasal plate. This plate was also observed in *Delturus carinotus*, *Isbrueckerichthys duseni*, and amongst the Hypoptopomatinae in *Acestridium martini*, *Parotocinclus jumbo*, and *Gymnotocinclus anosteos*.

82. Postrostral plate 2: (0) present, as a single element; (1) fused to postrostral plate 3; (2) fused to postrostral plate 1; (3) fused to infraorbital 2. CI = 0.600; RI = 0.800.

Loricariids have a series of postrostral plates in the lateroventral portion of the head. In the Hypoptopomatinae, four is the plesiomorphic number of postrostral plates (state 0, Fig. 3A). In *Pseudotothyris*, *Otothyris*, and in all analysed Hypoptopomatini (except for *Hypoptopoma*), postrostral plate 2 is apparently fused to postrostral plate 3 (state 1, Fig. 3B, C). In *Nannoplecostomus* this fusion occurs with postrostral plate 1 (state 2). Finally, in *Hisonotus depressicauda*, it seems to be fused to infraorbital 2 (state 3).

83. Contact between postrostral plate 4 (or posterior) and infraorbital series [modified; Lehmann, 2006 (2)]: (0) absent, with small plates in between; (1) present, with infraorbitals 2, 3, and 4; (2) present, with infraorbitals 3 and 4; (3) present, only with infraorbital 2; (4) present, with infraorbitals 2 and 3. CI = 0.231; RI = 0.545.

Miscellaneous

84. Odontode size at anterior margin of snout [modified; Schaefer, 1998 (39); Calegari, 2010 (46)]: (0) equally small, similar to others on the head, dorsal and ventrally; (1) unequally enlarged, odontodes at dorsal portion larger than the ventral ones; (2) equally enlarged, both in dorsal

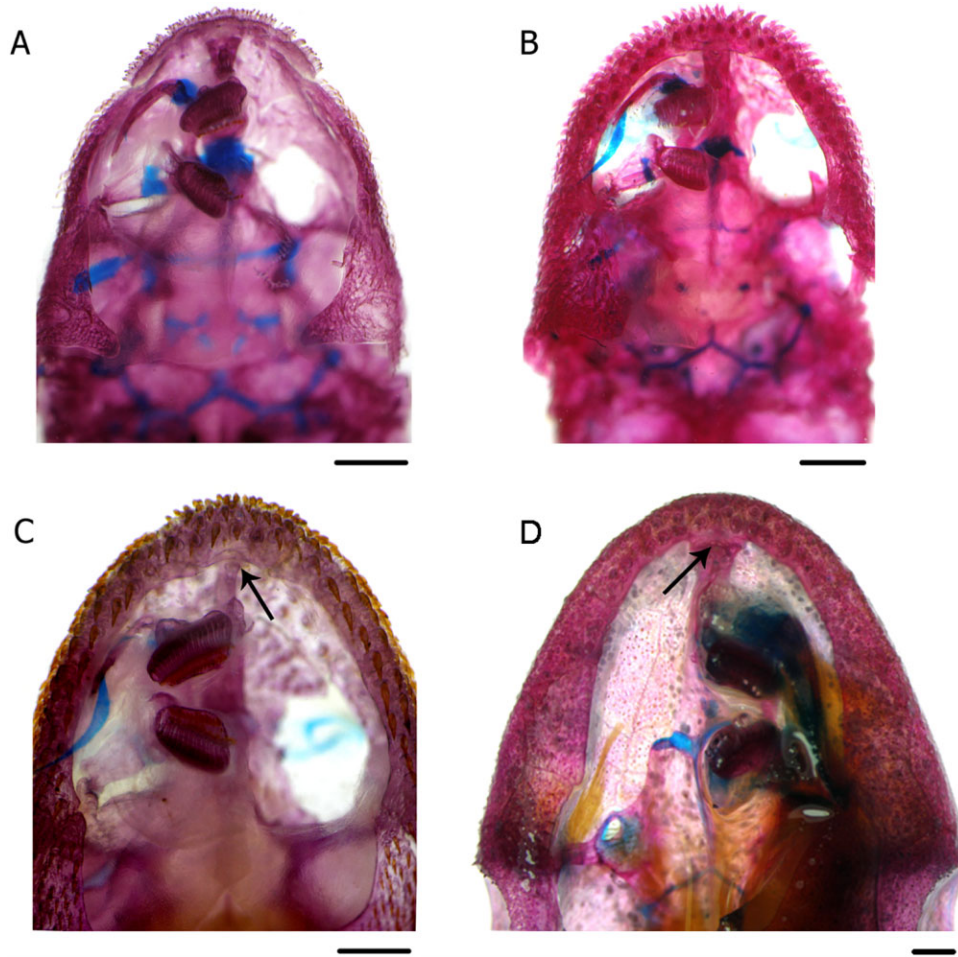


Figure 26. Skull in ventral view. A, *Pseudotothyris obtusa*, MCP 31726, 24.2 mm standard length (SL), female. B, *Otothyropsis marapoama*, DZSJRP 9937, 26.3 mm SL. C, *Hisonotus notatus*, DZSJRP 13852, 31.5 mm SL, male. D, *Hypoptopoma inexpectata*, DZSJRP 15807, 64.6 mm SL, female. Arrows show the notch (C) and the projection (D) at the ventromesial margin of the rostral plate. Scale bars = 1 mm.

and ventral portions; (3) unequally enlarged, odontodes at ventral portion larger than the dorsal ones. CI = 0.429; RI = 0.846.

Amongst the Loricariidae with one or more plates on the anterior margin of the snout, most possess small odontodes on these plates, similar to others on the head and trunk (state 0). This plesiomorphic condition is shared by *Delturus carinotus*, *Harttia krontei*, *Hypostomus careopinnatus*, all Neoplecostominae, and most of the Hypoptopomatinae. Amongst the Hypoptopomatinae we observed a tendency for enlargement of the odontodes in the most anterior portion of the snout. This enlargement may be homogeneous between the dorsal and ventral margins (state 2), as in the Hypoptopomatini (except for *Hypoptopoma* and *Niobichthys*), *Hisonotus*, *Lampiella*, *Nannoplecostomus*, *Otothyris*, *Parotocinclus*, and *Schizolecis* (Fig. 1A). Alternatively, the enlargement

may be unequal, with well-developed odontodes restricted either to the ventral margin (state 3, present in *Epactionotus* and *Hypoptopoma*) or to the dorsal margin (state 1, present in *Pseudotothyris*, Fig. 1B). The presence of well-developed odontodes only at the dorsal margin of the snout is a uniquely derived synapomorphy for *Pseudotothyris*, contrary to Schaefer (1998), who referred to this state as being shared by *Pseudotothyris* and *Otothyris*; *Otothyris*, according to our analysis, has well-developed odontodes in both the ventral and dorsal margins of the snout.

85. Odontodes shape at anterodorsal margin of snout: (0) with pointed margin (Fig. 1A, B; Martins & Langeani, 2011a: fig. 2c–f); (1) with rounded margin, leaf-shaped in dorsal view of head (Martins & Langeani, 2011a: fig. 2a, b). CI = 0.200; RI = 0.200.

86. Orientation of odontodes at anterior portion of snout: (0) recurved dorsally; (1) recurved in both directions, dorsally and ventrally (Fig. 1A, B). CI = 0.143; RI = 0.455.
87. Well-developed odontodes at posterior margin of parietosupraoccipital in adults [modified; Schaefer, 1998 (20)]: (0) absent; (1) present, three to five odontodes; (2) present, numerous, forming an oval area; (3) present, numerous, forming an elongate rectangular area. CI = 0.429; RI = 0.636.
88. Maxillary barbel: (0) free from the lip distally; (1) completely adnate to the lip. CI = 0.200; RI = 0.429.
89. Iris operculum [Schaefer, 1998 (42)]: (0) present; (1) absent. CI = 0.167; RI = 0.583.

The iris operculum is a projection that expands or retracts according to light conditions (Douglas, Collin & Corrigan, 2002). This structure is absent in *Lithogenes*. However, within the Loricariidae, the iris operculum is present in most species. Amongst the taxa analysed here, *Delturus carinotus*, *Harttia kronei*, *Hypostomus careopinnatus*, all Neoplecostominae, and most of the Hypoptopomatinae have an iris operculum present. In the Hypoptopomatini (except for *Otocinclus* and *Acestridium*), *Otothyris*, *Pseudotothyris*, *Schizolecis*, and *Microlepidogaster perforatus*, the iris operculum is absent. Some specimens of *Pseudotothyris* have the iris dorsoventrally flattened, which may work as a different control mechanism of light input.

90. First pelvic-fin ray dorsal skin flap, in males [Schaefer, 1998 (45)]: (0) absent; (1) present. CI = 0.200; RI = 0.500.

Males of *Delturus carinotus*, *Harttia kronei*, and *Hypostomus careopinnatus* do not have any skin flap on the pelvic fin (state 0). By contrast, males of most neoplecostomines and hypoptopomatines share the presence of a dorsal skin flap on the first pelvic-fin ray (state 1); the function of which is still unknown. Sometimes skin flaps are also present on other branched rays of the pelvic fin but are poorly developed. A dorsal skin flap on the first pelvic-fin ray has even been observed in some females, although underdeveloped, as related by Martins & Langeani (2012) for *Hisonotus piraicanjuba*. Amongst the Neoplecostominae and the Hypoptopomatinae, the absence of this structure in males, as found in *Kronichthys*, *Pareiorhina*, *Epactionotus*, *Schizolecis*, and many Hypoptopomatini members, is an apomorphic feature that has evolved many independently times.

91. Nasal chamber sexual dimorphism: (0) absent, males and females with equal nasal chamber

size; (1) present, males with dilated nasal chamber, wider and longer than in females. CI = 0.111; RI = 0.636.

Martins & Langeani (2011a: fig. 3), describing *Microlepidogaster dimorpha*, reported a sexual dimorphism characterized by a dilated nasal chamber in males. This kind of sexual dimorphism appears in many other hypoptopomatines, being more common than previously thought. In addition to the Hypoptopomatinae, we only found the character in *Pareiorhina rudolphi*. The character was considered undetermined for taxa for which specimens of both sexes are unavailable.

92. Pectoral-fin axillary slit [modified; Gauger & Buckup, 2005 (57)]: (0) absent in both adults and juveniles; (1) present only in juveniles; (2) present in both adults and juveniles. CI = 0.286; RI = 0.821.

A pectoral-fin axillary slit has been reported for many Hypoptopomatinae species and other Siluriformes, such as Aspredinidae, Auchenipteridae, Callichthyidae, Cetopsidae, Doradidae, Heptapteridae, Pimelodidae, and Pseudopimelodidae (Reis & Schaefer, 1998; Martins & Langeani, 2011b). Amongst other loricariids, a pectoral-fin axillary slit is also present in the Loricariinae, Hypostominae, and Neoplecostominae (Lithogeneinae had not yet been analysed). For *Isbrueckerichthys duseni*, *Neoplecostomus microps*, *Pareiorhina rudolphi* (Neoplecostominae), *Microlepidogaster arachas*, *Microlepidogaster longicolla*, *Pseudotocinclus tietensis*, and *Rhinolekos* (Hypoptopomatinae), the slit is present only in juvenile specimens, closing completely in adults (state 1). The pectoral-fin axillary slit in adults seems to have been lost independently many times. Rarely the slit is absent in both juveniles and adults (state 0), as observed in *Harttia kronei*, *Hypostomus careopinnatus*, *Otothyris*, and *Schizolecis*. The pectoral-fin axillary slit is frequently present in *Pseudotothyris* species, with the exception of specimens of two populations of *Pseudotothyris janeirensis* (MZUSP 80211, 80213) in which the slit is absent in adults; it is possible to see a mark in the slit position. The species with juveniles not examined, but whose adults always had the pectoral axillary slit absent were coded as polymorphic (0, 1) because we know that these are the only possibilities.

TOPOLOGY AND CHARACTER SUPPORT

Fifty-five equally parsimonious trees were recovered (overall length 760 steps; consistency index = 0.217; retention index = 0.566). The strict consensus tree is provided in Figure 27; the upper numbers on the

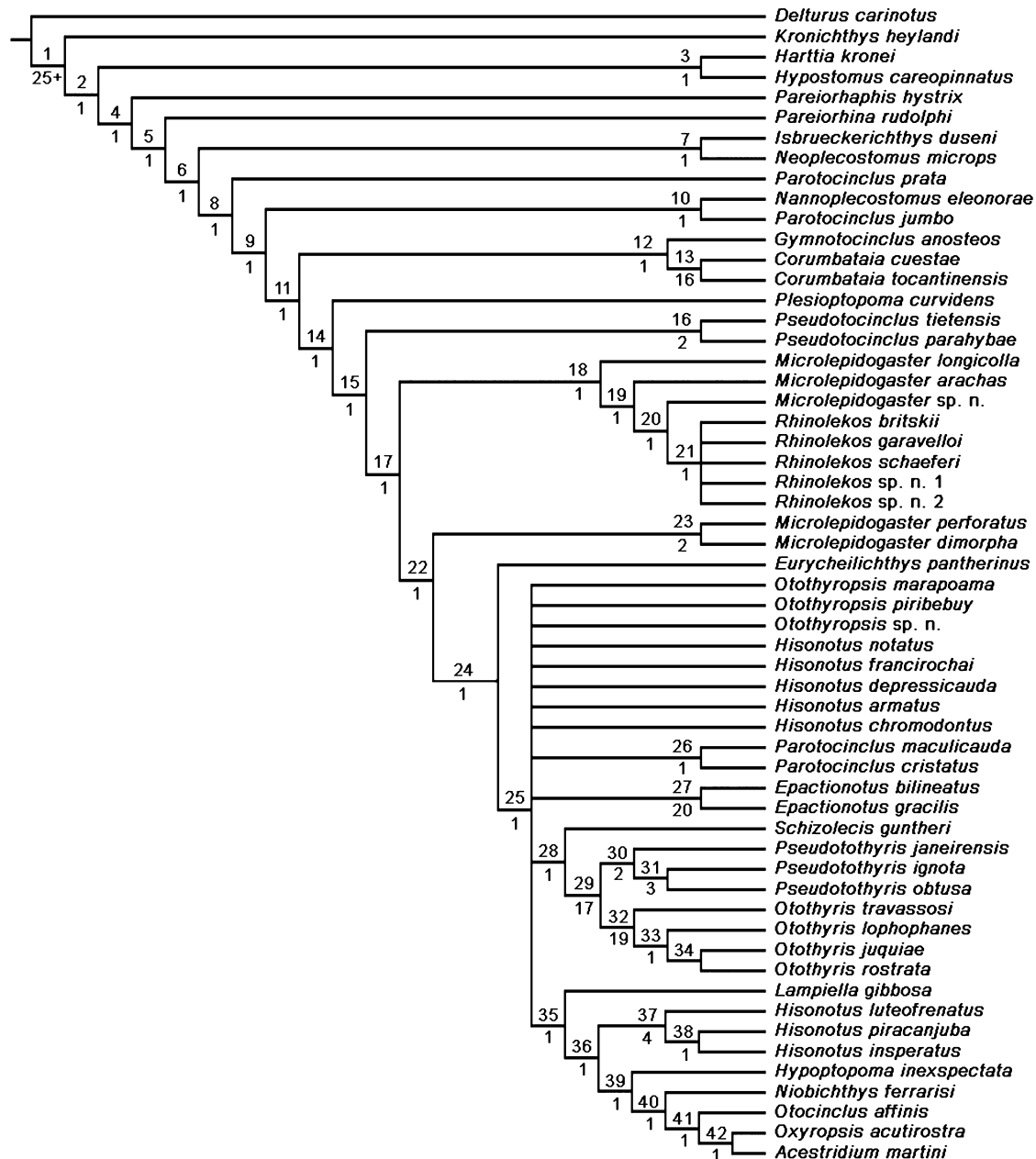


Figure 27. Strict consensus cladogram of 55 most parsimonious trees (760 steps; consistency index = 0.217; retention index = 0.566), showing the inter-relationships amongst Hypoptopomatinae species. Numbers above branches indicate the number of the clade and those below the branches correspond to the Bremer support values.

branch indicate the clade and the lower ones correspond to the Bremer support. A list of unambiguous synapomorphies for each clade and autapomorphies for each terminal taxon is given in Appendix 1.

General comments on Hypoptopomatinae

Hypoptopomatinae (*sensu* Schaefer, 1991, 1998) was recovered as a monophyletic group (clade 8), supported by three unambiguous synapomorphies: (1) suprapre-

opercle absent (char. 31, 0→1); (2) first anal-fin pterygiophore contacting the haemal spine of the 14th vertebra (char. 60, 5→0); (3) arrector fossae partially closed, opening relatively large (char. 64, 0→1).

We did not recover any of the six synapomorphies proposed by Schaefer (1998) to diagnose the subfamily. One of them, the arrector fossae completely closed (char. 30, state 2 in Schaefer, 1998) was recovered here in our analysis as a less inclusive synapomorphy,

appearing independently many times within the subfamily, mainly in the most derived clades; instead, the arrector fossae partially closed, with the opening relatively large, was the state optimized as a synapomorphy for Hypoptopomatinae.

The nasal capsule opened ventrally (char. 5, state 1 in Schaefer, 1998) and the presence of the metapterygoid channel (char. 13, state 1 in Schaefer, 1998) were also found in some Neoplecostominae members, and were not optimized here as synapomorphies for Hypoptopomatinae. These characters were probably recovered as synapomorphies by Schaefer (1998) because they are absent in *Neoplecostomus microps*, even though they are present in most neoplecostomines.

The presence of a median rostral snout plate (char. 34, state 1 in Schaefer, 1998), and the presence of enlarged odontodes on both the dorsal and ventral snout margins (char. 39, state 2 in Schaefer, 1998), were not optimized as synapomorphies because many recently described basal members of the Hypoptopomatinae maintain the plesiomorphic condition as found in loricariids, with the anterior portion of the snout naked or comprised of numerous small plates bearing poorly developed odontodes.

Finally, the last synapomorphy suggested by Schaefer (1998), the compound pterotic pierced by numerous enlarged fenestrae (char. 10, state 1 in Schaefer, 1998), was already considered by the author as ambiguous and after our subdivision of character 11 presented here, it no longer optimized as a synapomorphy.

More than 20 years have passed since the first phylogenetic hypothesis on the relationships of Hypoptopomatinae (Schaefer, 1991). Now, the diversity of the group is surprisingly greater than previously expected. In these last two decades, ten of the 20 valid Hypoptopomatinae genera have been described, and a similar situation is also true for the species – 56 in 1991, and 130 now, according to Eschmeyer (2012). The discovery of these new taxa, mainly the most basal ones, has had a great impact on phylogenetic studies of the Hypoptopomatinae. This justifies the divergent hypotheses presented by many authors, including us, since the first phylogenetic study for the subfamily (Schaefer, 1998; Gauger & Buckup, 2005; Ribeiro *et al.*, 2005; Lehmann, 2006; Calegari, 2010). Schaefer (1998) had already demonstrated the impact of the addition of new taxa on the available phylogenies. Other new species are being described and others are likely to be discovered in the near future; thus, we think that we are still far from a more definitive hypothesis concerning the phylogenetic relationships amongst the Hypoptopomatinae until we have addressed most of its real diversity.

Phylogenetic relationships amongst the Hypoptopomatinae genera

Only Hypoptopomatini was recovered as a monophyletic group in the present analysis, and the Otothyriini was found to be paraphyletic, as already suggested by other authors (Gauger & Buckup, 2005; Lehmann, 2006; Calegari, 2010).

We corroborated the monophyly of *Pseudotothyris*, *Otothyris*, and *Rhinolekos*, and also of *Corumbataia*, *Epactionotus*, and *Pseudotocinclus*, despite not analysing all of the valid species. *Microlepidogaster* was not recovered as monophyletic, and the present study is the first to address this possibility. *Hisonotus* and *Parotocinclus* were recovered as paraphyletic, as already suggested by other morphological and molecular studies (Schaefer & Provenzano, 1993; Gauger & Buckup, 2005; Lehmann, 2006; Cramer *et al.*, 2007, 2011; Chiachio *et al.*, 2008; Calegari, 2010). In addition, relationships amongst *Otothyropsis* species are also uncertain. *Parotocinclus* nomenclatural readjustments are in progress by P. Lehmann (pers. comm.) and *Hisonotus* is currently being analysed in a phylogenetic framework by one of us (F. O. M.).

Nannoplecostomus eleonora is a recently described genus with an uncertain position within the Loricariidae. Here, we found this taxon to belong to the Hypoptopomatinae, although it does not have the pectoral girdle exposed, the usual feature used to identify the group. This condition is also found in some specimens of *Parotocinclus jumbo*, the sister to *Nannoplecostomus*, according to our analysis. Despite this, *Nannoplecostomus* shares many other features with hypoptopomatines, including two synapomorphies (char. 31, state 1; char. 60, state 0) amongst the three proposed here. With respect to the pectoral girdle, the third synapomorphy, it is very similar to that found in *Gymnotocinclus* and *Microlepidogaster* sp. nov., in which the arrector fossae are almost totally closed, except for a fenestra where the muscle is ventrally exposed. Despite not being the synapomorphic condition for the Hypoptopomatinae clade, a closure of the arrector fossae is not found outside the subfamily. As in other hypoptopomatines, the head of *Nannoplecostomus* has a reduced number of plates when compared to other Loricariidae members. The snout has only one large median rostral plate and few prenasal plates, instead of numerous small plates covering the portion between the nares and the snout margin, as for most loricariids. Additionally, there are only three postrostral plates, and the plates between them and the infraorbital series are lacking. In other loricariids there is a higher number of postrostral plates, and they are not in contact with the infraorbital series because of the presence of many small plates between

them. Additionally, *Nannoplecostomus eleonora* has the first anal-fin pterygiophore contacting the haemal spine of the 14th vertebrae. This may be linked to the reduced number of vertebrae presented by the species (26 in the specimen observed by us). This process of loss of vertebrae and anteriorization of the anal-fin insertion is common to many Hypoptopomatinae species as commented upon above (see char. 60).

Finally, *Pseudotocinclus* was recovered inside the Hypoptopomatinae, as in all other previous morphological studies (Schaefer, 1991, 1998; Gauger & Buckup, 2005; Lehmann, 2006; Calegari, 2010), differing from the molecular results that include the genus in the Neoplecostominae (Cramer *et al.*, 2007, 2011; Chiachio *et al.*, 2008). Chiachio *et al.* (2008) went even further, proposing some morphological features that could reinforce its placement in the Neoplecostominae. According to them, *Pseudotocinclus* has the pectoral girdle very distinct from Hypoptopomatinae genera and similar to *Pareiorhina* and *Neoplecostomus*. However, the pectoral girdle in *Pseudotocinclus* is clearly different from the state present in the Neoplecostominae (arrector fossae completely opened, without ventral laminar shelves in either the cleithrum or coracoid); *Pseudotocinclus* arrector fossae are partially closed by the cleithrum and coracoid laminar expansions bearing odontodes, resulting in a pectoral girdle exposed laterally. This condition was also verified in other hypoptopomatines, such as *Rhinolekos*, *Parotocinclus jumbo*, and *Parotocinclus prata*. Chiachio *et al.* (2008) also suggested four other features distinguishing *Pseudotocinclus* from other Hypoptopomatinae: (1) eyes dorsally positioned, which is an error because the genus has eyes dorsolaterally placed; (2) preopercle exposed, present in all examined Neoplecostominae and Hypoptopomatinae, (except in the Hypoptopomatini); (3) abdomen covered by numerous small plates, which is the plesiomorphic condition for the Hypoptopomatinae, present in most of its species, mainly the most basal ones; and (4) 26 or more plates in the median lateral series, a feature also occurring in *Eurycheilichthys*, *Rhinolekos*, *Microlepidogaster longicolla*, *Epactionotus*, *Acestridium*, some *Oxyropsis*, and *Parotocinclus jumbo*. Therefore, based on morphological data *Pseudotocinclus* is a hypoptopomatine.

Phylogenetic relationships of Pseudotothyris

Schaefer (1991) questioned the validity of *Pseudotothyris* because of the lack of any uniquely derived synapomorphies for the genus. The author also suggested as inadequate the two proposed features by Britski & Garavello (1984) to diagnose the genus: the presence of small plates and small odontodes on the most anterior portion of the snout. Schaefer (1991) stated that small plates on the anterior portion of

the snout is a plesiomorphic condition amongst the Hypoptopomatinae, which is true; however, the pattern in *Pseudotothyris*, four medium-sized elongated plates, sequentially disposed, is clearly distinct from that found for the most basal members of the subfamily – snout with many small irregularly shaped plates, randomly distributed, frequently leaving a naked anteroventral area on the snout. Although not optimized as a synapomorphy for *Pseudotothyris* (see comments under char. 76), this feature is clearly important for diagnosing the genus amongst the Hypoptopomatinae. The odontodes of the most anterior portion of the snout, according to Schaefer (1991) are not distinguishable in shape and size from the other ones in the head; however, in all *Pseudotothyris* specimens examined by us, the odontodes of the anterodorsal margin of the snout are clearly larger than the ones present in the ventral portion, which are similar in size to the others on the head, a condition unique to *Pseudotothyris* amongst the Hypoptopomatinae.

Thus, *Pseudotothyris* is recovered as a monophyletic group (clade 30) supported by two unambiguous synapomorphies: (1) accessory element of ceratobranchial 4 stick-shaped (char. 37, 1→2); and (2) odontodes at the anterior margin of the snout well developed only in the dorsal portion (char. 84, 2→1). Within the Hypoptopomatinae, this last feature is an exclusive synapomorphy for the genus. It was previously observed by Schaefer (1998, char. 39, state 1); however, he also considered this feature to be present in *Otothyris*, a condition not verified by us. All *Otothyris* specimens examined here have well-developed odontodes dorsally and ventrally (Fig. 1).

Schaefer (1991) only included *Pseudotothyris obtusa* in his specimens examined; however, based on the new results presented here, the author examined two species: *Pseudotothyris obtusa* (MCP 12556, from Juquiá/SP) and *Pseudotothyris ignota* (MCP 10706, from Joinville/SC). In his re-analysis, Schaefer (1998) supposedly examined *Pseudotothyris obtusa* and *Pseudotothyris janeirensis*; however, the author examined only *Pseudotothyris ignota* (MCP 10706), as the specimen referred to as *Pseudotothyris janeirensis* is in fact *Otothyris travassosi* [USNM 300905, decoupled from MZUSP 39099, and cited by Garavello *et al.* (1998) as 'other material' in the *Otothyris travassosi* original description]. Based on these specimens, Schaefer (1991, 1998) proposed as the single synapomorphy for *Pseudotothyris* the absence of the subocular cheek plate (called by him the subopercular plate). This is our character 32, state 1 and was not recovered as a synapomorphy for the genus. Although the subocular plate is absent in *Pseudotothyris janeirensis*, the other two species of the genus are polymorphic for this feature, being the most common

situation the presence of the subocular plate. Additionally, we did not recover the synapomorphy proposed by Ribeiro *et al.* (2005): absence of the spinelet (our char. 55, state 0). Although the absence of the spinelet is shared by *Pseudotothyris obtusa* and *Pseudotothyris ignota* (and also verified in *Schizolecis guntheri*), this element is present in *Pseudotothyris janeirensis*, as well as in *Otothyris* species.

Our results also contradict Chiachio *et al.* (2008), who suggested that *Pseudotothyris* is paraphyletic. This study was, to date, the only one to include the two valid species of the genus (*Pseudotothyris obtusa* and *Pseudotothyris janeirensis*); however, according to the localities, the species identified as *Pseudotothyris obtusa* is *Pseudotothyris ignota* based on the results presented here. Furthermore, the specimens indicated as *Pseudotothyris janeirensis* (MHNG 2586.95), from rio Taiaçupeba, upper rio Tietê basin, upper rio Paraná drainage, are not that species. This lot, now in the Geneva Museum of Natural History, decoupled from MCP 20100, was previously identified by J. C. Garavello as *Hisonotus depressicauda*, which seems to be the case, as *Pseudotothyris* does not occur in the upper rio Paraná drainage.

Within the genus, the clade composed of *Pseudotothyris obtusa* and *Pseudotothyris ignota* (clade 31) is supported by three unambiguous synapomorphies: (1) hyomandibula posterior margin not sutured to compound pterotic (char. 23, 1→0); (2) spinelet absent (char. 55, 1→2); and (3) odontodes on lateral plates randomly distributed (char. 72, 0→2).

As already verified by Schaefer (1998), we also recovered the three coastal genera as a monophyletic group, *Schizolecis* + (*Pseudotothyris* + *Otothyris*) (clade 28). Our results diverge from Ribeiro *et al.* (2005), who positioned *Pseudotothyris* + *Otothyris* as the sister group of *Otothyropsis*, a genus with a distribution in the Paraná-Paraguay basin. Here, *Otothyropsis* species have an uncertain position.

The *Pseudotothyris* and *Otothyris* clade, already suggested as monophyletic by many morphological studies (Schaefer, 1991, 1998; Gauger & Buckup, 2005; Ribeiro *et al.*, 2005; Lehmann, 2006; Calegari, 2010), is supported by ten unambiguous synapomorphies: (1) compound pterotic with a very elongate posterior extension surpassing the rib of sixth vertebra (char. 10, 0→1); (2) all compound pterotic fenestrae large and irregular in shape (char. 11, 1→2), feature shared only by these genera, *Otothyropsis*, and *Acestridium*; (3) only four infraorbitals (char. 14, 1→2), shared by these genera and *Microlepidogaster* sp. nov.; (4) first element of infraorbital series absent (char. 15, 0→2), uniquely derived synapomorphy; (5) accessory process of ceratobranchial 1 short, reaching 50% or less of ceratobranchial length (char.

36, 1→0); (6) dorsal process of ceratobranchial 5 absent (char. 39, 1→0); (7) central neural spine of seventh vertebra poorly developed (char. 49, 1→0); (8) transverse process of the first dorsal-fin pterygiophore dorsally exposed and bearing odontodes (char. 58, 0→1), present also in *Pseudotocinclus tietensis*; (9) postrostral plate 2 absent (char. 82, 0→1); and (10) numerous well-developed odontodes at parietosupraoccipital posterior margin, distributed in a rectangular elongate area (char. 87, 0→3), present also in *Oxyropsis*.

Additionally, *Otothyris* was recovered as monophyletic and supported by nine unambiguous synapomorphies: (1) mesethmoid just slightly projected anteriorly relative to the condyle (char. 1, 1→0); (2) mesethmoid anterolateral margin expanded (char. 3, 1→0); (3) bifid neural spines of seventh vertebra anterodorsally fused (char. 50, 1→3), uniquely derived within the Hypoptopomatinae; (4) 12 caudal-fin branched rays (char. 62, 0→1), feature also present in some *Acestridium* species; (5) pectoral spine medial serrae present in juveniles and adults (char. 63, 1→2); (6) median plate series incomplete, with a gap of four or more plates (char. 68, 1→2); (7) mid-dorsal plate series truncated, plates reaching no more than the dorsal-fin length (char. 69, 1→2); (8) large abdominal plates (char. 74, 0→1); and (9) anterodorsal portion of snout with two rostral plates (char. 76, 1→2).

In conclusion, although the phylogenetic relationships within the clade *Schizolecis* + (*Pseudotothyris* + *Otothyris*) seem to be clear, the position of the clade within the subfamily is still uncertain.

COMPARATIVE MATERIAL

Delturinae – *Delturus carinotus*: MCP not catalogued. Loricariinae – *Harttia kronei*: DZSJRP 3798 (1 c&s), rio Ribeira de Iguape basin. DZSJRP 13697 (3), rio Ribeira de Iguape basin. Hypostominae – *Hypostomus careopinnatus*: DZSJRP 12447 (68 + 2 c&s), paratypes, rio Paraguay basin. Neoplecostominae – *Isbrueckerichthys duseni*: DZSJRP 13662 (3), rio Ribeira de Iguape basin. DZSJRP 13623 (3), rio Ribeira de Iguape basin. DZSJRP 13670 (5 + 1 c&s), rio Ribeira de Iguape basin. *Kronichthys heylandi*: DZSJRP 12498 (16 + 1 c&s), rio Iguape basin. DZSJRP 13263 (2), rio Ribeira de Iguape basin. *Neoplecostomus microps*: DZSJRP 2767 (1 c&s), rio Paraíba do Sul basin. DZSJRP 2768 (1 c&s), rio Paraíba do Sul basin. DZSJRP 4267 (9), rio Paraíba do Sul basin. DZSJRP 4270 (19), rio Tietê basin. *Pareiorhaphis hystrix*: DZSJRP 13714 (4 + 1 c&s), rio Uruguai basin. *Pareiorhina rudolphi*: DZSJRP 13713 (2 c&s), rio Tietê basin. Hypoptopomatinae – *Acestridium martini*: LBP 12907 (4 + 1 c&s), rio

Amazonas basin. *Corumbataia cuestae*: DZSJRP 7947 (30 + 2 c&s), rio Tietê basin. DZSJRP 8027 (176), rio Tietê basin. *Corumbataia tocantinensis*: MZUEL 4998 (3 of 22 + 2 c&s), rio Tocantins basin. *Epaactionotus bilineatus*: DZSJRP 11358 (3 + 1 c&s), rio Maquiné basin. MCP 23679 (9 of 40 + 1 c&s), rio Tramandaí basin. UFRGS 6564 (6 of 22), rio Tramandaí basin. *Epaactionotus gracilis*: UFRGS 1861 (7 of 251 + 1 c&s), rio Jordão basin. *Eurycheilichthys pantherinus*: DZSJRP 11429 (4 + 2 c&s), rio Uruguay basin. *Gymnotocinclus anosteos*: UFRGS 11296 (5 of 20 + 1 c&s), rio Tocantins basin. *Hisonotus armatus*: LIRP 8047 (33 of 66 + 2 c&s). *Hisonotus chromodontus*: MZUSP 95942 (3 + 1 c&s), rio Tapajós basin. *Hisonotus depressicauda*: DZSJRP 11422 (5 + 1 c&s), rio Tietê basin. *Hisonotus francirochai*: DZSJRP 7693 (66 + 2 c&s), rio Aguapeí basin. DZSJRP 8514 (26), rio Grande basin. *Hisonotus insperatus*: DZSJRP 5377 (5), rio Tietê basin. DZSJRP 10240 (10 + 1 c&s), rio Tietê basin. DZSJRP 10722 (17), rio Paraná basin. *Hisonotus luteofrenatus*: MZUSP 96783 (4 of 23 + 1 c&s), rio Tapajós basin. *Hisonotus notatus*: DZSJRP 13852 (45 + 2 c&s), rio São João basin. *Hisonotus piracanjuba*: DZSJRP 13233 (14 + 1 c&s), paratypes, rio Paranaíba basin. *Hypoptopoma inexpectata*: DZSJRP 15807 (48 + 2 c&s), rio Paraguay basin. *Lampiella gibbosa*: DZSJRP 13621 (2 + 1 c&s), rio Ribeira de Iguape basin. *Microlepidogaster arachas*: DZSJRP 15808 (28 + 3 c&s), paratypes, rio Paranaíba basin. *Microlepidogaster dimorpha*: DZSJRP 8750 (17 + 2 c&s), paratypes, rio Grande basin. DZSJRP 12332 (15 + 2 c&s), paratypes, rio Grande basin. *Microlepidogaster longicolla*: DZSJRP 12453 (4 + 1 c&s), paratypes, rio Paranaíba basin. LBP 9236 (11 + 1 c&s), rio Paranaíba basin. *Microlepidogaster perforatus*: MCP 17717 (1 c&s), rio Grande basin. MNRJ 31886 (1 c&s of 12), rio Grande basin. MZUSP 10216 (1), MZUSP 10217 (1), rio Grande basin. *Microlepidogaster* sp. nov.: MZUSP 95291 (12 + 1 c&s), rio São Francisco basin. *Nannoplecostomus eleonora*: MCP 44047 (14 + 1 c&s), paratypes, rio Tocantins basin. *Niobichthys ferrarisi*: MCP 34810, (2 + 1c&s), rio Negro basin. *Otocinclus affinis*: DZSJRP 7610, (24 + 1 c&s), rio Ribeira de Iguape basin. DZSJRP 7622 (8), rio Ribeira de Iguape basin. *Otothyris juquia*: MZUSP 51286 (12 of 14 + 1 c&s), paratypes, rio Ribeira de Iguape basin. *Otothyris lophophanes*: MNRJ 17702 (11), rio Surui basin. MNRJ 22985 (19 of 64 + 1 c&s), rio Itapemirim basin. *Otothyris rostrata*: MCN 18493 (15 + 1 c&s), rio Tramandaí basin. MHNCI 10322 (11 + 1 c&s), tributary to lagoa Caverá. *Otothyris travassosi*: MCP 18100 (15 + 1 c&s), rio Caraiva basin. MNRJ 22947 (19 of 68 + 1 c&s), rio Mucuri basin. *Otothyropsis marapoama*: LIRP 5641 (3 of 48 + 4 c&s), paratypes,

rio Tietê basin. DZSJRP 7887 (8), paratypes, rio Tietê basin. DZSJRP 7517 (31 + 1 c&s), rio Ivinhema basin. DZSJRP 9937 (10 + 2 c&s), rio Tietê basin. *Otothyropsis piribebuy*: MCP 44394, (2 of 25 + 2 c&s), paratypes, rio Paraguay basin. *Otothyropsis* sp. nov.: DZSJRP 2907 (18 + 3 c&s), rio São Francisco basin. *Oxyropsis acutirostra*: LBP 7193 (42 + 2 c&s), rio Negro basin. *Parotocinclus cristatus*: DZSJRP 15637 (54 + 2 c&s), rio Cachoeira basin. *Parotocinclus jumbo*: MZUSP 69514 (1 c&s), rio Paraíba do Norte basin. MZUSP 108754 (2), rio São Francisco basin. *Parotocinclus maculicauda*: DZSJRP 3137 (1 + 1 c&s), rio Ribeira de Iguape basin. DZSJRP 13618 (32), rio Ribeira de Iguape basin. *Parotocinclus prata*: LIRP 1136, 4 of 37 + 1 c&s), paratypes, rio São Francisco basin. *Plesioptopoma curvidens*: DZSJRP 16133 (67 + 2 c&s), rio São Francisco basin. *Pseudotocinclus parahybae*: MCP 45094 (6 + 1c&s), rio Paraíba do Sul basin. *Pseudotocinclus tietensis*: DZSJRP 6197 (4), rio Tietê basin. DZSJRP 12811 (2), rio Tietê basin. LBP 2964 (2 + 1 c&s), rio Tietê basin. *Rhinolekos britskii*: DZSJRP 5622 (37 + 2 c&s), rio Paranaíba basin. DZSJRP 6983 (6 + 1 c&s), rio Paranaíba basin. DZSJRP 7064 (2 + 1 c&s), paratypes, rio Paranaíba basin. DZSJRP 12190 (16 + 1 c&s), paratypes, rio Paranaíba basin. *Rhinolekos garavelloii*: DZSJRP 10477 (19 + 3 c&s), paratypes, rio Paranaíba basin. DZSJRP 12191 (33 + 4 c&s), paratypes, rio Paranaíba basin. *Rhinolekos schaeferi*: DZSJRP 12192 (2 + 1 c&s), paratypes, rio Paranaíba basin. *Rhinolekos* sp. nov. 1: DZSJRP 10522 (22 + 7 c&s), rio Paranaíba basin. *Rhinolekos* sp. nov. 2: MZUSP 95439 (29 + 4 c&s), rio Tocantins basin. *Schizolecis guntheri*: DZSJRP 2299 (5 + 1 c&s), rio Ribeira de Iguape basin. DZSJRP 6525 (24 + 1 c&s), Bertioga. DZSJRP 12500 (56), rio Iguaçú basin.

ACKNOWLEDGEMENTS

We are grateful to Carlos A. Lucena (MCP), Claudio Oliveira (LBP), Flávio A. Bockmann (LIRP), José L. Figueiredo (MZUSP), Luiz Roberto Malabarba (UFRGS), Marcelo R. Britto (MNRJ), Marco Aurélio Azevedo (MCN), Margarete Lucena (MCP), Oscar Shibatta (UEL), Osvaldo T. Oyakawa (MZUSP), Paulo A. Buckup (MNRJ), Roberto E. Reis (MCP), and Vinicius Abilhoa (MHNCI) for the loan of specimens. The authors were supported by fellowships from Fundação de Amparo à Pesquisa do Estado de São Paulo (FAPESP, 2009/11873-0 to F. O. M.; 2004/00545-8 to F. L.), and Conselho Nacional de Desenvolvimento Científico e Tecnológico (CNPq, 305.946/2011-0 to F. L.; 305053/2011-6 to H. A. B.).

REFERENCES

- Abell R, Thieme ML, Revenga C, Bryer M, Kottelat M, Bogutskaya N, Coad B, Mandrak N, Balderas SC, Bussing W, Stiassny MLJ, Skeleton P, Allen GR, Unmack P, Naseka A, Ng R, Sindorf N, Robertson J, Armijo E, Higgins JV, Heibel TJ, Wikranabayake E, Olson D, López HL, Reis RE, Lundberg JG, Sabaj Pérez MH, Petry P. 2008. Freshwater ecoregions of the world: a new map of biogeographic units for freshwater biodiversity conservation. *BioScience* **58**: 403–414.
- Armbruster JW. 1998. Phylogenetic relationships of the suckermouth armored catfishes of the *Rhinelepis* group (Loricariidae: Hypostominae). *Copeia* **1998**: 620–636.
- Armbruster JW. 2004. Phylogenetic relationships of the suckermouth armoured catfishes (Loricariidae) with emphasis on the Hypostominae and the Ancistrinae. *Zoological Journal of the Linnean Society* **141**: 1–80.
- Armbruster JW, Page LM. 1996. Redescription of *Aphanotorulus* (Teleostei: Loricariidae) with description of one new species, *A. ammophilus*, from the Rio Orinoco basin. *Copeia* **1996**: 379–389.
- Armbruster JW, Sabaj MH, Hardman M, Page LM, Knouft J. 2000. Catfish genus *Corymbophanes* (Loricariidae: Hypostominae) with description of one new species: *Corymbophanes kaiei*. *Copeia* **2000**: 997–1006.
- Arratia G, Gayet M. 1995. Sensory canals and related bones of tertiary siluriform crania from Bolivia and North America and comparison with recent forms. *Journal of Vertebrate Paleontology* **15**: 482–505.
- Boeseman M. 1968. The genus *Hypostomus* Lacépède 1803, and Surinam representatives (Siluriformes: Loricariidae). *Zoologische Verhandlungen* **99**: 1–89.
- Britski HA, Garavello JC. 1984. Two new southeastern Brazilian genera of Hypoptopomatinae and a redescription of *Pseudotocinclus* Nichols, 1919 (Ostariophysi, Loricariidae). *Papéis Avulsos de Zoologia* **35**: 225–241.
- Calegari B. 2010. Filogenia de Hypoptopomatinae com ênfase em *Microlepidogaster*, *Pseudotocinclus* e *Otothyropsis* (Siluriformes: Loricariidae), e descrições de novas espécies. Unpublished MSc. Dissertation, Pontifícia Universidade Católica do Rio Grande do Sul.
- Calegari B, Lehmann PA, Reis RE. 2011. A new species of *Otothyropsis* (Siluriformes: Loricariidae) from the rio Paraguay basin, Paraguay. *Neotropical Ichthyology* **9**: 253–260.
- Calegari B, Reis RE. 2010. A new species of *Microlepidogaster* (Siluriformes: Loricariidae: Hypoptopomatinae) from the upper rio Paraná basin, Brazil. *Neotropical Ichthyology* **8**: 625–630.
- Carvalho TP, Lehmann P, Reis RE. 2008. *Gymnotocinclus anosteos*, a new uniquely-plated genus and species of loricariid catfish (Teleostei: Siluriformes) from the upper rio Tocantins basin, central Brazil. *Neotropical Ichthyology* **6**: 329–338.
- Carvalho TP, Reis RE. 2009. Four new species of *Hisonotus* (Siluriformes: Loricariidae) from the upper rio Uruguay, southeastern South America, with a review of the genus in the rio Uruguay basin. *Zootaxa* **2113**: 1–40.
- Chiachio MC, Oliveira C, Montoya-Burgos JI. 2008. Molecular systematic and historical biogeography of the armored Neotropical catfishes Hypoptopomatinae and Neoplecostominae (Siluriformes: Loricariidae). *Molecular Phylogenetics and Evolution* **49**: 606–617.
- Cramer CA, Bonatto SL, Reis RE. 2011. Molecular phylogeny of the Neoplecostominae and Hypoptopomatinae (Siluriformes: Loricariidae) using multiple genes. *Molecular Phylogenetics and Evolution* **59**: 43–52.
- Cramer CA, Liedke AMR, Bonatto SL, Reis RE. 2007. The phylogenetic relationships of the Hypoptopomatinae and Neoplecostominae (Siluriformes: Loricariidae) as inferred from mitochondrial cytochrome c oxidase I sequences. *Bulletin of Fish Biology* **1/2 9**: 51–59.
- Douglas RH, Collin SP, Corrigan J. 2002. The eyes of suckermouth armoured catfish (Loricariidae, subfamily Hypostomus): pupil response, lenticular longitudinal spherical aberration and retinal topography. *The Journal of Experimental Biology* **205**: 3425–3433.
- Eschmeyer WN. 1998. *Catalog of fishes*. San Francisco: California Academy of Sciences.
- Eschmeyer WN. 2012. *Catalog of fishes*. California Academy of Sciences. Available at: <http://research.calacademy.org/research/ichthyology/catalog/fishcatmain.asp> Electronic version accessed 31 August 2012.
- Esteves K, Lobón-Cerviá J. 2001. Composition and trophic structure of a fish community of a clear water Atlantic rainforest stream in southeastern Brazil. *Environmental Biology of Fishes* **62**: 429–440.
- Ferraris JCJ. 2007. Checklist of catfishes, recent and fossil (Osteichthyes: Siluriformes), and catalogue of siluriform primary types. *Zootaxa* **1418**: 1–628.
- Fink SV, Fink WL. 1981. Interrelationships of the ostariophysan fishes (Teleostei). *Zoological Journal of the Linnean Society* **72**: 297–353.
- Fowler HW. 1954. Os peixes de água doce do Brasil (4ª entrega). *Arquivos de Zoologia do Estado de São Paulo* **9**: 1–400.
- Garavello JC, Britski HA, Schaefer SA. 1998. Systematics of the genus *Otothyris* Myers, 1927, with comments on geographic distribution (Siluriformes: Loricariidae: Hypoptopomatinae). *American Museum Novitates* **3222**: 1–19.
- Gauger MFW, Buckup PA. 2005. Two new species of Hypoptopomatinae from the rio Paraíba do Sul basin, with comments on the monophyly of *Parotocinclus* and the *Otothyriini* (Siluriformes: Loricariidae). *Neotropical Ichthyology* **3**: 509–518.
- Goloboff PA, Farris JS, Nixon KC. 2008. TNT, a free program for phylogenetic analysis. *Cladistics* **24**: 774–786.
- Gosline WA. 1945. Catálogo dos Nematognatos de água-doce da América do Sul e Central. *Boletim do Museu Nacional* **33**: 1–138.
- Gosline WA. 1947. Contribution to the classification of the loricariid catfishes. *Arquivos do Museu Nacional* **41**: 79–134.
- Lehmann PA. 2006. Anatomia e relações filogenéticas da família Loricariidae (Ostariophysi: Siluriformes) com ênfase

- na subfamília Hypoptopomatinae. Unpublished D. Phil. Thesis, Pontifícia Universidade Católica do Rio Grande do Sul.
- Martins FO, Langeani F. 2011a.** *Microlepidogaster dimorpha*, a new species of Hypoptopomatinae (Siluriformes: Loricariidae) from the upper rio Paraná system. *Neotropical Ichthyology* **9**: 79–86.
- Martins FO, Langeani F. 2011b.** *Rhinolekos*, a new genus with three new species of Hypoptopomatinae (Siluriformes: Loricariidae) from upper rio Paraná. *Neotropical Ichthyology* **9**: 65–78.
- Martins FO, Langeani F. 2012.** *Hisonotus piracanjuba*, a new species of Hypoptopomatinae (Siluriformes: Loricariidae) from the rio Paranaíba, upper rio Paraná system, central Brazil. *Ichthyological Exploration of Freshwaters* **23**: 29–36.
- Milne GA, Long AJ, Bassett SE. 2005.** Modelling Holocene relative sea-level observations from the Caribbean and South America. *Quaternary Science Reviews* **24**: 1183–1202.
- Miranda-Ribeiro A. 1911.** Fauna Brasiliense. Peixes. *Eleutherobranchios Aspirophoros*. *Arquivos do Museu Nacional do Rio de Janeiro* **16**: 1–504.
- Miranda-Ribeiro P. 1953.** Tipos das espécies e subespécies do prof. Alípio de Miranda Ribeiro depositados no Museu Nacional. *Arquivos do Museu Nacional do Rio de Janeiro* **42**: 389–417.
- Montoya-Burgos JI, Muller S, Weber C, Pawlowski J. 1998.** Phylogenetic relationships of the Loricariidae (Siluriformes) based on mitochondrial rRNA gene sequences. In: Malabarba LR, Reis RE, Vari RP, Lucena CAS, eds. *Phylogeny and classification of Neotropical fishes*. Porto Alegre: Edipucrs, 363–374.
- Provenzano F, Schaefer SA, Baskin JN, Royero-Leon R. 2003.** New, possibly extinct lithogenine loricariid (Siluriformes, Loricariidae) from northern Venezuela. *Copeia* **2003**: 562–575.
- Reis RE, Carvalho TP. 2007.** Família Loricariidae: Hypoptopomatinae. In: Buckup PA, Menezes NA, Ghazzi MS, eds. *Catálogo das espécies de água doce do Brasil*. Série Livros 23. Rio de Janeiro: Museu Nacional da Universidade Federal do Rio de Janeiro, 82–87.
- Reis RE, Pereira EHL, Armbruster JW. 2006.** Delturinae, a new loricariid catfish subfamily (Teleostei, Siluriformes), with revisions of *Hemipsilichthys* and *Delturus*. *Zoological Journal of the Linnean Society* **147**: 277–299.
- Reis RE, Schaefer SA. 1992.** *Eurycheilus pantherinus* (Siluroidei: Loricariidae), a new genus and species of Hypoptopomatinae from southern Brazil. *Copeia* **1992**: 215–223.
- Reis RE, Schaefer SA. 1998.** New Cascudinhos from southern Brazil: systematics, endemism, and relationships (Siluriformes, Loricariidae, Hypoptopomatinae). *American Museum Novitates* **3254**: 1–25.
- Ribeiro AC, Carvalho M, Melo ALA. 2005.** Description and relationship of *Otothyropsis marapoama*, a new genus and species of Hypoptopomatinae catfish (Siluriformes: Loricariidae) from rio Tietê basin, southeastern Brazil. *Neotropical Ichthyology* **3**: 489–498.
- Ribeiro AC, Lima FCT, Riccomini C, Menezes NA. 2006.** Fishes of the Atlantic Rainforest of Boracéia: testimonies of the Quaternary fault reactivation within a Neoproterozoic tectonic province in southeastern Brazil. *Ichthyological Exploration of Freshwaters* **17**: 157–164.
- Sabino J, Castro RMC. 1990.** Alimentação, período de atividade e distribuição espacial dos peixes de um riacho da floresta Atlântica (Sudeste do Brasil). *Revista Brasileira de Biologia* **50**: 23–36.
- Schaefer SA. 1987.** Osteology of *Hypostomus plecostomus* (Linnaeus), with a phylogenetic analysis of the loricariid subfamilies (Pisces: Siluroidei). *Contributions in Science, Natural History Museum of Los Angeles County* **394**: 1–31.
- Schaefer SA. 1991.** Phylogenetic analysis of the loricariid subfamily Hypoptopomatinae (Pisces: Siluroidei: Loricariidae), with comments on generic diagnoses and geographic distribution. *Zoological Journal of the Linnean Society* **102**: 1–41.
- Schaefer SA. 1997.** The Neotropical cascudinhos: systematics and biogeography of the *Otocinclus* catfishes (Siluriformes: Loricariidae). *Proceedings of the Academy of Natural Sciences of Philadelphia* **148**: 1–120.
- Schaefer SA. 1998.** Conflict and resolution: impact of new taxa on phylogenetic studies of the Neotropical cascudinhos (Siluroidei: Loricariidae). In: Malabarba LR, Reis RE, Vari RP, Lucena ZMS, Lucena CAS, eds. *Phylogeny and classification of Neotropical fishes*. Porto Alegre: Edipucrs, 375–400.
- Schaefer SA. 2003a.** Subfamily Hypoptopomatinae. In: Reis RE, Kullander SO, Ferraris CJ, eds. *Check list of the freshwater fishes of South and Central America*. Porto Alegre: Edipucrs, 321–329.
- Schaefer SA. 2003b.** Relationships of *Lithogenes villosus* (Siluriformes, Loricariidae): evidence from high-resolution computed microtomography. *American Museum Novitates* **3401**: 1–55.
- Schaefer SA, Provenzano F. 1993.** The Guyana Shield *Parotocinclus*: systematics, biogeography, and description of a new Venezuelan species (Siluroidei: Loricariidae). *Ichthyological Exploration of Freshwaters* **4**: 39–56.
- Schaefer SA, Provenzano F. 1998.** *Niobichthys ferrarisi*, a new genus and species of armored catfish from southern Venezuela (Siluriformes: Loricariidae). *Ichthyological Exploration of Freshwaters* **8**: 221–230.
- Taylor WR, Van Dyke GC. 1985.** Revised procedures for staining and clearing small fishes and other vertebrates for bone and cartilage study. *Cybium* **9**: 107–119.
- Weitzman SH, Menezes NA, Weitzman MJ. 1988.** Phylogenetic biogeography of the Glandulocaudini (Teleostei: Characiformes: Characidae) with comments on the distribution of other freshwater fishes in eastern and southeastern Brazil. In: Vanzolini PE, Heyer WR, eds. *Proceedings of a workshop on Neotropical distribution patterns*. Rio de Janeiro: Academia Brasileira de Ciências, 379–427.

APPENDIX 1.

List of unambiguous synapomorphies and autapomorphies for each clade and terminal taxon, respectively.

<i>Delturus</i>	<i>Pareiorhaphis hystrix:</i>	<i>Epactionotus</i>	Char. 36: 1 → 0
<i>carinotus:</i>	Char. 5: 0 → 1	<i>gracilis:</i>	Char. 40: 1 → 0
No autapomorphies	Char. 32: 1 → 0	Char. 7: 3 → 1	Char. 48: 1 → 2
<i>Harttia kronei:</i>	Char. 33: 0 → 1	Char. 18: 1 → 0	Char. 57: 0 → 1
Char. 10: 2 → 0	Char. 47: 1 → 2	Char. 77: 1 → 0	Char. 61: 2 → 1
Char. 37: 1 → 3	Char. 60: 5 → 4	Char. 83: 1 → 2	Char. 63: 1 → 2
Char. 43: 0 → 1	Char. 88: 0 → 1		Char. 65: 2 → 1
Char. 48: 1 → 0		<i>Eurycheilichthys</i>	Char. 66: 1 → 2
Char. 56: 1 → 3		<i>pantherinus:</i>	Char. 67: 1 → 0
Char. 60: 5 → 1	<i>Pareiorhina</i>	Char. 1: 1 → 0	Char. 68: 1 → 0
Char. 62: 0 → 1	<i>rudolphi:</i>	Char. 25: 0 → 1	Char. 69: 1 → 3
Char. 88: 0 → 1	Char. 23: 0 → 1	Char. 35: 0 → 1	Char. 74: 0 → 1
<i>Hypostomus</i>	Char. 29: 0 → 1	Char. 37: 1 → 3	Char. 91: 1 → 0
<i>careopinnatus:</i>	Char. 37: 1 → 3	Char. 39: 1 → 0	
Char. 3: 0 → 1	Char. 59: 0 → 1	Char. 41: 1 → 0	<i>Hisonotus</i>
Char. 14: 1 → 0	Char. 67: 0 → 1	Char. 42: 0 → 1	<i>depressicauda:</i>
Char. 21: 2 → 1	Char. 91: 0 → 1	Char. 44: 1 → 0	Char. 12: 0 → 1
Char. 31: 0 → 1		Char. 49: 1 → 0	Char. 13: 0 → 1
Char. 61: 0 → 2	<i>Acestridium martini:</i>	Char. 65: 2 → 1	Char. 22: 1 → 0
Char. 69: 1 → 0	Char. 5: 0 → 1	Char. 80: 1 → 0	Char. 50: 1 → 0
Char. 73: 0 → 2	Char. 8: 1 → 0	Char. 87: 0 → 1	Char. 51: 1 → 0
Char. 85: 0 → 1	Char. 11: 0 → 2		Char. 61: 2 → 1
Char. 86: 0 → 1	Char. 12: 0 → 1	<i>Gymnotocinclus</i>	Char. 79: 0 → 1
<i>Isbrueckerichthys</i>	Char. 19: 1 → 0	<i>anosteos:</i>	Char. 82: 0 → 3
<i>duseni:</i>	Char. 24: 2 → 1	Char. 4: 12 → 0	
Char. 14: 1 → 0	Char. 34: 0 → 1	Char. 6: 2 → 1	<i>Hisonotus</i>
Char. 33: 0 → 1	Char. 39: 0 → 1	Char. 9: 1 → 0	<i>francirochai:</i>
Char. 55: 1 → 2	Char. 48: 1 → 2	Char. 18: 1 → 2	Char. 7: 3 → 12
Char. 81: 1 → 0	Char. 52: 0 → 1	Char. 32: 1 → 0	Char. 12: 0 → 1
<i>Kronichthys</i>	Char. 54: 0 → 4	Char. 42: 0 → 1	Char. 13: 0 → 1
<i>heylandi:</i>	Char. 57: 0 → 2	Char. 52: 0 → 1	Char. 26: 0 → 1
Char. 3: 0 → 1	Char. 67: 0 → 1	Char. 67: 0 → 1	Char. 34: 1 → 0
Char. 17: 0 → 1	Char. 69: 3 → 5	Char. 81: 1 → 0	Char. 35: 0 → 1
Char. 23: 0 → 1	Char. 81: 1 → 0	Char. 83: 1 → 4	Char. 56: 1 → 3
Char. 27: 0 → 1			Char. 80: 1 → 0
Char. 33: 0 → 1	<i>Corumbataia</i>		Char. 87: 0 → 2
Char. 41: 0 → 1	<i>cuetae:</i>	<i>Hisonotus armatus:</i>	
Char. 51: 0 → 1	Char. 7: 2 → 3	Char. 6: 2 → 1	<i>Hisonotus</i>
Char. 63: 0 → 2	Char. 9: 1 → 2	Char. 22: 1 → 0	<i>insperatus:</i>
Char. 67: 0 → 1	Char. 10: 2 → 0	Char. 36: 1 → 0	Char. 10: 0 → 2
<i>Neoplecostomus</i>	Char. 23: 0 → 1	Char. 37: 1 → 3	Char. 29: 1 → 0
<i>microps:</i>	Char. 48: 1 → 2	Char. 56: 1 → 3	Char. 55: 1 → 2
Char. 1: 1 → 0	Char. 53: 2 → 0	Char. 57: 0 → 1	Char. 64: 4 → 2
Char. 4: 2 → 0	Char. 60: 0 → 1	Char. 68: 1 → 2	
Char. 9: 1 → 0		Char. 69: 1 → 3	<i>Hisonotus</i>
Char. 21: 2 → 0	<i>Corumbataia</i>	Char. 73: 1 → 2	<i>luteofrenatus:</i>
Char. 34: 1 → 0	<i>tocantinensis:</i>	Char. 74: 0 → 1	Char. 4: 0 → 2
Char. 35: 0 → 1	Char. 22: 1 → 0		Char. 23: 1 → 0
Char. 36: 1 → 0		<i>Hisonotus</i>	Char. 34: 1 → 0
Char. 86: 0 → 1	<i>Epactionotus</i>	<i>chromodontus:</i>	Char. 83: 1 → 2
	<i>bilineatus:</i>	Char. 9: 2 → 1	Char. 91: 1 → 0
	Char. 43: 0 → 1	Char. 13: 0 → 1	
	Char. 48: 1 → 0	Char. 19: 1 → 0	<i>Hisonotus notatus:</i>
	Char. 53: 1 → 0	Char. 24: 0 → 1	Char. 22: 1 → 0
	Char. 68: 1 → 2	Char. 26: 0 → 1	Char. 36: 1 → 0

Char. 37: 1 → 2
 Char. 39: 1 → 0
 Char. 45: 0 → 1
 Char. 48: 1 → 2
 Char. 49: 1 → 0
 Char. 50: 1 → 0
 Char. 51: 1 → 0
 Char. 69: 1 → 4
 Char. 73: 1 → 2
 Char. 74: 0 → 1
 Char. 79: 0 → 1

Hisonotus**piracanjuba:**

Char. 9: 1 → 2
 Char. 24: 1 → 0
 Char. 44: 0 → 1
 Char. 57: 1 → 2
 Char. 72: 0 → 2

Hypoptopoma**inexpectata:**

Char. 6: 2 → 1
 Char. 9: 1 → 0
 Char. 40: 1 → 0
 Char. 45: 0 → 2
 Char. 48: 1 → 2
 Char. 50: 1 → 0
 Char. 55: 1 → 2
 Char. 59: 1 → 2
 Char. 72: 0 → 1
 Char. 79: 01 → 2
 Char. 83: 1 → 4
 Char. 84: 2 → 3
 Char. 90: 1 → 0

Lampiella gibbosa:

Char. 3: 1 → 0
 Char. 19: 1 → 0
 Char. 60: 1 → 0
 Char. 66: 1 → 0

Microlepidogaster**arachas:**

No autapomorphies

Microlepidogaster**dimorpha:**

Char. 37: 1 → 2
 Char. 91: 0 → 1

Microlepidogaster**longicollis:**

Char. 34: 1 → 0
 Char. 56: 1 → 2
 Char. 64: 1 → 2
 Char. 69: 1 → 2
 Char. 85: 0 → 1
 Char. 86: 1 → 0

Microlepidogaster**perforatus:**

Char. 52: 0 → 1
 Char. 54: 0 → 1
 Char. 57: 0 → 1
 Char. 61: 2 → 1
 Char. 68: 0 → 2
 Char. 69: 1 → 2
 Char. 73: 1 → 2
 Char. 89: 0 → 1

Microlepidogaster**sp. nov.:**

Char. 11: 1 → 0
 Char. 14: 1 → 2
 Char. 24: 0 → 1
 Char. 34: 1 → 0
 Char. 35: 0 → 1
 Char. 39: 1 → 0
 Char. 43: 0 → 1
 Char. 44: 1 → 0
 Char. 53: 0 → 2
 Char. 60: 0 → 4
 Char. 64: 1 → 3
 Char. 67: 1 → 0
 Char. 68: 0 → 1
 Char. 83: 1 → 2
 Char. 85: 0 → 1

Nannoplecostomus**eleonorae:**

Char. 7: 2 → 3
 Char. 37: 1 → 3
 Char. 53: 2 → 0
 Char. 61: 0 → 1
 Char. 64: 1 → 3
 Char. 67: 0 → 1
 Char. 68: 0 → 3
 Char. 69: 1 → 3
 Char. 70: 0 → 1
 Char. 72: 2 → 1
 Char. 82: 0 → 2
 Char. 83: 1 → 2
 Char. 84: 0 → 2

Otocinclus affinis:

Char. 1: 1 → 0
 Char. 3: 1 → 2
 Char. 4: 0 → 3
 Char. 9: 1 → 2
 Char. 13: 0 → 1
 Char. 35: 0 → 3
 Char. 40: 1 → 0
 Char. 55: 1 → 0
 Char. 57: 0 → 1
 Char. 63: 2 → 1
 Char. 68: 0 → 4

Char. 69: 3 → 1
 Char. 72: 0 → 2
 Char. 80: 1 → 2
 Char. 83: 1 → 2
 Char. 87: 0 → 2

Otothyris juquiae:

Char. 18: 1 → 0
 Char. 38: 0 → 1
 Char. 40: 1 → 0

Otothyris**lophophanes:**

Char. 20: 0 → 1
 Char. 39: 0 → 1
 Char. 47: 0 → 3
 Char. 51: 1 → 0
 Char. 69: 2 → 3
 Char. 91: 1 → 0

Otothyris rostrata:

Char. 27: 1 → 0
 Char. 37: 1 → 3
 Char. 83: 2 → 1

Otothyris travassosi:

No autapomorphies

Otothyropsis**marapoama:**

Char. 11: 1 → 2
 Char. 12: 0 → 1
 Char. 13: 0 → 1
 Char. 22: 1 → 0
 Char. 24: 0 → 2
 Char. 34: 1 → 0
 Char. 36: 1 → 0
 Char. 38: 0 → 1
 Char. 44: 1 → 0
 Char. 50: 1 → 0
 Char. 68: 1 → 2
 Char. 72: 2 → 0
 Char. 73: 1 → 2
 Char. 80: 1 → 0

Otothyropsis**piribeby:**

Char. 2: 1 → 0
 Char. 11: 1 → 2
 Char. 13: 0 → 1
 Char. 15: 0 → 1
 Char. 16: 0 → 1
 Char. 19: 1 → 0
 Char. 22: 1 → 0
 Char. 26: 0 → 1
 Char. 36: 1 → 0
 Char. 38: 0 → 1
 Char. 39: 1 → 0
 Char. 44: 1 → 0

Char. 45: 0 → 1
 Char. 48: 1 → 2
 Char. 56: 1 → 3
 Char. 57: 0 → 1
 Char. 67: 1 → 0
 Char. 68: 1 → 2
 Char. 79: 0 → 1

Otothyropsis sp. nov.:

Char. 2: 1 → 0
 Char. 7: 3 → 1
 Char. 12: 0 → 1
 Char. 23: 1 → 0
 Char. 24: 0 → 2
 Char. 45: 0 → 1
 Char. 50: 1 → 0
 Char. 53: 1 → 0
 Char. 57: 0 → 1
 Char. 61: 2 → 1
 Char. 63: 1 → 0
 Char. 64: 2 → 1
 Char. 65: 2 → 1
 Char. 66: 1 → 2

Oxyropsis**acutirostra:**

Char. 3: 1 → 0
 Char. 17: 1 → 0
 Char. 44: 0 → 1
 Char. 55: 1 → 2
 Char. 64: 4 → 2
 Char. 65: 2 → 1
 Char. 73: 2 → 0
 Char. 83: 1 → 4
 Char. 87: 0 → 3
 Char. 92: 2 → 01

Parotocinclus jumbo:

Char. 1: 1 → 0
 Char. 24: 1 → 0
 Char. 50: 1 → 0
 Char. 73: 0 → 1
 Char. 77: 1 → 0
 Char. 81: 1 → 0
 Char. 85: 0 → 1
 Char. 88: 0 → 1

Parotocinclus**cristatus:**

Char. 9: 2 → 1
 Char. 19: 1 → 0
 Char. 22: 1 → 0
 Char. 27: 1 → 0
 Char. 37: 1 → 3
 Char. 41: 1 → 0
 Char. 52: 0 → 1
 Char. 57: 0 → 1
 Char. 61: 2 → 0

- Char. 63: 1 → 0
 Char. 67: 1 → 0
 Char. 72: 2 → 1
 Char. 84: 2 → 3
 Char. 87: 0 → 2
 Char. 92: 2 → 1
- Parotocinclus maculicauda:**
 Char. 11: 1 → 0
 Char. 44: 1 → 0
 Char. 69: 1 → 4
 Char. 74: 0 → 1
 Char. 79: 0 → 1
- Parotocinclus prata:**
 Char. 11: 0 → 1
 Char. 22: 1 → 0
 Char. 24: 1 → 0
 Char. 65: 0 → 3
 Char. 66: 0 → 1
 Char. 76: 0 → 2
- Plesioptopoma curvidens:**
 Char. 1: 1 → 0
 Char. 6: 2 → 0
 Char. 7: 2 → 3
 Char. 18: 1 → 0
 Char. 32: 1 → 0
 Char. 33: 0 → 1
 Char. 49: 1 → 0
 Char. 50: 1 → 0
 Char. 51: 1 → 0
 Char. 59: 1 → 2
 Char. 65: 12 → 3
 Char. 82: 0 → 1
 Char. 83: 1 → 4
 Char. 89: 0 → 1
- Pseudotocinclus parahybae:**
 Char. 12: 0 → 1
 Char. 17: 0 → 1
 Char. 34: 1 → 0
 Char. 37: 1 → 3
 Char. 39: 1 → 0
 Char. 51: 1 → 0
 Char. 60: 0 → 5
 Char. 66: 1 → 2
 Char. 72: 2 → 1
- Pseudotocinclus tietensis:**
 Char. 13: 0 → 1
 Char. 18: 1 → 0
 Char. 26: 0 → 1
- Char. 53: 0 → 2
 Char. 56: 1 → 3
 Char. 58: 0 → 1
- Pseudotothyris janeirensis:**
 Char. 32: 1 → 0
 Char. 48: 1 → 2
- Pseudotothyris obtusa:**
 Char. 22: 1 → 0
- Pseudotothyris ignota sp. nov.:**
 No autapomorphies
- Rhinolekos britskii:**
 Char. 12: 1 → 0
 Char. 37: 3 → 12
 Char. 86: 1 → 0
- Rhinolekos garavelloi:**
 Char. 22: 1 → 0
 Char. 24: 0 → 1
 Char. 46: 0 → 1
 Char. 53: 0 → 2
 Char. 54: 2 → 3
 Char. 60: 0 → 5
 Char. 68: 0 → 1
 Char. 83: 1 → 2
- Rhinolekos schaeferi:**
 Char. 4: 01 → 2
 Char. 13: 1 → 0
 Char. 25: 0 → 1
 Char. 34: 1 → 0
 Char. 35: 0 → 1
 Char. 37: 3 → 2
 Char. 41: 1 → 0
 Char. 54: 2 → 3
 Char. 86: 1 → 0
- Rhinolekos sp. nov. 1:**
 No autapomorphies
- Rhinolekos sp. nov. 2:**
 Char. 18: 1 → 0
 Char. 22: 1 → 0
 Char. 23: 1 → 0
 Char. 34: 1 → 0
 Char. 35: 0 → 1
 Char. 41: 1 → 0
 Char. 56: 3 → 2
- Schizolecis guntheri:**
 Char. 19: 1 → 0
 Char. 41: 1 → 0
 Char. 47: 0 → 1
- Char. 51: 1 → 0
 Char. 55: 1 → 2
 Char. 65: 2 → 1
 Char. 68: 1 → 0
 Char. 80: 1 → 0
 Char. 90: 1 → 0
 Char. 91: 1 → 0
- Niobichthys ferrarisi:**
 Char. 56: 1 → 2
 Char. 64: 4 → 2
 Char. 76: 3 → 0
 Char. 84: 2 → 0
- Node 1:**
 No synapomorphies
- Node 2:**
 Char. 1: 0 → 1
 Char. 34: 0 → 1
 Char. 44: 0 → 1
 Char. 50: 0 → 1
- Node 3:**
 Char. 57: 0 → 1
 Char. 59: 0 → 1
- Node 4:**
 Char. 4: 0 → 2
 Char. 9: 0 → 1
 Char. 53: 01 → 2
- Node 5:**
 Char. 7: 3 → 2
 Char. 27: 0 → 1
 Char. 51: 0 → 1
- Node 6:**
 Char. 3: 0 → 1
 Char. 40: 0 → 1
- Node 7:**
 Char. 59: 0 → 3
 Char. 71: 0 → 1
 Char. 88: 0 → 1
- Node 8:**
 Char. 31: 0 → 1
 Char. 60: 5 → 0
 Char. 64: 0 → 1
- Node 9:**
 Char. 18: 0 → 1
 Char. 29: 0 → 1
 Char. 83: 0 → 1
- Node 10:**
 Char. 17: 0 → 1
 Char. 34: 1 → 0
 Char. 38: 0 → 1
 Char. 51: 1 → 0
- Char. 76: 0 → 3
 Char. 78: 0 → 1
- Node 11:**
 Char. 59: 0 → 1
 Char. 65: 0 → 12
 Char. 73: 0 → 2
- Node 12:**
 Char. 27: 1 → 0
 Char. 57: 0 → 1
 Char. 64: 1 → 4
 Char. 88: 0 → 1
- Node 13:**
 Char. 2: 0 → 1
 Char. 17: 0 → 1
 Char. 20: 0 → 1
 Char. 38: 0 → 1
 Char. 45: 0 → 1
 Char. 49: 1 → 0
 Char. 66: 0 → 1
 Char. 87: 0 → 2
 Char. 91: 0 → 1
 Char. 92: 1 → 2
- Node 14:**
 Char. 5: 0 → 1
 Char. 10: 2 → 0
 Char. 53: 2 → 0
- Node 15:**
 Char. 23: 0 → 1
 Char. 61: 0 → 2
 Char. 66: 0 → 1
 Char. 67: 0 → 1
 Char. 70: 0 → 1
- Node 16:**
 Char. 7: 2 → 1
 Char. 47: 1 → 2
 Char. 69: 1 → 2
- Node 17:**
 Char. 24: 1 → 0
 Char. 73: 2 → 1
- Node 18:**
 Char. 11: 0 → 1
 Char. 37: 1 → 3
 Char. 57: 0 → 1
- Node 19:**
 Char. 4: 2 → 1
 Char. 10: 0 → 2
 Char. 61: 2 → 0
- Node 20:**
 Char. 13: 0 → 1
 Char. 56: 1 → 3
 Char. 65: 2 → 1

Node 21:

Char. 12: 0 → 1
 Char. 40: 1 → 0
 Char. 61: 0 → 1
 Char. 73: 1 → 2
 Char. 81: 1 → 0

Node 22:

Char. 19: 0 → 1
 Char. 92: 1 → 2

Node 23:

Char. 10: 0 → 2
 Char. 12: 0 → 1
 Char. 13: 0 → 1
 Char. 26: 0 → 1
 Char. 76: 0 → 2
 Char. 85: 0 → 1

Node 24:

Char. 4: 2 → 0
 Char. 5: 1 → 0
 Char. 63: 0 → 1

Node 25:

Char. 2: 0 → 1
 Char. 7: 2 → 3
 Char. 9: 1 → 2
 Char. 11: 0 → 1
 Char. 47: 1 → 0
 Char. 53: 0 → 1
 Char. 64: 1 → 2
 Char. 68: 0 → 1
 Char. 75: 0 → 1
 Char. 76: 0 → 3
 Char. 84: 0 → 2
 Char. 91: 0 → 1

Node 26:

Char. 7: 3 → 2
 Char. 26: 0 → 1
 Char. 34: 1 → 0
 Char. 50: 1 → 2
 Char. 53: 1 → 0
 Char. 59: 1 → 0
 Char. 73: 1 → 2

Node 27:

Char. 11: 1 → 0
 Char. 25: 0 → 1
 Char. 45: 0 → 1
 Char. 46: 1 → 0
 Char. 47: 0 → 1
 Char. 52: 0 → 1
 Char. 54: 0 → 1
 Char. 56: 1 → 3
 Char. 60: 1 → 0
 Char. 66: 1 → 2
 Char. 84: 2 → 3
 Char. 90: 1 → 0
 Char. 91: 1 → 0

Node 28:

Char. 2: 1 → 0
 Char. 9: 2 → 1
 Char. 13: 0 → 1
 Char. 17: 0 → 1
 Char. 24: 0 → 1
 Char. 26: 0 → 1
 Char. 34: 1 → 0
 Char. 35: 0 → 1
 Char. 53: 1 → 0
 Char. 57: 0 → 1
 Char. 66: 1 → 2
 Char. 72: 2 → 0
 Char. 76: 3 → 1
 Char. 78: 1 → 0
 Char. 89: 0 → 1

Node 29:

Char. 10: 0 → 1
 Char. 11: 1 → 2
 Char. 14: 1 → 2
 Char. 15: 0 → 2
 Char. 36: 1 → 0
 Char. 39: 1 → 0
 Char. 49: 1 → 0
 Char. 58: 0 → 1
 Char. 82: 0 → 1
 Char. 87: 0 → 3

Node 30:

Char. 37: 1 → 2
 Char. 84: 2 → 1

Node 31:

Char. 23: 1 → 0
 Char. 55: 1 → 2
 Char. 72: 0 → 2

Node 32:

Char. 1: 1 → 0
 Char. 3: 1 → 0
 Char. 50: 1 → 3
 Char. 62: 0 → 1
 Char. 63: 1 → 2
 Char. 68: 1 → 2
 Char. 69: 1 → 2
 Char. 74: 0 → 1
 Char. 76: 1 → 2

Node 33:

Char. 9: 1 → 2
 Char. 17: 1 → 0

Node 34:

Char. 13: 1 → 2
 Char. 23: 1 → 0
 Char. 46: 1 → 2
 Char. 68: 2 → 4

Node 35:

Char. 7: 3 → 2
 Char. 9: 2 → 1
 Char. 17: 0 → 1
 Char. 24: 0 → 1
 Char. 37: 1 → 2
 Char. 44: 1 → 0
 Char. 46: 1 → 0
 Char. 53: 1 → 0
 Char. 68: 1 → 0

Node 36:

Char. 11: 1 → 0
 Char. 64: 2 → 4

Char. 67: 1 → 0

Char. 69: 1 → 3

Char. 72: 2 → 0

Char. 73: 1 → 2

Char. 74: 0 → 1

Node 37:

Char. 22: 1 → 0

Char. 31: 1 → 0

Char. 36: 1 → 0

Char. 57: 0 → 1

Char. 76: 3 → 2

Node 38:

Char. 39: 1 → 0

Char. 48: 1 → 2

Char. 69: 3 → 2

Node 39:

Char. 8: 0 → 1

Char. 21: 2 → 1

Char. 24: 1 → 2

Char. 29: 1 → 0

Node 40:

Char. 7: 2 → 3

Char. 26: 0 → 1

Char. 34: 1 → 0

Char. 39: 1 → 0

Char. 49: 1 → 0

Char. 66: 1 → 2

Node 41:

Char. 30: 0 → 1

Char. 32: 1 → 0

Char. 50: 1 → 2

Char. 82: 0 → 1

Node 42:

Char. 6: 2 → 1

Char. 36: 1 → 0

Char. 56: 1 → 3

Char. 76: 3 → 2

Char. 90: 1 → 0